QUANTUM GRAVITY EFFECTS IN SCALAR, VECTOR AND TENSOR FIELD PROPAGATION

ANINDITA DUTTA
Bachelor of Science, West Bengal State University, 2012
Master of Science, RKM Vivekananda University, 2014

A Thesis
Submitted to the School of Graduate Studies
of the University of Lethbridge
in Partial Fulfillment of the
Requirements for the Degree

MASTER OF SCIENCE

Department of Physics and Astronomy
University of Lethbridge
LETHBRIDGE, ALBERTA, CANADA

QUANTUM GRAVITY EFFECTS IN SCALAR, VECTOR AND TENSOR FIELD PROPAGATION

ANINDITA DUTTA

Date of Defense: December 12, 2016

Dr. Arundhati Dasgupta Supervisor	Associate Professor	Ph.D.
Dr. Ken Vos Committee Member	Associate Professor	Ph.D.
Dr. Stacey Wetmore Committee Member	Professor	Ph.D.
Dr. Viqar Husain External Committee Member	Professor	Ph.D.
Dr. Mark Walton Chair, Thesis Examination Committee	Professor	Ph.D.

Dedication

To my **Parents**

for supporting me all the way.

And to my **Teachers** who made me who I am.

Abstract

Quantum theory of gravity deals with the physics of the gravitational field at Planck length scale (10^{-35} m). Even though it is experimentally hard to reach the Planck length scale, one can look for evidence of quantum gravity that is detectable in astrophysics. In this thesis, we try to find effects of loop quantum gravity corrections on observable phenomena. We show that the quantum fluctuation strain for LIGO data would be 10^{-125} on the Earth. The correction is, however, substantial near the black hole horizon. We discuss the effect of this for scalar field propagation followed by vector and tensor fields. For the scalar field, the correction introduces a new asymmetry; for the vector field, we found a new perturbation solution and for the tensor field, we found the corrected Einstein equations which are yet to solve. These will affect phenomena like Hawking radiation, black hole entropy and gravitational waves.

Acknowledgments

I would like to thank my supervisor Dr. Arundhati Dasgupta for her kind support and encouragement during this Master's project. Her positive outlook and confidence in my research inspired me and gave me confidence. I am also grateful to my supervisory committee members, especially to Dr. Ken Vos and Prof. Viqar Husain. They were very generous with their time and knowledge, and assisted me in each step to complete this thesis.

My sincere thanks to the School of Graduate Studies at University of Lethbridge for giving me this opportunity and funding me during my research. I would also like to thank all the students and the members of Department of Physics and Astronomy for their friendship and help.

This journey would not be possible without the support from my family. I am grateful to them for their encouragement and kind words when I needed it. My special thanks goes to my friend Partha Paul for helping me with Mathematica and proof reading of this thesis. I am also thankful to my teachers, especially to Dr. Ashik Iqubal, for advising me on the numerical set-up required in this project. To my friends from Lethbridge and roommates, thank you for listening, offering me advice, and supporting me through this entire process.

Contents

Contents vi

Lists of Abbreviations, Consants and Symbols viii

List of Figures xi

1 Introduction 1
- 1.1 This Thesis . . . 7
- 1.2 Outline . . . 9
- 1.3 Notations and Representation . . . 10
  - 1.3.1 General Notations . . . 10
  - 1.3.2 Coordinate System . . . 11

2 Classical Gravity 13
- 2.1 Special Theory of Relativity . . . 14
- 2.2 Riemannian Geometry and Einstein's Field Equation . . . 20
- 2.3 Scalar, Vector and Tensor Fields . . . 32
- 2.4 Schwarzschild Solution . . . 34
- 2.5 Conclusion . . . 38

3 Canonical Quantum Gravity and The Semi-classical Correction 39
- 3.1 Hamiltonian Formulation of General Relativity . . . 41
- 3.2 Ashtekar Variables and Loop Quantum Gravity . . . 50
- 3.3 Kinematical Coherent States in Loop Quantum Gravity . . . 56
- 3.4 Semi-classical Correction in Schwarzschild Space-time: New Result . . . 59
  - 3.4.1 Static and Spherical Metrics . . . 62
  - 3.4.2 Non-static Space-time . . . 63
  - 3.4.3 Non-spherical Space-time . . . 63
  - 3.4.4 The Strain . . . 64
- 3.5 Conclusion . . . 65

4 Effect on The Scalar Field 66
- 4.1 Corrected Scalar Field Evolution . . . 67
- 4.2 Numerical Solution: New Result . . . 70
- 4.3 Conclusion . . . 75

5 Effect on The Vector Field **77**
5.1 Electromagnetic Field in Curved Space-Time 78
5.2 Electromagnetic Field Propagation in Schwarzschild Background 80
5.3 Electromagnetic Field Propagation in Corrected Schwarzschild Black Hole: New Result 83
5.4 Conclusion 89

6 Conclusion **90**
6.1 Work in Progress: Effect on Gravitational Wave in Corrected Black Hole Background 91

Bibliography **95**

A RNPL Pogramming for Numerical Solution **104**

Lists of Abbreviations, Consants and Symbols

List of Abbreviations

ADM metric	Arnowitt, Deser and Misner metric
CMB	Cosmic Microwave Background
CODATA	Committee on Data for Science and Technology
EHT	Event Horizon Telescope
eV	electron-Volt
GPS	Global Positioning System
LHS	Left Hand Side
LIGO	Laser Interferometer Gravitational-Wave Observatory
RHS	Right Hand Side
RNPL	Rapid Numerical Prototyping Language

List of Constants

$\varepsilon_0 = 8.854 \times 10^{-12}\ m^{-3}Kg^{-1}S^4A^2$ .....Permittivity of the free space
$\hbar = 6.626 \times 10^{-34}\ m^2kg/s$ .....Planck constant
$\mu_0 = 1.256 \times 10^{-6}\ H/m$ .....Permeability of the free space
$c = 2.99 \times 10^8/\mathrm{m/s}$ .....Speed of light in a vacuum inertial frame
$G = 6.674 \times 10^{-11}\ m^3kg^{-1}s^{-2}$ .....Gravitational constant
$l_p = 1.62 \times 10^{-35}\ m$ .....Planck length

List of Symbols

$*F^{IJ}_{\mu\nu}$	Dual of the curvature $F^{IJ}_{\mu\nu}$
$\hat{i}, \hat{j}, \hat{k}$	Euclidean basis vectors in 3d
$\mathcal{L}_n$	Lie derivative along vector n^μ
$\mathcal{M}$	Four dimensional manifold
Π	Canonical momentum conjugate to N
Π^a	Canonical momentum conjugate to N^a
Π^{ab}	Canonical momentum conjugate to q^{ab}
$\Re$	Real part
Σ	Constant time three dimensional hypersurface

$\Box$	d'Alembertian operator
$\tilde{\beta}$	Immirzi parameter
A^{μ}	Four vector potential
A^{IJ}_{μ}	Spin connection
D_a	Covariant derivative defined on Σ
e	Edge
E^I	Triad
e^I_{μ}	Tetrad
$F^{IJ}_{\mu\nu}$	Curvature due to spin connection
H	Hamiltonian density
$h_e(A)$	Holonomy
$K_{\mu\nu}$	Extrinsic curvature
K_{ab}	Extrinsic curvature of Σ
L	Lagrangian density
N	Lapse function
N^{μ}	Shift vector
P^I_e	Momentum corresponding to holonomy
$P_l(\cos\theta)$	Legendre polynomial of order l
$q_{\mu\nu}$	Projector onto Σ
q_{ab}	Metric tensor on Σ
$R^{(3)\mu}_{\nu\rho\sigma}$	Three Riemann curvature
$R^{(3)}$	Three Ricci scalar
$R^{(3)}_{\mu\nu}$	Three Ricci tensor
r_g	Schwarzschild radius
r_*	Tortoise coordinate
Y_{lm}	Spherical harmonics
$\mathbf{B}$	Magnetic field
$\mathbf{E}$	Electric field
$\eta_{\mu\nu}$	Minkowski metric tensor
$\Gamma^{\lambda}_{\mu\nu}$	Affine connection
$\hat{e}_{\mu}$	Basis vector
Λ^{μ}_{ν}	Lorentz transformation matrix
$\mathbf{J}$	Current density
∇_{μ}	Covariant derivative
$\otimes$	Direct product
∂_{μ}	$\frac{\partial}{\partial x^{\mu}}$
ρ	Charge density
τ_P	Tangent space of the point P
φ	Scalar field
$\xi : M \to N$	ξ maps the elements of M to the elements of N
$\xi^{-1} : N \to M$	Inverse mapping between the sets M and N
C^p	Continuous and p-times differentiable map
$dr,\ d\theta,\ d\phi$	Infinitesimal Space coordinates in spherical polar coordinate system
dt	Infinitesimal time coordinate

dx, dy, dz	Infinitesimal space coordinates in Cartesian coordinate system
$F_{\mu\nu}$	Antisymmetric electromagnetic field
g	Determinant of the metric tensor
$G_{\mu\nu}$	Einstein tensor
$g_{\mu\nu}$	Metric tensor in curved space-time
M	Mass of the black hole
R	Ricci scalar
r, θ, ϕ	Space coordinates in spherical polar coordinate system
R^n	n-dimensional Euclidean space
$R^{\mu}_{\nu\rho\sigma}$	Riemann curvature
$R_{\mu\nu}$	Ricci tensor
S	Action
S^n	n-dimensional sphere
t	Time coordinate
$T^{\mu\nu}$	Stress-energy tensor
$T^{i_1 i_2 \ldots i_m}_{j_1 j_2 \ldots j_n}$	Tensor of rank (m,n)
u^{μ}	Four velocity
x, y, z	Space coordinates in Cartesian coordinate system
x^{μ}	Contravariant vector
x_{μ}	Covariant vector
Greek indices	run from 0 to 3
Latin indices	run from 1 to 3

List of Figures

1.1 Gravitational wave strain from a binary black hole system 3
1.2 Pictorial view of the Gravitational Lensing 4
1.3 Time dilation in the clocks for a GPS 5
1.4 Cartesian coordinate system 11
1.5 Spherical coordinate system 11

2.1 Light cone for an event 17
2.2 Parallel transport of a vector on a two sphere 26
2.3 Commutator of covariant derivatives 28

3.1 Edge intersecting surface S 55
3.2 An SU(2) coherent state 58

4.1 Plotting of the scalar field potential φ vs. x without correction 72
4.2 Plotting of the scalar field potential φ vs. x with twist term $\beta = x^2(x-1)^2$. 74
4.3 Plotting of scalar field potential φ vs. x with twist term $\beta = \sin^2(x^2(x-1)^2)$ 75

5.1 A(r) vs. r for $\tilde{\lambda} = 0$ 88

Chapter 1

Introduction

If I have seen

further than others,

it is by standing upon

the shoulders of giants.

– Isaac Newton

One of the most important discoveries in the history of science is the existence of gravity. Sir Isaac Newton (1642 – 1727), an English mathematician and physicist, realized that there must be a force between the Earth and a falling object and this force causes the object to accelerate towards the Earth. This insight resulted in the universal law of gravitation, " *Every object in the universe attracts every other object with a force directly proportional to the product of their masses and inversely proportional to the square of the distance between the centres of them*" [1]. This proportionality turns into an equation with the help of a proportionality constant namely gravitational constant denoted as G. The value of this constant was derived later by Henry Cavendish (1798) and it is $G = 6.754 \times 10^{-11} N.m^2/kg^2$ (The value of G recommended by CODATA in 2014 is $6.674 \times 10^{-11} N.m^2/kg^2$) [2].

Newton's laws have achieved many successes in explaining orbital rotations in our solar system, although it could not accurately explain the perihelion precession in the orbital motion of Mercury [3]. Later, this problem was resolved by Albert Einstein's 'General Theory of Relativity' in 1915 [4]. Einstein's theory defines gravity as a result of space-

time curvature. According to this theory, space and time are on the same footing, hence interchangeable. Although Einstein's gravity treats space and time very differently compared to Newtonian theory, general theory of relativity is able to explain everything that Newton's theory did as well as some natural phenomena that would not be justified by Newton's theory, e.g. bending of light and perihelion precession of Mercury [1].

One of the most important consequence of the general theory of relativity is the *Black Hole* [1]. A black hole is a region of space with very high gravity from which not even light can escape. It can be formed from the death of a massive star with sufficiently large mass or from primordial density fluctuations. The general theory of relativity predicts the space-time structure of a black hole and also explains the physics behind it. Direct detection of a black hole is quite challenging as it does not emit any detectable radiation. However, there is indirect evidence that confirms the existence of black holes [5]. Later in this thesis, we will explain the black hole more elaborately.

Another surprising outcome of the general theory of relativity is the existence of *Gravitational Waves*, which are basically ripples caused by a moving massive object in the space-time curvature. The gravitational wave propagates in free space with the speed of light. As the gravitational effect is very weak compared to other physical forces ($G \sim O(10^{-11})\ N\ m^2/kg^2$), it is a difficult task to get experimental evidence of a gravitational wave. Even though the existence of the gravitational wave was predicted by Einstein around 1916-1918 [6], it took almost 100 years to get experimental evidence of the wave. After a long period of constant effort and breathless waiting, in 2016, LIGO finally announced the experimental detection of gravitational waves [7]. This discovery not only opened a new window for research, but also set the standards for precision, by detecting an effect in space-time of order 10^{-21}. The first received gravitation wave data, as detected by LIGO, provide us the mass of the source black hole which was created by merging two black holes. They received a strain of order 10^{-21} as shown in Figure 1.1. The data also predicted the distance of the event from the Earth as well as the approximate radius of the source black

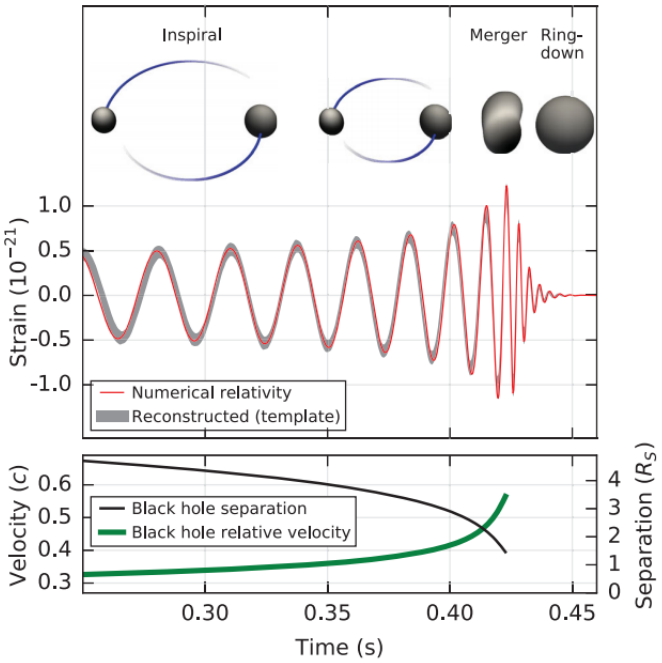

Figure 1.1: Gravitational wave strain from a binary black hole system [7].

hole [7].

Along with these consequences, general theory of relativity also has applications in observational astronomy, modern cosmology and GPS of the Earth [9]. *Gravitational lensing* is one of the important tools in observational astronomy [10]. According to the general theory of relativity, if there is a strong gravity source between the observer and a distant target object in space, then light coming from the object will bend around the gravity source. As a result, the observer sees multiple distorted images of the object as shown in Figure 1.2. In the figure, D is a high gravity source lying between the observer and the target object S. Lights coming from S are bending due to the presence of D; but the observer cannot follow the bend path of light and see real images of S. The distortion of S comes from the fact that, lights coming from different parts of S bend differently when they pass by D. This phenomena is useful to detect the presence of dark matter [11], to estimate the mass of the gravity source, etc. Modern cosmology is highly dependent on Einstein's relativistic theory. *The Big Bang* theory explains how the universe was born [12]. The general theory of relativity describes the physics of the evolution of the universe. It also

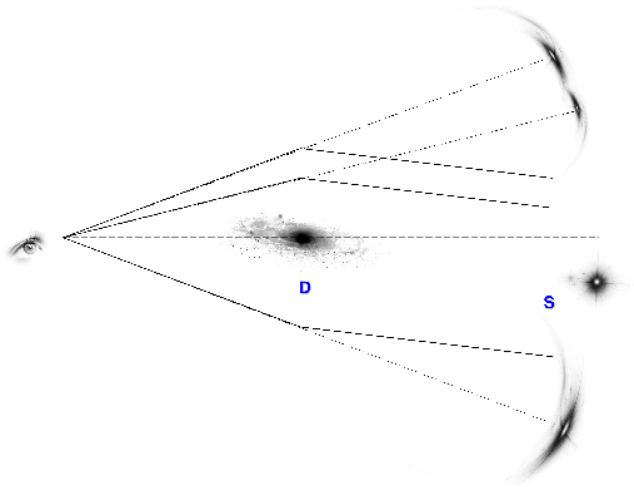

Figure 1.2: Pictorial view of the Gravitational Lensing. D is the gravity source and S is the target object [8].

explains the theory behind the expanding universe and the CMB [12].

In our daily life, the most useful application of the relativistic theory is the GPS [9]. GPS provides the location and time of a GPS receiver on or near the Earth and hence this system is very effective for airlines, military, even in our everyday technology like smart phones, cars, etc. The GPS satellites revolve around the earth in outer space and they contain clocks that are needed to be synchronized properly in order to get an accurate signal. GPS technology uses both special and general theory of relativity in order to improve the system's accuracy. According to the special theory of relativity, clocks on the satellites should be 7 microseconds/day slower due to their motion [9]. On the other hand, according to the general theory of relativity, clocks on the ground should be 45 microseconds/day slower because of the effective curvature of the space-time near the Earth [9]. In Figure 1.3, the left part is showing the effect due to special theory of relativity where the rotating clocks are slower than the stationary clocks. The right part of Figure 1.3 is showing the effect of general theory of relativity where the clock, sitting on the Earth, is slower than the clock sitting on higher altitude. Altogether, there should be 38 microseconds/day correction in the GPS. There are also other ideas, like time travel [13], worm holes [14]. that originate from the general theory of relativity.

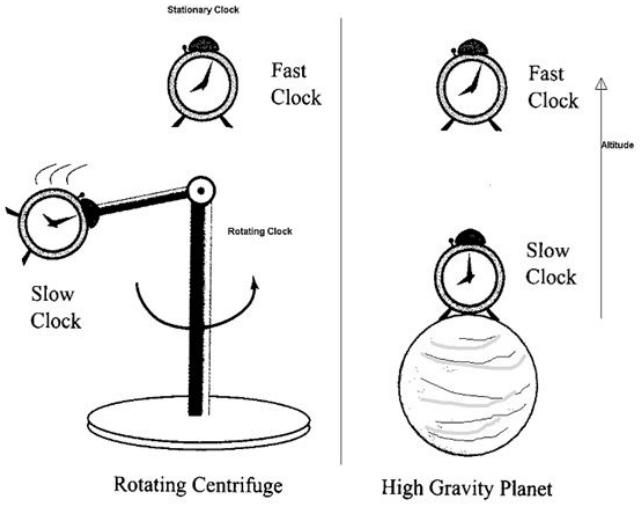

Figure 1.3: Time dilation in the clocks for a GPS. Time depends on gravity and the rotation of the system [15].

When Einstein's relativity theory was dealing with the physics of a space-time, there was a parallel theory developing in the same epoch. This theory is known as *Quantum Theory* [16] and it explains the physics of atoms and photons. Quantum theory reveals that the energy of a system is quantized rather than continuous and a system exchanges energy in the form of a quanta or multiple of the quanta. In 1918, Max Planck won the Nobel Prize in physics for his work on the quanta of energy [17]. Einstein won the Nobel Prize in 1921 for his theory of the *photoelectric effect* based on Planck's theory [18]. Modern quantum theory started in 1926 with the realisation that any particle, including light, has both particle and wave nature [19]. Schrödinger presented the wave-like equation for a hydrogen atom that agreed nicely with experimental results [19]. Moreover, in 1927, Heisenberg wrote his first paper in quantum mechanics formulating the uncertainty principle. This principle states that both the position and momentum of a particle cannot be determined precisely at the same time [20, 21]. In 1927, Dirac's work on the quantum theory of radiation gave birth to quantum field theory [22]. According to this theory, the fields are the physical quantity

and particles are the excited state of the field. Quantum theory is quite well-developed now and this theory has been rigorously verified in experiments [23].

Quantum mechanics and quantum field theory, both have a huge application in different fields of technology including supercomputers, semiconductors, superconductors, particle accelerators, ultra-precise clocks [24, 25, 26, 27]. Quantum mechanics is needed in biophysics, condensed matter and quantum chemistry [28]. Three of the four fundamental interactions of the universe, viz. electromagnetic interaction, strong and weak interactions, have been quantized using quantum field theory and experimentally well-verified [29]. However, quantisation of the gravitational interaction is still not mathematically well-formulated [30].

Understanding physics behind how the universe works, becomes even more challenging when one introduces quantum theory in general relativity. Starting from 1930 to the present, the quantum theory of gravity has come a long way through different formalisms and methodologies [31]. However, it is still a developing area of physics with many unanswered questions. For now, we do not have any experimental evidence of quantum gravity because of the inability of constructing a proper instrumental set up to study the weak effect at the quantum length scale (Planck length scale $\sim O(10^{-35}m)$) [32]. Therefore, none of the quantum gravity theory has been verified yet. Although there are a number of candidate models trying to quantize gravity theoretically, *String theory* and *Loop quantum gravity* are the most promising theories among the models [33]. Throughout this thesis, we will follow the loop quantum gravity approach. It is to be noted that there is no consistent theoretical model to explain all the features of the quantum gravity. Hence, it is expected we will have some 'yet to be answered' questions at the very end of this thesis. Research is still continuing and hopefully we will able to answer all the queries in the very near future.

1.1 This Thesis

There is no straight forward method to quantize gravity theoretically and observe the gravity quanta "graviton" experimentally. The theories "General relativity" and "relativistic quantum mechanics" both of the theories work great on their own. However, the combination of these two theories does not lead us to a fruitful solution, rather ends up with infinite number of divergences. Therefore, theorists have been trying to quantize gravity in different approaches in order to avoid the divergences [31]. Many of these theoretical approaches are quite successful in providing a quantum description of the space-time even though none of them are experimentally verified, hence unreliable. Experimentally detectable evidence for the quantum nature of gravity is still not achieved by the modern technology. One of the main reasons is the weakness of the gravitational interaction. In order to get a detectable quantum gravity effect at Planck length scale, we need to produce extremely high energy ($\approx 10^{30}\ eV$) where the latest generation can only produce $10^{13}\ eV$ [34]. However, given a classical space-time, quantum fluctuations, though infinitesimal, might affect phenomena which are observable. This is not unusual in quantum physics as tiny quantum fluctuations produce the *Casimir effect* detectable in 'classical' quantum plates [35]. The main purpose of this thesis is to find an observable effect due to a semi-classical correction found in loop quantum gravity coherent states.

A quantum effect can be implemented as a semi-classical correction in the classical space-time. Even though the correction is too small to detect directly, it might generate a non-trivial effect in the space-time due to the non-linearity of the mathematical equations describing the system. The semi-classical correction has been computed for the Schwarzschild black hole space-time which is a solution of the Einstein's equations. The computed correction has broken the spherical symmetry of the Schwarzschild black hole. Due to the non-linearity of the Einstein's equations, the correction effect might take a chaotic form near the unstable orbits of the Schwarzschild black hole under certain con-

ditions [36]. In this thesis, we have observed different field propagation in this corrected black hole background. The correction will distort this background space-time and hence effects of the distortion can be calculated on the field propagation. We have studied the correction effect in the scalar and vector propagation near the black hole event horizon where this quantum effect is maximum. For the tensor propagation, we have the equations which are to be solved numerically. As a result, we have found non-trivial loop quantum gravity correction effects in each of the fields.

- For the scalar field propagation, the semi-classical correction is introducing a left-right asymmetry in the propagation of a Gaussian wave near the black hole horizon. We have studied the effect using a toy model wave-equation and solved the equation numerically with proper boundary conditions. We have shown the correction effect is not only breaking the symmetry of the solution, but the velocity of propagation also depends on the correction. The scalar field equation with the actual quantum gravitational correction term also shows assymmetry as the toy model, we have taken. However, this work is still in progress and will be presented soon. The outcome of this research might have some consequences for Hawking radiation [37], which can be observed experimentally [38].

- For the vector field propagation in the corrected black hole background, the semi-classical correction is generating a radial component of the vector potential which is missing in the classical solution. The angular component of the vector potential will also have correction. As the black hole entropy depends on the vector potential, our result might have a non-trivial effect on the entropy of the system. In the upcoming years, we are also expecting to have an *event horizon telescope* that would be able to observe the high gravity zone [39]. As telescope technology is based on the light wave propagation, i.e. vector field propagation, the correction effect might give a relevant prediction of observation.

- For the tensor field propagation, i.e. the gravitational wave propagation, we have found non-trivial equations that might be analysed numerically. The equations, we found, are quite complicated to solve as there is no symmetry in the system, and the solutions will be in most general form. In particular, there is no 'odd' and 'even' parity modes of the spherical gravitational wave. However, this complexity might bring good news as we are looking for a chaotic effect in the system. A gravity wave has already been detected [7] at the end of 2015. Therefore, we can expect better technology that might be able to detect this quantum correction effect in the near future.

1.2 Outline

We will start this thesis with a brief demonstration of the background theories: Einstein's special theory of relativity and general theory of relativity, in Chapter 2. In this chapter, it will be shown that the curvature of the space-time due to the presence of the matter and energy can be depicted as the cause of gravitational force. This phenomenon can be represented by Einstein's field equations. The simplest vacuum solution of these equations, characterizing an uncharged non-rotating black hole space-time, namely Schwarzschild black hole, will also be derived.

In Chapter 3, quantum theory of gravity will be introduced. The quantum gravity theory is a big field of research by itself and consists of different ideas of quantization. For our purpose, mainly the basic theories relevant to this thesis will be discussed and we will use the results directly in later calculations.

The original work of this thesis will begin in Chapter 4. In this chapter, a correction will be calculated from loop quantum gravity coherent state in Schwarzschild black hole background and we will observe this quantum effect of gravity on the scalar field propagation in the Schwarzschild black hole background. The result of this research will be calculated numerically.

Next in Chapter 5, quantum gravity effect will be discussed on the vector field propagation with the black hole background. We will analyse the outcome of the correction effect on the vector field.

Finally, we conclude in the last chapter and summarize the findings based on what we are looking for and what we have found. We also discuss quantum gravity effect on the tensor field propagation which is a work in progress. Some new research possibilities related to this thesis will also be recommended in this chapter.

1.3 Notations and Representation

1.3.1 General Notations

- In this thesis, we will deal with the three and four dimensional coordinate systems. The three dimensional space coordinates x, y, z will be expressed as x_i or x^i where the index $i = 1,2,3$ respectively. The index i will be replaced often by j or k or other Latin letters. Hence coordinates with Latin indices will represent the three dimensional space. On the other hand, four dimensional space-time coordinates t, x, y, z will be expressed as x_μ or x^μ where the index $\mu = 0,1,2,3$ respectively. Again, the index μ can be replaced by ν, τ or any Greek letters. Therefore, the coordinates with Greek indices will represent the four dimensional space-time. Accordingly, the partial derivative operators ∂_i and ∂_μ denote the partial derivative operation $\frac{\partial}{\partial x}$ for i, $\mu = 1$.

- We have used Einstein summation convention in the entire thesis. There will be summation over any repeated index. For example in three dimensions, $x^i x_i = x^1 x_1 + x^2 x_2 + x^3 x_3$ [40].

- The 'Prime' sign over a mathematical variable denotes the derivative with respect to space coordinates unless it is stated otherwise. Example: For an arbitrary factor A, $A' \equiv \frac{dA}{dx}$. The 'dot' sign over a mathematical variable implies the derivative with

respect to time coordinate. Example: For a factor A, $\dot{A} \equiv \frac{dA}{dt}$.

- Bold mathematical characters are denoted as the vector quantities. For example, for a vector quantity B, $\mathbf{B} \equiv \vec{B}$.

1.3.2 Coordinate System

In this section we will discuss the coordinate system briefly [41]. A coordinate system uniquely defines the position of a point in space. Cartesian coordinate system is one of the simplest systems in geometry.

In three dimension, the Cartesian coordinate system is made of three perpendicular axes X, Y, Z and the intersection of the three axes is known as the origin. The position of a point P is given by a set of three unique numbers (x,y,z) where x, y, z are the distances of the point from the origin along the X, Y, Z axes respectively as shown in Figure 1.4. The infinitesimal path difference between two points in this coordinate system is given by $ds^2 = dx^2 + dy^2 + dz^2$.

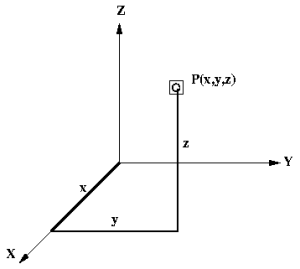

Figure 1.4: Cartesian coordinate system

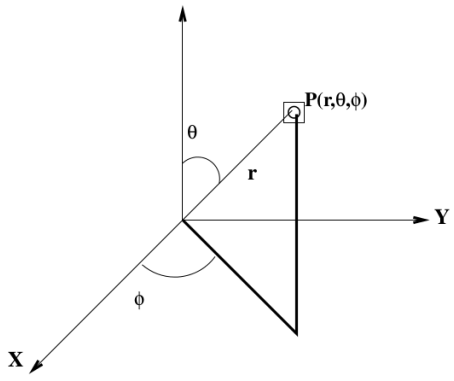

Figure 1.5: Spherical coordinate system

Spherical coordinate system is another way to define the position of a point in space. In Figure 1.5, the position of the point P has been defined with three unique numbers (r,θ,ϕ) where r is the radial distance from the origin to the point P, θ is the polar angle between the Z axis and the radial distance, ϕ is the azimuthal angle between the X axis and the radial projection on the X-Y plane. The infinitesimal path difference between two points in this coordinate

system is given by $ds^2 = dr^2 + r^2 d\theta^2 + r^2 \sin^2\theta \, d\phi^2$.

Later in this thesis, we will introduce time t as a coordinate. In order to determine the location of a point in four dimensional space-time, we would need a time axis along with three space axes. This time axis is perpendicular to each of the space axes. However, in mathematical calculations, it would be considered that the time axis is imaginary. The infinitesimal path difference between two points in four dimensional space-time is given by, $ds^2 = -dt^2 + dx^2 + dy^2 + dz^2$ or $ds^2 = -dt^2 + dr^2 + r^2 d\theta^2 + r^2 \sin^2\theta \, d\phi^2$. We have used natural units here with $c = 1$. Sometimes, in this thesis, we will use natural units with $c = \hbar = G = 1$ for convenience [42]. It is to be noted there is a $-ve$ sign associated with the time coordinate, i.e, the four dimensional path difference is following the sign convention (- + + +) [43]. We will be using this convention through out this thesis. One can always alter the sign convention to (+ - - -) with a $+ve$ time and $-ve$ space components, but the physics of the system will still be the same. However, in order to avoid the confusion, a particular sign convention should be followed entirely in a mathematical calculation.

Chapter 2

Classical Gravity

Black holes are where

God divided by zero.

– A. Einstein

The central idea of this chapter is to show that gravity arises due to the curvature of the geometry of a four dimensional space-time. According to the principle of least action, a moving particle should always choose the path that will extremize the action of the system [44]. Typically, for Newtonian mechanics the chosen path is the shortest possible straight line between the starting and ending positions. For example, if you leave a ball at the higher side of an inclined plane, the ball will slide along a straight line on the plane. Now the question is, what will be the trajectory of the ball if the inclined plane is a curved surface. Obviously, the ball will follow the curved surface. So, the geometry of the space has an important role in the movement of the particle. This example is just an over-simplified model of the actual scenario for the curvature in the space-time. However, the point is, if a space-time is significantly curved, even the trajectory of light can bend [45].

This chapter is a review chapter based on Einstein's theory of special and general theory of relativity. We will start this chapter with the idea of flat space-time described by special theory of relativity. In the following section, we will discuss the required differential geometry in order to compute the mathematical model for the curved space-time. We will also discuss Einstein's field equations that describe any geometry in curved space-time. Finally

the simplest solution of Einstein's field equations, namely Schwarzschild solution, will be presented. In this work, the background space-time is taken to be Schwarzschild black hole space-time. Therefore, a brief discussion on the nature of this space-time would be relevant in this context.

2.1 Special Theory of Relativity

Special theory of relativity is an experimentally well-verified theory developed by Einstein in 1905 [46]. This theory has introduced modification to Newtonian mechanics for systems with high velocity comparable to the velocity of light. The original Newtonian mechanics can describe the physics only when the dimension of the system is somewhere between micron length and cosmological length, the reference frame is inertial, i.e. the frame is not accelerating with respect to obeserver's reference frame, does not have many degrees of freedom, in addition, the particles within the system does not approach the velocity of light. Special theory of relativity introduces modifications to macroscopic high velocity system with small degrees of freedom. This theory is based on two postulates proposed by Einstein [1],

Principle 1: *The laws of physics are the same in any inertial frame, regardless of position or velocity*.

Principle 2: *The speed of light in free space is constant (generally defined as c) in all inertial frame of reference*.

Special theory of relativity considers *time* on the same footing as *space*. Hence, instead of using the three dimensions of space and one absolute time, a unified four dimensional *space-time* coordinate system is defined. An individual point in the four dimensional space-time is called a *world-point* compared to *position* in three dimensional space [46, 47, 48].

The geometry of any space-time can be described by the *line element*: the infinitesimal path difference between two world-points in the space-time. In three dimensional Cartesian coordinate, the line element ds describing a *Euclidean geometry* is given by the *metric* ds^2 as,

$$ds^2 = dx^2 + dy^2 + dz^2 \ . \tag{2.1}$$

However, in four dimensional space-time geometry, the line element in natural unit $c = 1$ is described as,

$$\begin{aligned} ds^2 &= -dt^2 + dx^2 + dy^2 + dz^2 \\ \Rightarrow ds^2 &= \eta_{\mu\nu} dx^\mu dx^\nu \ , \end{aligned} \tag{2.2}$$

where μ, ν runs from 0 to 3. The geometry defined by equations (2.2) is different from the Euclidean geometry because of the $-ve$ sign presented in the metric. This geometry is often called *Minkowski space* or *flat space-time* [1]. The second equation in the equations (2.2) is a tensor form of the metric where $\eta_{\mu\nu}$ is known as Minkowski metric tensor given by a 4×4 matrix,

$$\eta_{\mu\nu} = \begin{pmatrix} -1 & 0 & 0 & 0 \\ 0 & 1 & 0 & 0 \\ 0 & 0 & 1 & 0 \\ 0 & 0 & 0 & 1 \end{pmatrix} \ . \tag{2.3}$$

Also, it is important to note that the quantity ds^2 is invariant in all inertial frames of reference and $\eta_{\mu\nu}$ is a symmetric tensor. Inverse metric of $\eta_{\mu\nu}$ is given by $\eta^{\mu\nu}$ such that $\eta_{\mu\nu}\eta^{\mu\tau} = \delta^\tau_\nu$ [1].

Depending on the positivity or negativity of ds^2, one can portray different scenario in the

four dimensional space-time. Considering a particle movement just in x direction, two points in the space-time is separated by the distance, $ds^2 = -dt^2 + dx^2$.

(i) When $ds^2 > 0$: The pair of world-points is said to be *space-like* separated, e.g., $dt = 0$, $dx \neq 0$ or $dt < dx$. It implies that two points can be space-like separated but no information can be exchanged between them as it violates the causality.
(ii) When $ds^2 < 0$: The pair of world-points is said to be *time-like* separated, e.g., $dt \neq 0$, $dx = 0$ or $dt > dx$. It implies that two points which are time-like separated can exchange information as one is in the causal past of the other.
(iii) When $ds^2 = 0$: The pair of world-points is said to be *light-like/null* separated, e.g., $dx = dt$. In this case, points are connected with light rays. One can say this is the boundary of the time-like and space-like region.

Locus of the null separated points from an event O in a space-time is known as the *light cone* (shown in Figure 2.1). The light cone is a three dimensional surface in a four dimensional space-time. The direction of the light rays from point O defines the $future$ and *past* in the light cone. The light rays diverging from the event O, form the future light cone whereas, light rays converging at point O form the past light cone. The point O is representing the *present* [49].

An event inside the light cone is time-like separated with respect to O, an event on the surface of the light cone is light-like separated with respect to O, and an event outside the light cone is space-like separated with respect to point O. The locus of the point O with time defines the *world line* of the event. Particles with non-zero rest mass follow the time-like world line and particles with zero rest mass (e.g. photon) follow the light-like world line. No real particle has been found yet that has a space-like world line. In order to measure the distance along the particle's world line, a new quantity *proper time* has been introduced such that,

$$d\tau^2 = -\frac{ds^2}{c^2} \, . \tag{2.4}$$

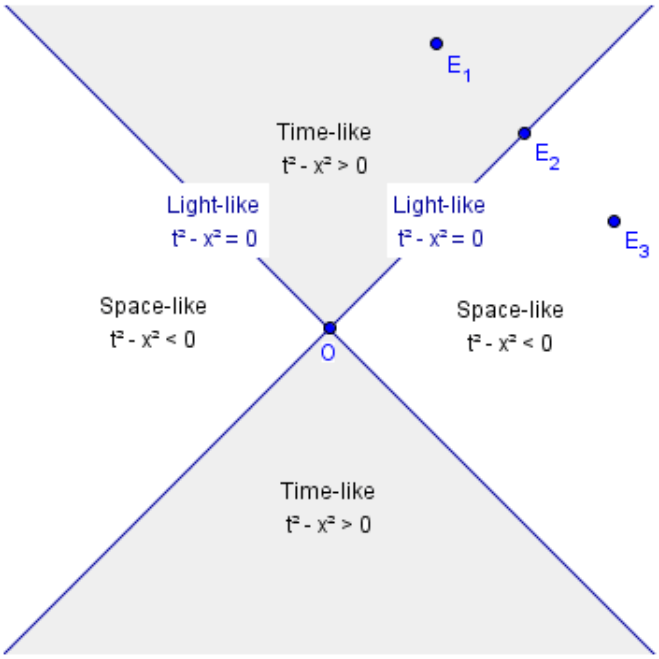

Figure 2.1: Light cone for a event O. Space-like, time-like and light-like separated points with respect to O are shown with points E_1, E_2, E_3 [50].

This is the time measured by the inertial frame along its own world line. This is the way Einstein introduced time as a coordinate in the geometry of a system [51].

A new transformation law for this relativistic theory was proposed by Einstein instead of *Galilean transformation* used in Newtonian mechanics [46]. According to the principle of the Special Theory of Relativity, as ds^2 is invariant in different inertial frames, the transformation from the coordinates (t,x,y,z) to (t',x',y',z') should preserve the form of the equation (2.2). This transformation is known as *Lorentz transformation* [52] (It is to be noted that the 'prime' sign over (t,x,y,z) is denoting the transformed coordinates, it is not representing the derivative of space). If we consider one inertial frame is moving with a constant velocity v along x axis with respect to the other inertial frame, the Lorentz

transformation between two frames are given by,

$$\begin{aligned} t' &= \gamma(t - vx/c^2) \\ x' &= \gamma(x - vt) \\ y' &= y \\ z' &= z\,, \end{aligned} \tag{2.5}$$

with $\gamma = \frac{1}{\sqrt{1-v^2/c^2}}$. However, the inverse transformation is given by,

$$\begin{aligned} t &= \gamma(t' + vx'/c^2) \\ x &= \gamma(x' + vt') \\ y &= y' \\ z &= z'\,. \end{aligned} \tag{2.6}$$

In the tensor form, the Lorentz transformation can be written as,

$$x'^{\nu} = \Lambda^{\nu}_{\mu} x^{\mu}\,, \tag{2.7}$$

where Λ^{ν}_{μ} is the Lorentz transformation metric. For the boost along the x direction with velocity v, the metric takes the form,

$$\Lambda^{\nu}_{\mu} = \begin{pmatrix} \gamma & -\beta\gamma & 0 & 0 \\ -\beta\gamma & \gamma & 0 & 0 \\ 0 & 0 & 1 & 0 \\ 0 & 0 & 0 & 1 \end{pmatrix}, \tag{2.8}$$

where $\beta = \frac{v}{c}$.

The special theory of relativity gives us a few consequences that are experimentally

verified [53, 54]. One of the important consequence is *the relativity of simultaneity*. Time interval Δt also transforms as the first equation of the equations (2.5). If $\Delta t = 0$, i.e., two events are occurring at the same time in different locations ($\Delta x \neq 0$) observed from one inertial reference frame, then we find $\Delta t' \neq 0$, i.e., the events are not simultaneous as observed from another inertial frame of reference. The same equation also yields the *time dilation* property for an event. If an event is observed from an inertial frame of reference for a time period Δt, the same event in the same location ($\Delta x = 0$) will appear to take a longer time period, $\Delta t' = \gamma \Delta t$ as observed from another inertial reference frame. The second equation of the equations (2.6) gives us the paradox of *length contraction*. Suppose the length of a rod measured in its inertial reference rest frame is Δx. If the length is measured simultaneously from another reference frame, the length will appear contracted as $\Delta x' = \frac{\Delta x}{\gamma}$.

Now let us consider a particle moving with a velocity u' along x axis in a reference frame S'. If S' is moving with the velocity v along x axis with respect to another inertial reference frame S, then the velocity of the particle observed by S,

$$u = \frac{dx}{dt} = \frac{u' + v}{1 + \frac{u'v}{c^2}} \, . \tag{2.9}$$

It is to be noted that with the limit $u', v \ll c$, the velocity will follow the Galilean transformation rule $u = u' + v$. Also, for $u' = c$, one can find from equation (2.9) that $u = c$. Hence this theory states that the velocity of light is independent of the frame of reference.

Special theory of relativity has achieved huge success for the relativistic systems, specially in the astrophysics and cosmology [55]. Maxwell's equations are found to be special relativistic theory invariant but not Newtonian gravity. Though Newtonian gravity could explain most of the planetary motion of our solar system, it could not justify the perihelion precession of the Mercury. In 1915, Einstein published his article on *General Theory of Relativity* where gravity was visualized in a completely unique way [56]. In general theory of relativity, gravity is defined as a consequence of curvature in four dimensional

space-time rather than an attractive force between two objects as defined in Newtonian theory. The curvature in space-time is caused by the presence of matter or energy. This new theory not only explains the perihelion precession of Mercury [4], but also reveals some other astrophysical phenomena including bending of light rays, gravitational time dilation, existence of gravity wave and black holes [56, 1].

2.2 Riemannian Geometry and Einstein's Field Equation

Manifold and Differential Manifold:

Einstein's general theory of relativity is a generalization of the special theory of relativity where the Minkowskian flat space-time is replaced by a curved space-time. In order to study the physics in the curved space-time, first we need to build the basic formalism to describe the curved space-time. In this section, we will study the basic mathematics to obtain the curvature of a given geometry. We will be using *Riemannian Geometry* for this purpose [57]. We will begin our study with the understanding of the *Manifold*.

Definition 2.1. A manifold is defined as an n-dimensional space (any kind of topological space) which is locally equivalent to n-dimensional Euclidean space R^n. An n-dimensional manifold will have open sets homeomorphic to Euclidean geometry. If time is included, then the manifold is locally equivalent to Minkowski space-time [57].

For example, an n-dimensional sphere S^n is a manifold where a circle is S^1 sphere, a 2-sphere is S^2 etc. It is obvious that an n-dimensional Euclidean space R^n is also a manifold as it is locally Euclidean. There are some geometries that cannot be regarded as a manifold, e.g., a one dimensional line intersecting a two dimensional plane. Here the intersection point cannot be mapped into a Euclidean space. In order to study a concrete example, let us define a map. *Map* ξ is defined as a relationship between two sets M and N such that $\xi : M \to N$, i.e., for each element of M, there is one element for N. For the S^1 circle with

unit radius, we can write the circle as an union of open sets, each of which maps to R [58],

$$\begin{aligned}
\xi_1 &:= \{(x,y)|x>0\} \qquad \phi_1(x,y) := y \\
\xi_2 &:= \{(x,y)|x<0\} \qquad \phi_2(x,y) := y \\
\xi_3 &:= \{(x,y)|y>0\} \qquad \phi_3(x,y) := x \\
\xi_4 &:= \{(x,y)|y<0\} \qquad \phi_4(x,y) := x \,,
\end{aligned} \tag{2.10}$$

where the constraint equation is $x^2+y^2=1$. Thus the circle is mapped into a real Euclidean line. It is to be noted that even though the circle is written as a function of both x and y, the constraint equation reduces one degree of freedom making it one dimensional geometry.
Note: There is also an *inverse mapping* that exists such that $\xi^{-1}: N \to M$ and for an element a of set M, $\xi.\xi^{-1}(a) = a$.

In general relativity, the 4-dimensional space-time is a special class of manifold which is differentiable and is known as a *differential manifold*. Let us consider a map $\xi: R^m(x) \to R^n(y)$, such that,

$$\begin{aligned}
y_1 &= \xi^1(x_1,x_2,...,x_m) \\
y_2 &= \xi^2(x_1,x_2,...,x_m) \\
&\vdots \\
y_n &= \xi^n(x_1,x_2,...,x_m)\,.
\end{aligned} \tag{2.11}$$

Any of these functions can be referred to as a C^p map where the function is continuous and p times differentiable. A *smooth* manifold should have a C^∞ mapping.

Tangent Space, Vector and Dual Vector:

Now let us define a *tangent space* on a differential manifold. First we consider a manifold

M with smooth functions such that a C^∞ map $f : M \to R$ exists and we draw curves on this space through an arbitrary point p. Now we can define an operator in that space, named *directional derivative*, which maps $f \to \frac{df}{d\lambda}$ at p where λ is a parameter along the curve.

Definition 2.2. A tangent space τ_p is defined as a space of the directional derivative operators along the curves through the point p [59].

The directional derivative operator is actually representing a *vector* which can be defined as an arrow in the space-time with a notion of direction. It is often convenient to decompose a vector into components along a set of *basis* vectors, where the basis vectors are independent of each other. Any abstract vector $\mathbf{A}$ can be written as a linear combination of basis vectors $\hat{e_\mu}$ and its components A^μ,

$$\mathbf{A} = A^\mu \hat{e_\mu} \ , \tag{2.12}$$

where the index μ is assigned to the numbers of dimension of the space and takes the values 0,1,2,3... accordingly. Sometimes, in physics, we loosely refer a vector $\mathbf{A}$ as its components A^μ when the basis vectors are known. On a differential manifold at each point x, we can find a *tangent space* where we can define vectors $\mathbf{V} = V^\mu \frac{\partial}{\partial x^\mu} = V^\mu \partial_\mu$ (∂_μ represents the basis on the tangent space and V^μ are the components). The way V^μ transform under change of coordinates gives them the label *contravariant vectors*. Under a coordinate transformation $\mu \to \mu'$, the contravariant vector component changes as,

$$V^{\mu'} = \frac{\partial x^{\mu'}}{\partial x^\mu} V^\mu \ . \tag{2.13}$$

We can also define *dual vectors* corresponding to the vectors such that the dual vectors map vectors to real numbers. There is an easy way to visualize the difference between a vector and a dual vector as shown in reference [59]. If we visualize a vector as an arrow, then a dual vector can be visualized as a series of parallel surfaces. When the arrow 'vector' passes through the parallel surfaces 'dual-vector' the vector is said to be mapped by the dual

vector. The dual vector maps the vector into real number which can be visualized as the number of surfaces the arrow pierces. Mathematically, the dual vector ω is expressed as,

$$\omega = \omega_\mu \hat{e^\mu} \ , \tag{2.14}$$

where $\hat{e^\mu}$ are the basis dual vectors and ω_μ are the components. Therefore, we can also define a dual space to the tangent space known as the *cotangent space* such that the dual vectors $\omega = \omega_\mu dx^\mu$ maps the tangent vectors to the space of real numbers (dx^μ are the basis of the cotangent space and ω_μ are the components). The way, the ω_μ transform under coordinate transformation, gives them the label *covariant vectors*. Under a coordinate transformation $\mu \to \mu'$, the covariant vector components change as,

$$\omega_{\mu'} = \frac{\partial x^\mu}{\partial x^{\mu'}} \omega_\mu \ . \tag{2.15}$$

Note: It is to be noted that contravariant vector components are referred to with upper indices and the basis vectors are referred to with lower indices. For the covariant vector, the components are referred to with lower indices and the basis vectors are referred to with upper indices.

Tensors:

A generalization of vectors and dual vectors leads us to define another quantity named *tensor*. We can define tensor T that transforms in both of the tangent and cotangent space, e.g. $T = T^{ij}_{lmk} \partial_i \otimes \partial_j \otimes dx^l \otimes dx^m \otimes dx^k$, where T is a $T(2,3)$ type tensor. A tensor of (m,n) type should have m number of contravariant indices and n number of covariant indices. Therefore, from this point of view, a scalar is a $(0,0)$ type tensor, a vector is a $(1,0)$ type tensor and a dual vector is a $(0,1)$ type tensor. It can be said that while a dual vector maps a vector to a real number, *a tensor is a multilinear map from a collection of vectors and dual vectors to real numbers*. An N dimensional two tensor ((2,0),(0,2) or (1,1) type) can

be written as an $N \times N$ matrix. On our four dimensional manifold, all the tensors are 4×4 matrices. For example, in the special theory of relativity, the Minkowski metric tensor $\eta_{\mu\nu}$ can be written as a 4×4 matrix as shown in equation (2.3) and it is a tensor of type (0,2).

One of the characteristics of the differential manifold is the concept of the distance function. As we have already seen in equation (2.3), the line element in the space-time can be represented in terms of $\eta_{\mu\nu}$ which is the diagonal metric tensor of the Minkowski space-time. The generalization of this tensor to arbitrary curved geometries is $g_{\mu\nu}$ which is a symmetric metric tensor. With this metric, the notion of distance is $ds^2 = g_{\mu\nu}dx^\mu dx^\nu$. In this way, the metric of space-time is used to map a contravariant tensor to a covariant tensor.

$$V_\mu = g_{\mu\nu}V^\nu \ . \tag{2.16}$$

A metric tensor contains all the information that we need to describe the curvature of the manifold and it has a non-vanishing determinant $g = |g_{\mu\nu}|$. As $g_{\mu\nu}$ is symmetric in μ and ν, it has 10 independent components. The inverse metric tensor $g^{\mu\nu}$ can also be defined as $g^{\mu\nu}g_{\mu\lambda} = \delta^\nu_\lambda$. Later in this chapter, we will derive the metric tensor components for the Schwarzschild black hole space-time.

Another important tensor in general relativity is the *Stress-energy tensor* $T^{\mu\nu}$ [57]. This is a type (2,0) symmetric tensor which provides the information of the energy, momenta, pressure, etc. of the system. The quantity $T^{\mu\nu}$ stands for *flux of four-momentum* p^μ *across a surface of constant* x^β [59]. Thus the components T^{00} refers to the energy density, $T^{0i} = T^{i0}$ refers to the energy flux or momentum density, and T^{ij} refers to the momentum flux or stress of the system. In general relativity, any matter or field can be described as a perfect fluid which is 'isotropic in its rest frame' [12]. For a perfect fluid with density ρ and pressure p, the stress-energy tensor is given by,

$$T^{\mu\nu} = (\rho + p)u^\mu u^\nu + p\eta^{\mu\nu} \ , \tag{2.17}$$

where u^μ is the four-velocity of the system.

Derivative, Parallel Transport and Geodesic:

Now we will see how vectors and tensors behave with change of space-time point. When a vector or tensor moves on the manifold, we need to introduce a *connection* which is characterized by the curvature of the manifold. In flat space-time, change of any vector or tensor can be mapped by the partial derivative operator where no connection is needed. In flat space-time, the derivative of a vector V^ν in the direction x^μ is given by $\partial_\mu V^\nu$ and it is sufficient to describe the whole scenario. However in curved geometries, the vector components also get rotated. To measure this rotation, we introduce an *affine connection* [59] (also called Christoffel symbols) $\Gamma^\lambda_{\mu\nu}$ on the differential manifold. The total derivative, symbolically ∇_μ, is defined as the regular partial derivative and the connection. This total derivative is known as the *covariant derivative.*

Definition 2.3. A derivative operator on a manifold $\mathcal{M}$, which takes a tensor field of type $T(k,l)$ to type $T(k,l+1)$ is known as a covariant derivative [57].

For the covariant vector V_ν, the covariant derivative is given by,

$$\nabla_\mu V_\nu = \partial_\mu V_\nu - \Gamma^\alpha_{\mu\nu} V_\alpha \ . \tag{2.18}$$

For the contravariant vector V^ν, the covariant derivative is given by,

$$\nabla_\mu V^\nu = \partial_\mu V^\nu + \Gamma^\nu_{\mu\alpha} V^\alpha \ . \tag{2.19}$$

The affine connection is not a tensor because under a coordinate transformation, it does not transform like a tensor. Also it is symmetric in the lower two indices. This property will be shown later when we obtain an expression for this connection. In general, for an arbitrary

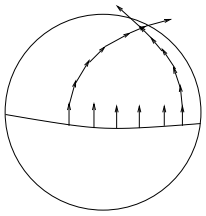

Figure 2.2: Parallel transport of a vector on the surface of a two sphere. The vector is rotated at the ending point after following a different path [60].

tensor, one can write,

$$\begin{aligned}\nabla_\sigma V^{\mu_1\mu_2\mu_3\ldots\mu_k}_{\nu_1\nu_2\nu_3\ldots\nu_k} = \;& \partial_\sigma V^{\mu_1\mu_2\mu_3\ldots\mu_k}_{\nu_1\nu_2\nu_3\ldots\nu_k} + \Gamma^{\mu_1}_{\sigma\lambda} V^{\lambda\mu_2\mu_3\ldots\mu_k}_{\nu_1\nu_2\nu_3\ldots\nu_k} + \Gamma^{\mu_2}_{\sigma\lambda} V^{\mu_1\lambda\mu_3\ldots\mu_k}_{\nu_1\nu_2\nu_3\ldots\nu_k} + \ldots \\ & - \Gamma^{\lambda}_{\sigma\nu_1} V^{\mu_1\mu_2\mu_3\ldots\mu_k}_{\lambda\nu_2\nu_3\ldots\nu_k} - \Gamma^{\lambda}_{\sigma\nu_2} V^{\mu_1\mu_2\mu_3\ldots\mu_k}_{\nu_1\lambda\nu_3\ldots\nu_k} - \ldots \,. \end{aligned} \tag{2.20}$$

Now we have the mathematical tools to find the derivative of a vector or tensor in a curved manifold. Here, we will discuss the notion of *parallel transport*.

Definition 2.4. If a vector remains parallel to itself when transported along a curve, then it is said to be parallel transported [59].

In flat space-time, the parallel transport of a vector does not depend on the path. However, in curved space-time, the choice of path is important while parallel transporting a vector. In the Figure 2.2, it has been shown that, the vector might not return to the same point to be coincident with itself. This is the sign of existence of curvature in the manifold. A vector is said to be parallel transported along a path if $t^\mu \nabla_\mu V^\nu = 0$, where t^μ represents the tangent vector to the curve.

With the understanding of parallel transport, the next logical discussion is about the *Geodesic*. We know in flat space-time a force-free particle moves in a straight line which is the shortest distance possible between two points. However, in curved space-time, the curve that connects the shortest distance between two points, is called the geodesic. In terms of parallel transport, one can say,

Definition 2.5. A geodesic is a curve which parallel transports its own tangent vector [59].

A force-free particle follows a geodesic in the curved space-time. The equation of motion of a test particle in a particular space-time can be derived by taking the variation on the metric. According to the variational principle, the world line between two time-like separated points of a test particle would extremize the proper time. This statement leads us to write,

$$\delta \int ds = 0 \, . \tag{2.21}$$

For the flat space-time, the line element is $ds = \sqrt{-\eta_{\mu\nu} dx^\mu dx^\nu}$ and hence the equation of motion can be expressed as,

$$\frac{d^2 x^\mu}{d\tau^2} = 0 \, . \tag{2.22}$$

On the other hand, for the curved space-time with $ds = \sqrt{-g_{\mu\nu} dx^\mu dx^\nu}$, the equation of motion can be written as,

$$\frac{d^2 x^\mu}{d\tau^2} + \Gamma^\mu_{\alpha\beta} \frac{dx^\alpha}{d\tau} \frac{dx^\beta}{d\tau} = 0 \tag{2.23}$$

$$\Rightarrow u^\nu \nabla_\nu u^\mu = 0 \, , \tag{2.24}$$

where u^ν is the four-velocity of the particle. The above equation is a set of four equations with the free index $\mu = 0, 1, 2, 3$. These equations of motion of a particle in a curved space-time are known as *geodesic equations* [57]. It is to be noted that the geodesic equations are free particle equations without any force. If a particle moves under some forces, then the force terms can be added on the LHS of the equation (2.23). For the time-like geodesic, we consider proper time τ as the parameter along the geodesic. However, for the light-like geodesic, time is not defined any more; hence we introduce some affine parameter that characterizes the geodesic [59].

Curvature and Gravity:

Curvature of a space-time can be quantified by a quantity called *Riemann Curvature*. We al-

ready know the fact that a vector changes while parallel transported along different paths on the manifold. The change of the vector carries the information of the curvature. In order to quantify the curvature, we refer to Figure (2.3). In this figure we parallel transport a vector from P to Q along two different paths. Path 1 is following path I and II, and path 2 is following path III and IV as labelled in the figure. The change along path 1 is found as $\nabla_\mu \nabla_\nu V^\rho$ (We assume that the tangent vectors to path I and II are constants). Similarly the change along path 2 is $\nabla_\nu \nabla_\mu V^\rho$. Next we take the difference of the two paths, and find that,

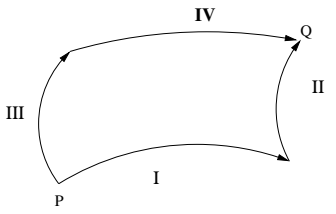

Figure 2.3: Commutator of covariant derivatives [61].

$$\begin{aligned}
\nabla_\mu \nabla_\nu V^\rho - \nabla_\nu \nabla_\mu V^\rho &= [\nabla_\mu, \nabla_\nu] V^\rho \\
&= (\partial_\mu \Gamma^\rho_{\nu\sigma} - \partial_\nu \Gamma^\rho_{\mu\sigma} + \Gamma^\rho_{\mu\lambda}\Gamma^\lambda_{\mu\sigma} - \Gamma^\rho_{\nu\lambda}\Gamma^\lambda_{\mu\sigma}) V^\sigma \\
&\quad -\Gamma^\rho_{\mu\sigma}\Gamma^\sigma_{\nu\lambda} V^\lambda - \Gamma^\rho_{\nu\sigma}\Gamma^\sigma_{\mu\lambda} V^\lambda \,, \qquad (2.25)
\end{aligned}$$

where $[\nabla_\mu, \nabla_\nu]$ is the standard commutator bracket in mechanics. The first bracketed part in the equation (2.25) is known as the *Riemann Curvature* of the manifold and given by [59],

$$R^\rho_{\sigma\mu\nu} = \partial_\mu \Gamma^\rho_{\nu\sigma} - \partial_\nu \Gamma^\rho_{\mu\sigma} + \Gamma^\rho_{\mu\lambda}\Gamma^\lambda_{\mu\sigma} - \Gamma^\rho_{\nu\lambda}\Gamma^\lambda_{\mu\sigma} \,. \qquad (2.26)$$

A nonzero Riemann tensor signifies the existence of curvature. The other quantity in equation (2.25) measures torsion, and is zero for space-times which are 'metric' compatible, i.e., the parallel transport of a metric along any path is zero.

$$\nabla_\lambda g_{\mu\nu} = 0 \,. \qquad (2.27)$$

The above equation can be solved to give a formula for the affine connection, which is

symmetric in the lower indices.

$$\Gamma^{\lambda}_{\mu\nu} = \frac{1}{2} g^{\lambda\rho} \left(\partial_{\nu} g_{\mu\rho} + \partial_{\mu} g_{\lambda\nu} - \partial_{\lambda} g_{\mu\nu} \right) \ . \tag{2.28}$$

There are few symmetries associated with the Riemann tensor and it is easy to see if we lower all of the indices using the relation $R_{\rho\sigma\mu\nu} = g_{\rho\lambda} R^{\lambda}_{\sigma\mu\nu}$. The symmetries in the tensor $R_{\rho\sigma\mu\nu}$ can be described as follows:

- Antisymmetric in the first two indices such that, $R_{\rho\sigma\mu\nu} = -R_{\sigma\rho\mu\nu}$.
- Symmetric in the first two pair of indices to the second two pair of indices such that, $R_{\rho\sigma\mu\nu} = R_{\mu\nu\rho\sigma}$.
- Follower of the relation $R_{\rho\sigma\mu\nu} + R_{\rho\nu\sigma\mu} + R_{\rho\mu\nu\sigma} = 0$.

After applying these constraints it is easy to calculate the number of the independent components of the Riemann tensor. For the four dimensional space-time, it has 20 independent components. Along with the above mentioned symmetries, there is a differential identity for the Riemann tensor,

$$\nabla_{\lambda} R_{\rho\sigma\mu\nu} + \nabla_{\rho} R_{\sigma\lambda\mu\nu} + \nabla_{\sigma} R_{\lambda\rho\mu\nu} = 0 \ . \tag{2.29}$$

The above identity is known as *Bianchi identity* [43].
Sometimes it is possible to use a contracted form of the Riemann tensor. This contracted form is known as the *Ricci tensor* and it is given by [59],

$$\begin{aligned} R_{\mu\nu} &= R^{\alpha}_{\mu\alpha\nu} \\ &= \partial_{\alpha} \Gamma^{\alpha}_{\mu\nu} - \partial_{\nu} \Gamma^{\alpha}_{\mu\alpha} + \Gamma^{\alpha}_{\sigma\alpha} \Gamma^{\sigma}_{\nu\mu} - \Gamma^{\alpha}_{\sigma\nu} \Gamma^{\sigma}_{\alpha\mu} \ . \end{aligned} \tag{2.30}$$

It is to be noted that the Ricci tensor is symmetric as $R_{\mu\nu} = R_{\nu\mu}$. With further contraction,

one will end up with the *Ricci scalar* [59],

$$\begin{aligned} R &= g^{\mu\nu}R_{\mu\nu} = R^{\mu}_{\mu} \\ &= g^{\mu\nu}(\partial_{\alpha}\Gamma^{\alpha}_{\mu\nu} - \partial_{\nu}\Gamma^{\alpha}_{\mu\alpha} + \Gamma^{\alpha}_{\sigma\alpha}\Gamma^{\sigma}_{\nu\mu} - \Gamma^{\alpha}_{\sigma\nu}\Gamma^{\sigma}_{\alpha\mu}) \ . \end{aligned} \tag{2.31}$$

If we contract the identity equation (2.29) with $g^{\mu\sigma}g^{\nu\lambda}$, we will get the following,

$$\nabla^{\mu}R_{\rho\mu} = \frac{1}{2}\nabla_{\rho}R \ . \tag{2.32}$$

This equation can be re-written as,

$$\nabla^{\mu}G_{\mu\nu} = 0 \ , \tag{2.33}$$

where $G_{\mu\nu}$ is known as the *Einstein tensor* and it is defined as [59],

$$G_{\mu\nu} = R_{\mu\nu} - \frac{1}{2}Rg_{\mu\nu} \ . \tag{2.34}$$

Now we have a formalism for a curved manifold described by the Riemann tensor, Ricci tensor and Ricci scalar. The curvature, we have computed here, is referred as 'intrinsic curvature'. This curvature can be measured by the observer who is staying on the same dimension as the manifold. For our four dimensional manifold, the intrinsic curvature is measured by the observers who are on the four dimensional manifold by themselves. There is also 'extrinsic curvature' which can be measured on a manifold embedded in higher dimensional manifold. Thus we can measure the extrinsic curvature of a three dimensional manifold while we are staying on a four dimensional space-time. We will study extrinsic curvature in the next chapter.

Given the above description of curvature quantities, we can try to measure gravity. For

a Newtonian potential φ, one can write,

$$\nabla^2\varphi = 4\pi G\rho \ , \tag{2.35}$$

where ρ is the mass density. If we want to compute a similar equation for the curved space-time, we need to generalize the above equation for the tensor field. As all generally covariant (transform appropriately under coordinate transformations) physical quantities can be written as vectors or tensors; The mass density can be depicted as the time-time component of the energy-momentum tensor $T_{\mu\nu}$. In addition, in the weak field limit, the components of $G_{\mu\nu}$ reduces to $\nabla^2\varphi$. Motivated from this, the Einstein's equations for general $T_{\mu\nu}$ are given by [59],

$$R_{\mu\nu} - \frac{1}{2}Rg_{\mu\nu} = \frac{8\pi G}{c^4}T_{\mu\nu} \ . \tag{2.36}$$

In Natural units with $c = G = 1$, Einstein's equations are,

$$R_{\mu\nu} - \frac{1}{2}Rg_{\mu\nu} = 8\pi T_{\mu\nu} \ . \tag{2.37}$$

The above expression is a set of 10 equations for different values of μ, ν. In the low energy limit, the Einstein equations coincide with the Newtonian counterpart. However, it is to be noted that one side of the expression (2.37) characterizes the geometry of the manifold where the other side describes the matter/energy associated with the system. Thus these equations link the curvature of the space-time with the matter or energy of the system. Einstein's equations are non-linear and hence the combination of two solutions of these equations cannot provide a third solution. The expression (2.37) can also be derived from the Einstein-Hilbert action [59],

$$S = \frac{1}{16\pi}\int d^4x\sqrt{-g}\, R + S_{matter} \ , \tag{2.38}$$

where g is the determinant of metric tensor $g_{\mu\nu}$. In the absence of a matter field, i.e, in a

vacuum $S_{matter} = 0$ and hence $T_{\mu\nu} = 0$. Therefore, in the vacuum, the RHS of the equations (2.37) vanish.

2.3 Scalar, Vector and Tensor Fields

In this section, we will briefly discuss about the scalar, vector and tensor fields, and their relation with Einstein's equations. When a system contains a huge number of particles (ideally, the number of particles $\to \infty$), we consider the system as a field. The spin of the particles defines the nature of the field. The equation of motion of a particle in a field is derived from the action principle. In order to do so, first we need to find the action of a field. We will begin our study with the scalar field followed by the vector and tensor fields.

Scalar Field:

A scalar field is associated with spin-0 scalar particles like Higgs bosons [62]. The action for a scalar field φ can be written as,

$$S_{matter} = -\int d^4x\sqrt{-g}\left[\frac{1}{2}g^{\mu\nu}(\partial_\mu\varphi)(\partial_\nu\varphi) + V(\varphi)\right] , \tag{2.39}$$

where $V(\varphi)$ is some potential depending on the scalar field. The variation of this action with respect to the field variable φ leads to the Klein-Gordon equation,

$$\partial_\mu[\sqrt{-g}g^{\mu\nu}(\partial_\nu\varphi)] = 0 . \tag{2.40}$$

The above equation is the equation of motion of a scalar field φ with the background space-time defined by the metric tensor $g^{\mu\nu}$. Solutions of this equation can give us the information of the background space-time in terms of some physical quantity like temperature. In fact, for a background Schwarzschild black hole, the solutions generate different thermal modes that lead us to Hawking radiation [63]. In Chapter 4, we will study the effect on the scalar field while the background space-time gets corrected.

Vector Field:

A vector field is associated with vector particles of spin 1. One of the most important vector fields in physics is the electromagnetic field, where the corresponding vector particle is the photon. In order to describe the electromagnetic field, we introduce an antisymmetric tensor $F_{\mu\nu}$ whose components are the electric and magnetic field [47]. $F_{\mu\nu}$ can be written as a 4×4 matrix for the electric field $\mathbf{E} = E_1\hat{i}+E_2\hat{j}+E_3\hat{k}$ and the magnetic field $\mathbf{B} = B_1\hat{i}+B_2\hat{j}+B_3\hat{k}$ [47],

$$F_{\mu\nu} = \begin{pmatrix} 0 & -E_1 & -E_2 & -E_3 \\ E_1 & 0 & B_3 & -B_2 \\ E_2 & -B_3 & 0 & B_1 \\ E_3 & B_2 & -B_1 & 0 \end{pmatrix} . \tag{2.41}$$

From the above expression, one can find $F^{\mu\nu}F_{\mu\nu} = 2(B^2 - E^2)$. $F_{\mu\nu}$ is known as electromagnetic field tensor and it can be written in terms of the vector potential A_μ [47],

$$F_{\mu\nu} = \partial_\mu A_\nu - \partial_\nu A_\mu \, . \tag{2.42}$$

If we define the four-current density as j^μ, the action for the electromagnetic field is [47],

$$S = \int d^4x \left[-\frac{1}{4\mu_0} F^{\mu\nu}F_{\mu\nu} + j^\mu A_\mu \right] , \tag{2.43}$$

where μ_0 is the permeability of the free space. Variation of this action provides Maxwell's equations which will be discussed in the Chapter 5. Solutions of Maxwell's equations can give us information about the background space-time in terms of the entropy [64]. We will study the effect on the vector field due to the correction of the background.

Tensor Field:

A tensor field is associated with particles of spin-2 or higher. The gravitational field can be considered as a tensor field though we are yet to find the particles. We assume that the quanta of the gravitational field is a spin-2 particle known as a *graviton* [65]. The action for the gravitational field with matter is simply the Einstein-Hilbert action as shown in equation (2.38). Therefore, without the matter field, the action is [59],

$$S = \frac{1}{16\pi}\int d^4x\sqrt{-g}\,R\,. \tag{2.44}$$

Variation of this action provides the Einstein's equations. The gravitational wave solution is a linearised solution of the Einstein's equations, where the metric tensor $g_{\mu\nu}$ is written as the Minkowskian metric tensor $\eta_{\mu\nu}$ with a small perturbation $h_{\mu\nu}$. Here the background we have considered is a Minkowskian flat space-time. One can also find the gravitational wave solution with a black hole background. The recent detection of a gravitational wave has confirmed that it is possible to get information about background space-time [7] by studying the detected wave. In Conclusion chapter of this thesis, we will discuss the effect on the tensor field with a corrected background. This is a work in progress.

2.4 Schwarzschild Solution

Schwarzschild solution is one of the most important exact solutions of *Einstein's Field Equations* [66]. This static solution portrays a non-rotating electrically neutral spherically symmetric space-time. Let us start with the flat space-time Minkowski metric in spherical coordinates with $c = 1$ described by the equation,

$$ds^2 = -dt^2 + dr^2 + r^2 d\theta^2 + r^2\sin^2\theta\, d\phi^2\,.$$

For the curved space-time, one can generalize the above equation as,

$$ds^2 = -Adt^2 + Bdr^2 + Cr^2 d\theta^2 + Dr^2 \sin^2\theta \, d\phi^2 \ , \tag{2.45}$$

where A, B, C, D are the arbitrary function of the coordinates [67]. Now symmetries of the space-time would impose some constraints in the choice of the coefficients A, B, C, D.

- As the space-time is spherically symmetric, none of the coefficients will depend on θ and ϕ. Moreover, for the angular part of the metric, we can write $C = D = 1$ with our choice of scale.

- The static nature of the space-time indicates that all of the coefficients will be independent of time t and its derivatives. This condition leads us to write $A = A(r)$ and $B = B(r)$.

- The solution is electrically neutral, i.e. uncharged. So, the coefficients will be independent of charge.

- In the vacuum, RHS of the expression (2.37) will vanish leaving,

$$R_{\mu\nu} - \frac{1}{2} g_{\mu\nu} R = 0 \ . \tag{2.46}$$

Thus the constrained metric can be written as,

$$ds^2 = -A(r)dt^2 + B(r)dr^2 + r^2 d\theta^2 + r^2 \sin^2\theta d\phi^2 \ , \tag{2.47}$$

with the metric components,

$$\begin{aligned} g_{00} = -A(r), \qquad & g_{11} = B(r) \\ g_{22} = r^2, \qquad & g_{33} = r^2 \sin^2\theta \ . \end{aligned} \tag{2.48}$$

The inverse of the metric components are given by,

$$\begin{aligned} g^{00} &= -1/A(r), \qquad g^{11} = 1/B(r) \\ g^{22} &= 1/r^2, \qquad g^{33} = 1/(r^2 \sin^2\theta) \; . \end{aligned} \tag{2.49}$$

We will proceed further to calculate the affine connection using equation (2.28) with the metric components given by equations (2.48) and (2.49). After a few lines of calculation, one can easily find the existing Christoffel symbols,

$$\begin{aligned} \Gamma^0_{01} &= \frac{A'}{2A} \\ \Gamma^1_{00} = \frac{A'}{2B}, \quad \Gamma^1_{11} &= \frac{B'}{2B}, \qquad \Gamma^1_{22} = -\frac{r}{2B}, \quad \Gamma^1_{33} = -\frac{r}{2B}\sin^2\theta \\ \Gamma^2_{21} &= \frac{1}{r}, \qquad \Gamma^2_{33} = -\sin\theta\cos\theta \\ \Gamma^3_{31} &= \frac{1}{r}, \qquad \Gamma^3_{23} = \cot\theta \; . \end{aligned} \tag{2.50}$$

Also, using equation (2.30), it can be shown that in this special space-time $R_{\mu\nu}$ exists if $\mu = \nu$. Hence by inserting the values of the Christoffel symbols from equations (2.50), one can write from equation (2.30),

$$\begin{aligned} R_{00} &= -\frac{A''}{2B} + \frac{A'}{4}\frac{B'}{B^2} + \frac{(A')^2}{4AB} - \frac{A'}{rB} \\ R_{11} &= \frac{A''}{2A} - \frac{A'}{2A}\frac{B'}{2B} - \frac{(A')^2}{4A^2} - \frac{B'}{rB} \\ R_{22} &= \frac{rA'}{2AB} - \frac{r}{2}\frac{B'}{B^2} + \frac{1}{B} - 1 = \frac{R_{33}}{\sin^2\theta} \; . \end{aligned} \tag{2.51}$$

Also, from the equation (2.31), it can be obtained,

$$R = -\frac{A''}{AB} + \frac{A'B'}{2AB^2} + \frac{(A')^2}{2A^2B} - \frac{2A'}{rAB} + \frac{2B'}{rB^2} + \frac{2}{r^2}\left(1 - \frac{1}{B}\right) \; . \tag{2.52}$$

Finally gathering all the equations together, Einstein's equations (2.46) provide,

$$\begin{aligned} \frac{B'}{B} - \frac{1}{r}(B-1) &= 0 \\ \frac{A'}{A} - \frac{1}{r}(B-1) &= 0\,. \end{aligned} \tag{2.53}$$

The solutions of the above equations are,

$$\begin{aligned} B &= \frac{1}{1-\frac{X}{r}} \\ A &= 1-\frac{X}{r}\,, \end{aligned} \tag{2.54}$$

with an arbitrary constant X. The value of X can be determined by taking the weak field approximation. For a weak gravitational field, the space-time can be approximated as a Newtonian space-time with the gravitational potential $\frac{GM}{r}$. With this approximation, one finds,

$$X = 2GM \tag{2.55}$$

Therefore, in natural units with $c = G = 1$, the complete Schwarzschild metric defining a spherically symmetric static uncharged non-rotating space-time, known as *Schwarzschild black hole*, can be presented as,

$$ds^2 = -\left(1-\frac{2M}{r}\right)dt^2 + \left(\frac{1}{1-\frac{2M}{r}}\right)dr^2 + r^2 d\theta^2 + r^2\sin^2\theta d\phi^2\,, \tag{2.56}$$

where M is the mass of the black hole. At $r = 2M$, the second term in the equation (2.56) diverges. This is a coordinate singularity of the Schwarzschild metric in this coordinate system. In other coordinate systems such as Eddington-Finkelstein coordinate, this singularity can be omitted [68]. From equation (2.56), for a particle moving radially ($d\theta = d\phi = 0$), it can be seen that for $r < 2M$, the sign of the time component will be positive and that of the radial component will be negative. This implies that the time coordinate becomes real

whereas the radial component becomes imaginary for $r < 2M$. Therefore the region $r < 2M$ can be considered as space-like where two events are not causally connected. Similarly the region $r > 2M$ is time-like, and the $r = 2M$ surface is light-like. These properties of the Schwarzschild black hole is true for any θ and ϕ while the particle is moving radially. The surface at $r = 2M$ is called the *event horizon* of the Schwarzschild black hole. Classically, no information can be received beyond the event horizon. It is to be noted that we found the event horizon considering only the radial geodesic of the particle while setting $d\theta = d\phi = 0$. We can always choose a particular plane of observation where θ is constant, i.e., $d\theta = 0$. In general, for a particle moving in spiral geodesic, $d\phi \neq 0$ as well as $dr \neq 0$. However at the event horizon, the particle will still experience the change of sign in the radial coordinate and will fall in the space-like region. The metric defined by equation (2.56) also diverges at $r = 0$. But this singularity of the geometry cannot be omitted at all, even in other coordinate systems. This singularity is known as the space-time singularity of the black hole [69]. Black holes can be formed when a star collapses and shrinks within its event horizon. A solar mass black hole will be formed if the mass of the sun is confined approximately in three kilometres. A realistic collapse occurs for stars with masses greater than the Chandrasekhar limit [70], whereas primordial black holes can have smaller masses.

2.5 Conclusion

General relativity explains the classical theory of gravity in four dimensional space-time quite nicely. Most importantly it provides the equations that can describe the space-time dynamics theoretically. Now it is time to construct the quantum theory of gravity just like the other fundamental fields [29]. We shall discuss the quantum theory of gravity and semi-classical corrections to classical gravity in the next chapter. We shall then discuss the details of scalar, vector and tensor field propagation on the semi-classically corrected geometries.

Chapter 3

Canonical Quantum Gravity and The Semi-classical Correction

Whether you can go back
in time is held in the grip of
the law of quantum gravity
– Kip Throne

In modern days of physics, general relativistic theory and quantum field theory are the two most useful theories required to describe the fundamental interactions of the universe. General relativity describes how the energy of a system is modifying the curvature of the space-time where quantum field theory describes the physics of a quantum system in the flat space-time. However, the quantum theory of the gravitational field cannot be described by the existing relativistic theory and quantum field theories [71]. Although there is no experimental evidence yet, speaking from the point view of well-accepted mathematical structure, the most prominent quantization approaches of gravity are *String Theory* [72] and *Loop Quantum Gravity* [73]. Quantization of a field can be studied in two schemes: *perturbative approach* and *canonical formulation*. The perturbative approach to quantize gravity in general relativity does not provide a meaningful result as it generates infinite number of divergences in the theory [71]. String theory follows the perturbative approach where the divergences are avoided by considering a string-like particle instead of a point particle [72]. On the other hand, loop quantum gravity follows the canonical quantization

of general relativity. In this thesis, we will follow the framework of loop quantum gravity and hence, will focus on the canonical formulation in this chapter.

Loop quantum gravity predicts that the space has a web-like pattern made of loops. The surface area surrounded by a single loop is $\propto l_p^2$ [74]. John Wheeler and Bryce Dewitt were the first to give the idea of a foam-like space-time structure and formulate the wave function of geometries. This wave function follows a non-trivial equation called the *Wheeler-Dewitt Equation* [75, 76, 77]. One can say that the Wheeler-Dewitt equation is the Schrödinger equation for the gravitational field. However, time was still a problem in this equation as it follows the regular Hamiltonian formulation of general relativity that freezes time. Moreover, this equation is extremely complicated with the regular variables of general relativity. Later, in 1988, Rovelli and Smolin came up with loop-like solutions of the Wheeler-Dewitt equation. They substituted the Einstein's variables with a new set of variables where the field is quantized after constructing the Hamiltonian of the system [78]. These new variables are the phase space variables of loop quantum gravity and they make Wheeler-Dewitt equation mathematically well-behaved. These variables were suggested by A. Ashtekar and are named after him [79].

This chapter is a brief review of the loop quantum theory of gravity based on canonical formulation and also a semi-classical correction will be computed for the Schwarzschild black hole. We will start this chapter with the Hamiltonian formulation of gravity followed by the derivation of the Wheeler-Dewitt equation. Then we will introduce the Ashtekar variables from the Holst action and loop quantum gravity will be discussed briefly. Next we will construct a suitable coherent state for loop quantum gravity. Finally, we will find a semi-classical correction for the coherent state of the Schwarzschild black hole. The effects of this quantum gravity correction will be discussed in the next few chapters.

3.1 Hamiltonian Formulation of General Relativity

In this section we will discuss the classical Hamiltonian formulation of general relativity. We will start with the important work by Arnowitt, Deser and Misner (ADM formalism) [80] on the metric formulation of the four dimensional manifold $\mathcal{M}$. For the canonical formulation on four dimensional space-time, we have to make an assumption that the manifold $\mathcal{M}$ can be decomposed into three dimensional space and one separate time such that $\mathcal{M} = \mathcal{R} \times \xi$. Here the time $t \in \mathcal{R}$ and ξ is the three dimensional manifold without boundary. This is called 3+1 decomposition of the four dimensional manifold [81]. If X^μ defines the coordinates of $\mathcal{M}$, then we can define a three dimensional hypersurface Σ at constant time t such that $\Sigma_t := X_t(\xi)$ with $X_t(x) = X(t,x)$ where x^a are the coordinates of ξ. Therefore X_t can be considered as a map $X_t : \xi \to \mathcal{M}$. The change of vector X^μ with time can be expressed as,

$$\frac{\partial X^\mu(t,x)}{\partial t} = N(X)n^\mu(X) + N^\mu(X) \ , \tag{3.1}$$

where n^μ are the unit normal vectors on Σ_t and $g_{\mu\nu}n^\mu n^\nu = -1$. The coefficient of n^μ, in equation (3.1), is known as the *lapse function* [80]. $N(X)$ has nonzero values everywhere on the hypersurface as $\frac{\partial X^\mu(t,x)}{\partial t}$ is time-like. The vector $N^\mu(X)$ is known as the *shift vector* which is tangential on Σ [80].

As we have defined the manifold $\mathcal{M}$ in a canonical form, the next step is to define the tensor fields on the manifold. Therefore, we introduce the projector $q_{\mu\nu}$ and the extrinsic curvature $K_{\mu\nu}$,

$$\begin{aligned} q_{\mu\nu} &= g_{\mu\nu} + n_\mu n_\nu \\ K_{\mu\nu} &= q^\rho_\mu q^\sigma_\nu \nabla_\rho n_\sigma \ . \end{aligned} \tag{3.2}$$

These two symmetric tensors are known as the *first and second fundamental form* of Σ, respectively [81]. Both of these tensors are spatial as they vanish while contracted with the normal vector n^μ. From the symmetry of the $K_{\mu\nu}$, it can be expressed in terms of the *Lie*

derivative of g [59],

$$\begin{aligned} K_{\mu\nu} &= \frac{1}{2} q^{\rho}_{\mu} q^{\sigma}_{\nu} (\nabla_{\rho} n_{\sigma} + \nabla_{\sigma} n_{\rho}) \\ &= \frac{1}{2} q^{\rho}_{\mu} q^{\sigma}_{\nu} (\mathcal{L}_n g_{\rho\sigma}) \\ &= \frac{1}{2} (\mathcal{L}_n g)_{\mu\nu} \ , \end{aligned} \tag{3.3}$$

where $(\mathcal{L}_n g)$ implies the change in g while it is parallel transported along normal vector n. More details on Lie derivatives can be found in reference [59]. Next we need to construct a covariant derivative for $q_{\mu\nu}$ just like ∇_{ρ} was for $g_{\mu\nu}$. In general relativity, we have seen that the covariant derivative is a combination of partial derivatives and a connection, and also $\nabla_{\rho} g_{\mu\nu} = 0$. Similarly, if we define the new covariant derivative as D_{ρ}, then it should satisfy,

$$D_{\rho} q_{\mu\nu} = 0 \ . \tag{3.4}$$

It should also be commutative such that $D_{\mu} D_{\nu} f = D_{\nu} D_{\mu} f$ for some scalar f. Therefore the reasonable choice for the covariant derivative must be,

$$D_{\mu} \equiv q^{\nu}_{\mu} \nabla_{\nu} \ . \tag{3.5}$$

The covariant derivative operation on a vector u_{ν} is,

$$D_{\mu} u_{\nu} = q^{\sigma}_{\mu} q^{\rho}_{\nu} \nabla_{\sigma} u_{\rho} \ , \tag{3.6}$$

for $u_{\mu} n^{\nu} = 0$.

With all these mathematical tools, we will compute the Riemannian curvature on the foliated manifold. Following the similar approach as in equation (2.25) in Chapter 2, we

introduce the Riemannian curvature $R^{(3)\,\sigma}_{\mu\nu\rho}$ on the three hypersurface Σ,

$$\begin{aligned} R^{(3)\,\sigma}_{\mu\nu\rho} &= D_\mu D_\nu u_\rho - D_\nu D_\mu u_\rho \\ &= [q^{\mu'}_{\mu} q^{\nu'}_{\nu} q^{\rho'}_{\rho} \nabla_{\mu'} q^{\nu''}_{\nu'} q^{\rho''}_{\rho'} \nabla_{\nu''} u_{\rho''} - q^{\nu'}_{\nu} q^{\mu'}_{\mu} q^{\rho'}_{\rho} \nabla_{\nu'} q^{\mu''}_{\mu'} q^{\rho''}_{\rho'} \nabla_{\mu''} u_{\rho''}] \,. \end{aligned} \tag{3.7}$$

It is to be noted that the 'prime' signs are used here in order to refer different coordinates; they are not representing the derivative of the coordinates. The above equation can be simplified using the equations (3.2). Thus it can be written in terms of the extrinsic curvature $K_{\mu\nu}$ and four-curvature $R^{(4)\,\sigma}_{\mu\nu\rho}$ which is our Riemannian curvature in four dimensional geometry as defined in Chapter 2,

$$R^{(3)}_{\mu\nu\rho\sigma} = q^{\mu'}_{\mu} q^{\nu'}_{\nu} q^{\rho'}_{\rho} q^{\sigma'}_{\sigma} R^{(4)}_{\mu'\nu'\rho'\sigma'} + K_{\rho\nu} K_{\mu\sigma} - K_{\rho\mu} K_{\nu\sigma} \,. \tag{3.8}$$

This equation is known as *Gauss equation* [82]. As the three Riemannian curvature is now defined, we can also find the three Ricci scalar,

$$\begin{aligned} R^{(3)} &= R^{(3)}_{\mu\nu\rho\sigma} q^{\mu\rho} q^{\nu\sigma} \\ &= q^{\mu\rho} q^{\nu\sigma} R^{(4)}_{\mu\nu\rho\sigma} + K^{\mu\nu} K_{\mu\nu} - K^2 \,. \end{aligned} \tag{3.9}$$

Again as we have seen in Chapter 2, the four Ricci scalar is $R^{(4)} = R^{(4)}_{\mu\nu\rho\sigma} g^{\mu\rho} g^{\nu\sigma}$. This equation is re-written using the first equation of (3.2),

$$R^{(4)} = q^{\mu\rho} q^{\nu\sigma} R^{(4)}_{\mu\nu\rho\sigma} - [n^\nu \nabla_\mu \nabla_\nu n^\mu - n^\nu \nabla_\nu \nabla_\mu n^\mu] \,. \tag{3.10}$$

The bracketed term, in the above equation, can be expanded using the equations (3.2),

$$[n^\nu \nabla_\mu \nabla_\nu n^\mu - n^\nu \nabla_\nu \nabla_\mu n^\mu] = 2[K^2 - K_{\mu\nu} K^{\mu\nu} + \nabla_\mu (n^\nu \nabla_\nu n^\mu - n^\mu \nabla_\nu n^\nu)] \,. \tag{3.11}$$

Finally, combining the equations (3.9), (3.10) and (3.11), one can find,

$$R^{(4)} = R^{(3)} + (K_{\mu\nu}K^{\mu\nu} - K^2) - 2[\nabla_\mu(n^\nu\nabla_\nu n^\mu - n^\mu\nabla_\nu n^\nu)] \ . \tag{3.12}$$

The above equation is known as the *Codacci equation* and together with equation (3.8), they are called the *Gauss-Codacci equations* [82].

Now it is time to transform the coordinates from the four dimensional manifold $\mathcal{M}$ to the three dimensional manifold ξ. For this purpose, we define a coordinate transformation $X^\mu(X) \to x^a$ such that,

$$X^\mu_{,a}(X) := \frac{\partial X^\mu(x,t)}{\partial x^a}|_{X(x,t)=X} \ . \tag{3.13}$$

As $X^\mu_{,a}(X)$ is tangential to the spatial slice, it is obvious that,

$$n_\mu X^\mu_{,a} = 0 \ . \tag{3.14}$$

With these transformations, we find the spatial metric tensor q_{ab} and the extrinsic curvature K_{ab} of the three hypersurface ,

$$\begin{aligned} q_{ab} &= g_{\mu\nu}X^\mu_{,a}X^\nu_{,b} \\ K_{ab} &= X^\mu_{,a}X^\nu_{,b}K_{\mu\nu} = X^\mu_{,a}X^\nu_{,b}\nabla_\mu n_\nu \ . \end{aligned} \tag{3.15}$$

Thus, the above expressions lead us to write,

$$\begin{aligned} K &= K_{ab}q^{ab} \\ K_{\mu\nu}K^{\mu\nu} &= K_{ab}K_{cd}q^{ac}q^{bd} \ . \end{aligned} \tag{3.16}$$

Now as we have seen in equation (3.3), the extrinsic curvature can be expressed in terms of Lie derivative of g. Similarly in the (x,t) coordinate system, if we define the lapse function

$N(x,t) := N(X)$ and the shift vector $N^a := q^{ab}X^\mu_b g_{\mu\nu}N^\nu$, then the three extrinsic curvature is,

$$K_{ab} = \frac{1}{2N}[\dot{q}_{ab} - (\mathcal{L}_{\vec{N}}q)_{ab}] \ . \tag{3.17}$$

The covariant derivative with the spatial coordinates is given by,

$$D_a u_b = X^\mu_{,a} X^\mu_{,b} D_\mu u_\nu \ , \tag{3.18}$$

from where, with a little bit of algebra, we can easily find that,

$$D_a u_b = \partial_a u_b - \Gamma^c_{ab} u_c \ . \tag{3.19}$$

The connection Γ^c_{ab} is the three affine connection defined on the spatial hypersurface and can be written in terms of spatial metric tensor q_{ab}. Similarly one can write the three Riemannian curvature and Ricci scalar with the spatial coordinates. Therefore, in spatial coordinates, equation (3.12) can be written as,

$$R^{(4)} = R^{(3)} + K_{ab}K^{ab} - (K^a_a)^2 \ , \tag{3.20}$$

where we have used the equation (3.14). Therefore the ADM metric, in (x,t) coordinates, can be expressed as [80],

$$ds^2 = (-N^2 + q_{ab}N^a N^b)dt^2 + 2q_{ab}N^a dx^a dt + q_{ab}dx^a dx^b \ . \tag{3.21}$$

All the mathematical quantities are now defined in the canonical formulation of general relativity. With these tools, we can write the Einstein-Hilbert action defined by equation (2.44) in Chapter 2,

$$S = \frac{1}{16\pi}\int_{\mathcal{R}} dt \int_\xi d^3x\sqrt{q}\ |N|[R^{(3)} + K_{ab}K^{ab} - (K^a_a)^2] \ , \tag{3.22}$$

where $q \equiv \det(q_{ab})$.

In order to construct a canonical form of this theory, we perform a Legendre transformation from the Lagrangian density L to the Hamiltonian density H [83]. The action defines the Lagrangian density L such that, $S = \int_t dt\ L$. Therefore, from equation (3.22), it is easy to write,

$$L = \int d^3x\sqrt{q}|N|[R^{(3)} + K_{ab}K^{ab} - (K^a_a)^2] \ . \tag{3.23}$$

At this point, we can find the canonical momenta of the system for the variables q_{ab}, N, N^a. In this case, the Lagrangian density is not a function of $\dot{N}$ and $\dot{N}^a$. As a result, the canonical momenta corresponding to N and N^a will vanish providing two *primary constraints* in the system,

$$\begin{aligned} \frac{\delta L}{\delta \dot{N}} &= \Pi(t,x) = 0 \\ \frac{\delta L}{\delta \dot{N}^a} &= \Pi_a(t,x) = 0 \ , \end{aligned} \tag{3.24}$$

where Π and Π^a are defined as the canonical momenta corresponding to N and N^a, respectively. However, as K_{ab} is a function of $\dot{q_{ab}}$, the canonical momentum corresponding to q_{ab} is given by,

$$\frac{\delta L}{\delta \dot{q}_{ab}} = \Pi^{ab}(t,x) = \frac{1}{8\pi}\sqrt{q}(K^{ab} - q^{ab}K) \ . \tag{3.25}$$

The Hamiltonian of the system is defined as,

$$H = \int d^3x(\Pi\dot{N} + \Pi_a\dot{N}^a + \Pi^{ab}\dot{q}_{ab}) - L \ . \tag{3.26}$$

After doing some simple algebra, we can find,

$$H = \int d^3x(\Pi\dot{N} + \Pi_a\dot{N}^a + N\mathcal{H} + N_a\mathcal{H}^a) \ , \tag{3.27}$$

where we have defined,

$$\begin{aligned} \mathcal{H} &= -\sqrt{q}R^{(3)} + \frac{1}{\sqrt{q}} G_{abcd}\Pi^{ab}\Pi^{cd} \\ \mathcal{H}^a &= -2D_b\Pi^{ab} \ , \end{aligned} \tag{3.28}$$

with

$$G_{abcd} = \frac{1}{2\sqrt{q}}(q_{ac}q_{bd} + q_{ad}q_{bc} - q_{ab}q_{cd}) \ . \tag{3.29}$$

The first equation of the equations (3.28) is the *Hamiltonian constraint* and the second equation is the *momentum constraint* of the system. The quantity G_{abcd} is known as the *Dewitt metric*[84] . Thus we have defined the manifold $\mathcal{M}$ with the phase space variables (q_{ab}, N, N^a; Π^{ab}, Π, Π^a) at a fixed time t.

In order to find the quantum theory of this canonical formulation, we need to construct the Poisson bracket of these variables [29]. The fundamental Poisson brackets are defined as,

$$\begin{aligned} \left\{\Pi(t,\mathbf{x}), N(t,\mathbf{x}')\right\} &= \delta^3(\mathbf{x}-\mathbf{x}') \\ \left\{\Pi^a(t,\mathbf{x}), N^b(t,\mathbf{x}')\right\} &= q^{ab}\delta^3(\mathbf{x}-\mathbf{x}') \\ \left\{\Pi^{ab}(t,\mathbf{x}), q_{cd}(t,\mathbf{x}')\right\} &= 8\pi\ (\delta^a_c\delta^b_d + \delta^a_d\delta^b_c)\ \delta^3(\mathbf{x}-\mathbf{x}') \ . \end{aligned} \tag{3.30}$$

Using the above relations, one can find the constraints,

$$\begin{aligned} \{\Pi, H\} &= \mathcal{H} \\ \{\Pi^a, H\} &= \mathcal{H}^a \ . \end{aligned} \tag{3.31}$$

Now following the regular quantum mechanical approach, the phase space variables can be

defined in operator form,

$$\begin{aligned} \hat{\Pi} &:= -i\frac{\delta}{\delta N} \\ \hat{\Pi}_a &:= -i\frac{\delta}{\delta N^a} \\ \hat{\Pi}^{ab} &:= -8\pi i\frac{\delta}{\delta q_{ab}} \, . \end{aligned} \tag{3.32}$$

Thus if we define a Hilbert space wave function ψ on this manifold, due to the constraint in the system, ψ will be independent of N and N^a as,

$$\frac{\delta\psi}{\delta N} = \frac{\delta\psi}{\delta N^a} = 0 \, . \tag{3.33}$$

Hence it is obvious that the wave function is only a function of q_{ab}. On the other hand, from the momentum constraint of the system, we can write,

$$\hat{\mathcal{H}}^a\psi(q_{ab}) = 0 \, . \tag{3.34}$$

Considering the second equation of (3.28), the above equation implies,

$$D_b\frac{\delta\psi}{\delta q_{ab}} = 0 \, , \tag{3.35}$$

which means the wave function depends entirely on the induced metric tensor q_{ab} as $D_a q_{bc} = 0$. From the Hamiltonian constraint of the system, we can write,

$$\hat{\mathcal{H}}\psi = 0 \, , \tag{3.36}$$

where the operator $\hat{\mathcal{H}}$ can be computed from the first equation of (3.28). The above equation is known as *Wheeler-Dewitt equation* which describes the dynamics of the system [84]. This equation can be seen as the *Schrödinger equation for the gravitational field*. This equa-

tion has not been solved yet completely.

Problems of Canonical Quantum Gravity:

There are some problems with the canonical approach to quantize gravity. The details of the problems and the probable solutions are discussed in references [30, 85]. Here we will just point out the problems and proceed to the next section.

- One of the main problems with the canonical quantization of general relativity is the *problem of time*. The Wheeler-Dewitt equation is frozen in time as the RHS of the equation (3.36) vanishes unlike the regular form of Schrödinger's equation,

$$\hat{\mathcal{H}}\psi = i\frac{\partial\psi}{\partial t} \ . \tag{3.37}$$

  Thus there is no notion of time and the evolution of the system is frozen. However, the problem of time contains a number of further facts that are associated with other problems. These additional problems are categorized, e.g., sandwich problem, multiple choice problem, global time problem, foliation dependence problem, etc. A detailed discussion can be found in references [30, 85].

- There are some technical problems associated with the Wheeler-Dewitt equation. For example, the operator ordering problem and the regularization problem are two basic problems that can provide different forms of the Hamiltonian operator.[85]

- The mathematical structure of the Hamiltonian operator is quite complicated. We face unavoidable mathematical complicacy while trying to solve equation (3.36) with the canonical variables of general relativity. This is because the quantum operators are highly non-linear in the canonical variables.

The very last problem of the complicated structure of equation (3.36) has been resolved by a pair of new canonical variables proposed by Ashtekar [79]. These new variables yield a

loop-like structure of the space-time. In the next section, we will discuss the new variables as the solution of the *Holst action* [86] and will introduce the loop quantum gravity theory.

3.2 Ashtekar Variables and Loop Quantum Gravity

The Einstein-Hilbert action of general relativity is entirely a function of the space-time metric tensor $g_{\mu\nu}$. There is another formulation of space-time, first proposed by A. Palatini [87], where the metric and the connection are taken as independent variables. In this formulation, the variables are defined as *tetrad* e^I_μ and the corresponding *spin connection* A^{IJ}_μ where,

$$g_{\mu\nu} = e^I_\mu e^J_\nu \eta_{IJ} \ , \tag{3.38}$$

with Minkowskian metric η_{IJ} and $I,\ J = 0,1,2,3$ are the Minkowskian indices. The spin connection A^{IJ}_μ can be defined in terms of covariant derivative of an arbitrary vector V^I in Minkowskian space-time,

$$\mathcal{D}_\mu V_I = \nabla_\mu V_I + A^J_{\mu I} V_J \ . \tag{3.39}$$

Therefore, we can define a curvature $F^{IJ}_{\mu\nu}$ which is a function of spin connections, and also can write an action in terms of the tetrad and curvature. Later in 1995, S. Holst re-wrote the Palatini action with a dual curvature [86] ,

$$S = \frac{1}{2}\int d^4x\, e e^\mu_I e^\nu_J \left(F^{IJ}_{\mu\nu} - \alpha * F^{IJ}_{\mu\nu}\right) , \tag{3.40}$$

where e is the determinant of e^μ_I, α is a complex parameter that depends on the system, $*F$ is the dual of F and defined as, $*F^{IJ}_{\mu\nu} = \frac{1}{2}\varepsilon^{IJ}_{KL}F^{KL}_{\mu\nu}$ with the Levi-Civita operator ε^{IJ}_{KL} [43]. Now we can do a 3+1 decomposition of the tetrad on a three hypersurface Σ such that,

$$e_{0I} = N n_I + N^a e_{aI} \ , \tag{3.41}$$

where N and N^a is our well-known lapse function and shift vector, respectively; n_I is the normalised gradient to the time coordinate and e_{aI} is the *triad* defined as,

$$q_{ab} = e^I_a e^J_b \delta_{IJ} \ . \tag{3.42}$$

With a gauge choice of $e_{a0} = 0$, i.e., $n_I = (1,0,0,0)$, the Holst action, for $t =$ constant surface, is given by,

$$S = \frac{1}{2}\int dt \int d^3x \, \varepsilon^{IJK}\varepsilon^{abc} e_{aI} \, (e_{bJ}\hat{F}_{ctK0} + N^d e_{dJ}\hat{F}_{bcK0} + \frac{1}{2}N\hat{F}_{bcJK}) \ , \tag{3.43}$$

where I,J,K are the Lorentz indices corresponding to the internal space and a,b,c are indices of the three-hypersurface. Here 't' index is the time component corresponding to the spatial indices a,b,c; whereas '0' is the time component corresponding to Lorentz indices I,J,K.

If we redefine the variables as $E^a_J = e e^a_J \alpha$ and write the curvature explicitly in terms of connection, then the following time derivative can be identified from equation (3.43),

$$E^{aJ}\partial_t(\alpha \, A_{aJ0} - \frac{1}{2}\varepsilon_{JMN}A^{MN}_a) \neq 0 \tag{3.44}$$

Therefore, we can redefine the bracketed term of the above equation as,

$$\alpha \, \tilde{A}_{aJ} = \alpha \, A_{aJ0} - \frac{1}{2}\varepsilon_{JMN}A^{MN}_a \tag{3.45}$$

One can also find,

$$\begin{aligned} A_{aIJ} &= -\varepsilon_{IJK}\Gamma^K_a \\ A_{aI0} &= K_{aI} \ , \end{aligned} \tag{3.46}$$

where Γ_a^K is the solution of,

$$\mathcal{D}_a e_b^J = D_a e_b^J + A_{aI}^J e_b^I = 0 \ . \tag{3.47}$$

D_a is defined in equation (3.19). Therefore, defining $\tilde{A} := A$, we can write the new canonical variables as,

$$\begin{aligned} A_a^I &= \Gamma_a^I - \tilde{\beta} K_{ab} e^{Ib} \\ E_I^a &= \frac{1}{\tilde{\beta}} (\det e) e_I^a \ , \end{aligned} \tag{3.48}$$

where $\tilde{\beta} = \frac{1}{\alpha}$ is known as *Immirzi parameter*. In principle, it can take any non-zero value [88]. However, in this thesis, it is set to 1, which makes the connection A real valued. The variables defined in equations (3.48) are the Ashtekar variables that are the basis variables in loop quantum gravity. This is a SU(2) representation of gravity with SU(2) connection A_a^I and densitized triad E_I^a [82].

Now for the Hamiltonian formulation, the constrained equations should be computed. With the variables discussed above, one can write the constrained equations,

$$\begin{aligned} G_I(E) &= \mathcal{D}_a E_I^a \ , \\ V_a(A,E) &= E_I^b F_{ab}^I \ , \\ H(A,E) &= \varepsilon^{IJK} E_I^a E_J^b F_{abK} - 2\frac{\tilde{\beta}^2+1}{\tilde{\beta}^2} (E_I^a E_J^b + E_J^a E_I^b)(A_a^I - \Gamma_a^I)(A_b^J - \Gamma_b^J) \ , \end{aligned} \tag{3.49}$$

where F is the curvature of the three hypersurface. Here G_I is the *Gauge constraint* corresponding to the SU(2) gauge introduced with the triads, V_a is the *diffeomorphism constraint* that generates diffeomorphism on the spatial slice Σ, and H is the *Hamiltonian constraint* that generates diffeomorphism orthogonal to Σ [89]. As the Hamiltonian of general rela-

tivity vanishes on the constraint surface, one can write in natural units,

$$H_{grav}[N,N^A,A,E] = \frac{1}{8\pi}\int_\Sigma NH(A,E) + N^a V_a \ , \tag{3.50}$$

where N and N^a are the lapse function and shift vector respectively.

Now in equation (3.50), the new variables are integrable in metric independent way and hence able to form more feasible functionals to deal with in the phase-space. For that we obtain a discretised manifold. The discretisation is done using graphs connecting vertices with edges e. It is to be noted that the triad e_I is different from the edge e.

Definition 3.1. The *edge* e in Σ is defined as an equivalence class of analytic maps [0,1] $\rightarrow$ Σ. Two maps will be equivalent if they can be re-parametrized by preserving the orientation [82].

An edge e generates from the *vertex* $e(0)$ and converges to the ending vertex $e(1)$. A *graph* γ on Σ is defined as the set of edges where two distinct edges intersect at most their endpoints. Set of edges on a graph γ is denoted by $E(\gamma)$ where set of vertices are denoted by $V(\gamma)$.

Therefore the phase space variables are defined as,

$$h_e(A) = \mathcal{P}\exp(\int_e A.dx) \tag{3.51}$$

$$P_e^I = \int_S E.dS \ . \tag{3.52}$$

The first variable $h_e(A)$ is known as *holonomy* and the corresponding momentum is defined by the variable P_e^I. Here $\mathcal{P}$ stands for path-ordering the power expansion of the exponential such that the connection variables are ordered from left to right with the parameter along the edge on which they depend increasing.

The holonomy is a SU(2) matrix variable and can be compared to the 'position' of the quantum mechanics. Therefore, it can also be treated like a 'position operator' which

is the quantum representation of the variable 'position'. Under SU(2) gauge, holonomy transforms as,

$$h_e(A) \to h_e^g(A) = g(e(0))h_e(A)g^{-1}(e(1)) \ . \tag{3.53}$$

Also it follows the following algebraic properties,

$$h_{e_1 \circ e_2}(A) = h_{e_1}(A)h_{e_2}(A), \tag{3.54}$$

$$h_{e^{-1}}(A) = h_e^{-1}(A) \ . \tag{3.55}$$

In order to find basis eigenstate of the holonomy such that the holonomy operator will act as a multiplicative operator, we have to take the basis as the functions of the holonomy. Therefore, one can consider a suitable SU(2) representation given by $\Pi^j_{mn}(h(e))$ [90]. Here j labels the SU(2) representation, $m,n = -j..+j$. These can be understood, in analogy with angular momentum eigenstates, as SU(2) is isomorphic to SO(3). The angular momentum L^2 has eigenvalues $j(j+1)$ in the jth eigenstate, and the $L_x \pm iL_y$, raise and lower the L_z eigenvalues from $-j..+j$. In SU(2) group, the j is allowed to have half integer values, and each representation has dimensions $(2j+1)\times(2j+1)$. The basis states for one edge can also be labelled as $|jmn>$ in the Dirac notation.

In analogy to the quantization of N harmonic oscillator, we can build a complete set of states from the vacuum by using 'creation operators' (the operators which are $\Pi^j_{mn}(h(e))$). One can write the creation operator corresponding to the holonomy as follows,

$$(d_{j_1}\Pi^{j_1}_{m_1 n_1}(e_1))...(d_{j_N}\Pi^{j_N}_{m_N n_N}(e_N))|\psi> \ , \tag{3.56}$$

where $d_j = \sqrt{2j+1}$ and we have assumed all edges (e) are different.

The states where the edges meet in vertices, can be defined as *spin network* functions $|T_{\{j,m,n;;graph\}}>$. This spin network states form an orthonormal basis in the Hilbert space. They are built by using *intertwiners* at the vertices such that the vertices have trivial repre-

sentation of SU(2) group action. The inner product of spin network states are given by,

$$< T_{\{j,m,n;graph\}} | T_{\{j',m',n';graph'\}} >= \delta_{graph,graph'} \prod_e \delta_{j_e,j_{e'}} \prod_e \delta_{m_e,m_{e'}} \prod_e \delta_{n_e,n_{e'}} \ , \qquad (3.57)$$

where $\prod_e$ implies the products over all the edges e.

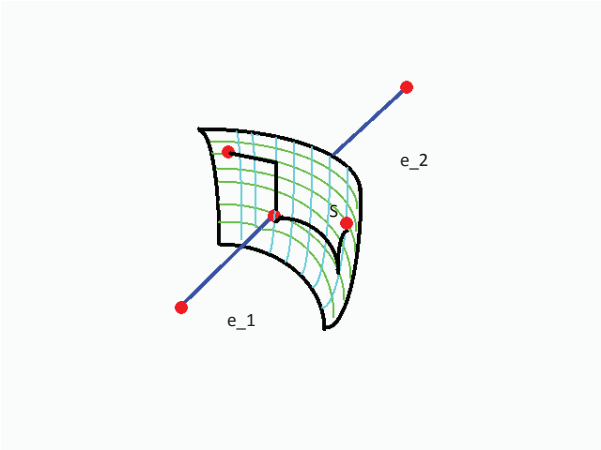

Figure 3.1: Edge intersecting surface S [91].

Next we will see the how the momentum operator acts on the spin network. If we take one edge, then,

$$P_e(S)\Pi^j_{mn}(e)|\psi> \propto L^{e_1}_e(\Pi^j(e_1)\Pi^j(e_2))_{mn}|\psi> + R^{e_2}_e(\Pi^j(e_1)\Pi^j(e_2))_{mn}|\psi> \ , \qquad (3.58)$$

where we have divided the edge into two edges e_1 and e_2. Here L and R are the left and right invariant derivatives respectively. The square of these operators when acting on the spin networks have eigenvalues $j(j+1)$, if the system is in the jth representation of SU(2).

Using this, area operator of a surface can be written as,

$$A_r(s) = \lim_{\text{partition}\to S} \Sigma_{\text{plaquets in S}} \sqrt{\Sigma_l E_l^2} \ , \qquad (3.59)$$

where a surface has been divided into smaller plaquets intersected by the edges.

It can shown that the area operator has discretized spectra proportional to $j(j+1)l_p^2$. In this section, we have discussed only those topics of loop quantum gravity, that will be useful for further progress of this thesis. More details on loop quantum gravity can be found in reference [92]. Next we will proceed to the section where we will study the coherent states in loop quantum gravity.

3.3 Kinematical Coherent States in Loop Quantum Gravity

Our aim is to study the quantum fluctuation effect on the system that can be observed physically. In order to accomplish that, we choose a state, with minimum uncertainty, called a *coherent state*. In quantum theory, coherent states of an operator are described as semi-classical states which are closest to the classical expectation value of the operator. Loop quantum gravity coherent states should be the states with minimum uncertainty peaked at classical values of the h_e and P_e^I for one edge. Excitation to the coherent states in loop quantum gravity represent the graviton state [82].

Usually for a quantum harmonic oscillator, coherent states are introduced as eigenstates of annihilation operator [29]. In order to define a suitable annihilation operator of a linear system, a Hamiltonian should be defined. However, in loop quantum gravity we neither have a linear system, nor a proper Hamiltonian. Thus we need a different strategy in order to construct a reasonable coherent state in this theory.

For an n-dimensional harmonic oscillator of mass m and angular frequency ω, we can define the Hamiltonian as,

$$H = \left(\frac{p^2}{2m} + \frac{1}{2}m\omega^2 x^2\right) = \omega z\bar{z}\,, \tag{3.60}$$

where the annihilation function is z and the creation function is $\bar{z}$. The annihilation function can be expressed as,

$$z = \frac{1}{\sqrt{2}}\left(\sqrt{m\omega}\,x - \frac{ip}{\sqrt{m\omega}}\right)\,. \tag{3.61}$$

In quantum mechanics, the annihilation operator is expressed as,

$$\hat{z} = \frac{\sqrt{m\omega}}{\sqrt{2}} \sum_n \frac{(-i)^n}{n!} \frac{[\hat{C}, \hat{x}]_n}{(i\hbar)^n} \ , \tag{3.62}$$

where complexifier $\hat{C} = \frac{\hat{p}^2}{2m\omega}$. Now we define a state ψ such that,

$$\psi_x := e^{-t\hat{C}/\hbar^2} \delta_x \ , \tag{3.63}$$

with the classical parameter $t := -\frac{\hbar}{m\omega}$ and δ_x is the eigen-distribution of the operator $\hat{x}$. Next we extend ψ_x in the complex plane by transforming $x \to x - \frac{ip}{m\omega}$ such that $\psi_{x-\frac{ip}{m\omega}} \to \psi_z$. Under the annihilation operator we will get,

$$\hat{z}\psi_z = z\psi_z \ . \tag{3.64}$$

Therefore ψ_z is the expected coherent state of the system which is a eigenstate of the annihilation operator.

For loop quantum gravity, we will need to find the SU(2) annihilation operator and the coherent state in a similar method. The annihilation operator is found to be [82],

$$\hat{g}_e = \sum_n \frac{(-i)^n}{n!} [\hat{C}, \hat{h_e}]_n = e^{-\frac{\tilde{t}(T^I)^2}{8}} e^{-\frac{iT^I \tilde{P}_e^{Icl}}{2}} \hat{h}_e^{cl} \ , \tag{3.65}$$

where the superscript '*cl*' represents the classical value of the corresponding variable, T^I are the SU(2) basis, i.e., the Pauli matrices, $\tilde{t} = \frac{l_p^2}{a}$ is a semi-classical parameter that depends on a dimensional constant a characterizing the system. For the Schwarzschild black hole, a is taken to be the square of the radius of the event horizon r_g and hence $\tilde{t} = \frac{l_p^2}{r_g^2}$. Therefore, in momentum representation, the coherent state for one edge is given by,

$$|\psi^{\tilde{t}}(g_e)> = \sum_{jmn} e^{-\tilde{t}j(j+1)/2} \pi_j(g_e)_{mn} |jmn> \ . \tag{3.66}$$

In the above equation, $|jmn>$ represent the spin network states where j is the quantum number of SU(2) Casimir operator and m,n are the azimuthal quantum numbers running from $-j$ to j. However, the coherent states peaked at h_e^{cl} and $P_e^{I_{cl}}$ with the maximum probability and the fluctuations from the exact classical values are controlled by a semi-classical parameter $\tilde{t}$. In the classical limit $\tilde{t} \to 0$, the coherent states perfectly coincide with the classical values. Details of the above calculation is shown in reference [82]. A schematic diagram of the probability amplitude of a SU(2) coherent state, as decribed in equation (3.66), is shown in Figure 3.2. In Figure 3.2, it can seen that the coherent state is peaked up with maximum probablity at $\tilde{t} = 0$. Even though the annihilation operator has not been

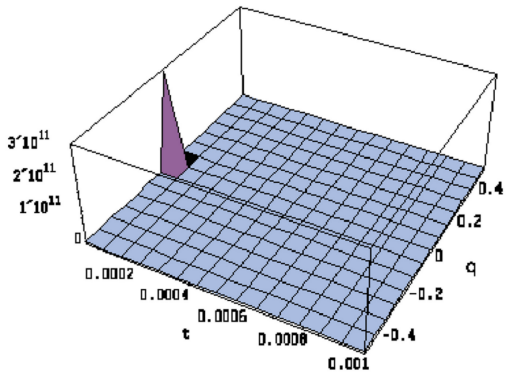

Figure 3.2: An SU(2) coherent state [93].

constructed from a physical Hamiltonian, the coherent state in equation (3.66) is the most suitable choice for now. The properties of coherent states including over-completeness, peakedness, expectation value, small fluctuation and Ehrenfest properties have been proved for this choice [94, 95, 96]. Therefore, we can consider equation (3.66) as our required coherent state and we will find a semi-classical correction in this coherent state in the next section.

3.4 Semi-classical Correction in Schwarzschild Space-time: New Result

In order to find the semi-classical fluctuation in the classical expectation value we use the coherent state defined in equation (3.66). The expectation value for the momentum with the first order correction in $\tilde{t}$ is given by,

$$< \psi^{\tilde{t}} | \hat{P}_e^I | \psi^{\tilde{t}} >= P_e^I (1 + \tilde{t} \tilde{f}(P)) \, , \tag{3.67}$$

where $\tilde{f}(P)$ is the function of gauge invariant momenta $P_e = \sqrt{P_e^I P_e^I}$ and given by [36],

$$\tilde{f}(P_e) = \frac{1}{P_e} \left(\frac{1}{P_e} - \coth(P_e) \right) \, . \tag{3.68}$$

Details of the function $\tilde{f}(P)$ is provided in reference [36] and it was also shown that the coherent states is defined on Lemaitre slicing of the Schwarzschild space-time. Thus we start with the metric [97],

$$ds^2 = -d\tau^2 + \frac{dR^2}{\left[\frac{3}{2r_g} (R - \tau) \right]^{2/3}} + \left[\frac{3}{2} (R - \tau) \right]^{4/3} r_g^{2/3} (d\theta^2 + \sin^2 \theta d\phi^2) \, , \tag{3.69}$$

where these coordinates are related with the Schwarzschild coordinates such that,

$$\begin{aligned} \sqrt{\frac{r}{r_g}} dr &= (dR \pm d\tau) \, , \\ dt = \frac{1}{1 - f^2} (d\tau \pm f dR), \qquad & f = \left(\frac{2 r_g}{3(R - \tau)} \right)^{2/3} \, . \end{aligned} \tag{3.70}$$

Now, with the limit that the area of the two-surface goes to zero, from equation (3.52), one can approximate the integration over two-surface S_e,

$$P_e^I = S_e E_e^I \, . \tag{3.71}$$

From the relation (3.42) and the second equation of (3.48) with $e = \sqrt{q}$,

$$qq^{ab} = E^{aI}E^{bI} = \frac{P^I_{e_a}}{S_{e_a}}\frac{P^I_{e_b}}{S_{e_b}} \ . \tag{3.72}$$

Therefore, it is obvious that,

$$q = \det\frac{P^I_{e_a}}{S_{e_a}} = P \ . \tag{3.73}$$

The above equations lead us to write,

$$q^{ab} = \frac{1}{P}\frac{P^I_{e_a}}{S_{e_a}}\frac{P^I_{e_b}}{S_{e_b}} \ . \tag{3.74}$$

Thus in order to find the correction in the metric, we need to calculate the expectation value,

$$< \psi|\frac{P^I_{e_a}}{S_{e_a}}\frac{P^I_{e_b}}{S_{e_b}}|\psi > \ . \tag{3.75}$$

It is to be noted that the indices a, b take values 1,2,3 corresponding to the coordinates r', θ, ϕ respectively. For now, we focus on the corrections to $(r,\ t)$ sector of the metric; however, there will be corrections for θ and ϕ coordinates as well. One can write the radial component of the intrinsic metric with induced radial coordinate r' as,

$$q^{r'r'} = \frac{1}{P}\left[\left(\frac{P_{e'_r}}{S_{e'_r}}\right)^2 + 2\tilde{f}\tilde{f}\left(\frac{P_{e'_r}}{S_{e'_r}}\right)\frac{P_{e'_r}}{S_{e'_r}}\right] \ , \tag{3.76}$$

where $P_{e'_r} = \sqrt{P^I_{e'_r}P^I_{e'_r}}$. In the limit $S_{e'_r} \to 0$, using the equation (3.72), the momentum can be approximated as,

$$P_{e'_r} = \frac{2r'^2\sin\theta\delta\theta\delta\phi}{r_g^2} \ , \tag{3.77}$$

where $S_{e'_r} = 2\delta\theta\delta\phi$. It is to be noted that the infinitesimal surface is not a function of $\sin\theta$. This implies that the surface is not bounded to be spherical anymore. Moreover, in the region $r > r_g$, the correction function $\tilde{f}(P_{r'}/S_{e'_r}) \approx 1/(P_{r'}/S_{e'_r})$. The cross-term metric such

as $q^{r'\theta}$ or $q^{r'\phi}$ will be equal to zero and no correction will survive as $P_{e_a} \cdot P_{e_b} = 0$. In order to visualize the correction in the Schwarzschild coordinate, a coordinate transformation has been done where the metric components transform like,

$$\begin{aligned} g^{tt} &= \frac{dt}{d\tau}\frac{dt}{d\tau}g^{\tau\tau} + \frac{dt}{dR}\frac{dt}{dR}g^{RR} \\ g^{rr} &= \frac{dr}{d\tau}\frac{dr}{d\tau}g^{\tau\tau} + \frac{dr}{dR}\frac{dr}{dR}g^{RR} \\ g^{rt} &= \frac{dr}{d\tau}\frac{dt}{d\tau}g^{\tau\tau} + \frac{dr}{dR}\frac{dt}{dR}g^{RR} \,. \end{aligned} \tag{3.78}$$

From equations (3.70), one can obtain,

$$\begin{aligned} \frac{dt}{d\tau} &= \frac{1}{1-f^2}, \qquad \frac{dt}{dR} = \pm\frac{1}{1-f^2}\left(\frac{2r_g}{3(R-\tau)}\right)^{2/3}, \\ \frac{dr}{dR} &= \sqrt{\frac{r_g}{r}}, \qquad \frac{dr}{d\tau} = \pm\sqrt{\frac{r_g}{r}} \,. \end{aligned} \tag{3.79}$$

Finally considering equations (3.79) and equations (3.78) together, we get the correction in metric component g^{tr} as,

$$g^{tr} = \pm 2\frac{1}{1-f^2}\left(\frac{r_g}{r}\right)^{3/2}\tilde{t}\tilde{f}\left(\frac{P_{e_r}}{S_{e_r}}\right) \,. \tag{3.80}$$

Thus a nonzero g^{tr} term has been added to the Schwarzschild metric. Clearly, this cross metric component exists due to the nonzero value of the function $\tilde{f}\left(\frac{P_{e_r}}{S_{e_r}}\right)$. It is also to be noted that $\tilde{f}\left(\frac{P_{e_r}}{S_{e_r}}\right)$ is a non-linear function of $\sin\theta$ according to the equation (3.68) and hence, it breaks the spherical symmetry of the Schwarzschild space-time. The inverse metric component of g^{tr} is given by $g^{tr}/(g^{tt}g^{rr})$. For the Schwarzschild coordinate, as $(g^{tt}g^{rr}) = 1$, the inverse component remains in the same form as g^{tr}. However, the corrections in other cross terms like $g_{r\theta}, g_{r\phi}$ etc. will vanish due to the choice of gauge. Also, it must be noted that even though we discuss this specific correction, obtained from the Hall coherent states in loop quantum gravity, our calculations will be true for any such g_{tr} term generated by

quantum fluctuations. These fluctuations can arise from various other approaches to quantisation. Now we shall briefly analyse what this correction implies.

3.4.1 Static and Spherical Metrics

In most discussions of quantum corrected collapse one addresses the spherically symmetric metrics, and those which are static. Let us recollect what the static metric is and what we mean by spherical symmetry. A metric is said to be stationary if the metric has isometries whose orbits are asymptotically time-like. This signifies the existence of a *Killing vector* ξ which generates these isometries [1],

$$\mathcal{L}_\xi g_{ab} = 0 \ . \tag{3.81}$$

If in addition there exists spatial hyper surfaces Σ which are orthogonal to the Killing orbits, the space-time is said to be static. This also translates to the condition of hypersurface orthogonality using Frobenius theorem [81].

$$\xi_{[a} \nabla_b \xi_{c]} = 0 \ , \tag{3.82}$$

If the Killing parameter is used as a time coordinate 't', then $\xi = \frac{\partial}{\partial t}$ and the space-like hypersurfaces orthogonal to the orbits of the Killing vector are described using coordinates of x^1, x^2, x^3. The metric appears as

$$ds^2 = -g_{tt}\, dt^2 + g_{ij}\, dx^i dx^j \ . \tag{3.83}$$

The spherical symmetry is imposed by requiring that the metric has SO(3) isometries, and that implies component g_{tt} is a function of r . The g_{ij} can be written in spherical coordinates as:

$$g_{rr}(r) dr^2 + r^2 (d\theta^2 + \sin^2\theta d\phi^2) \ . \tag{3.84}$$

3.4.2 Non-static Space-time

Relaxing the requirement of hypersurface orthogonality, one obtains the 'stationary metric'

$$ds^2 = -\left(g_{tt}dt - \omega_i dx^i\right)^2 + h_{ij}dx^i dx^j \ , \tag{3.85}$$

with the introduction of a 'twist vector' ω_i. The Kerr metric has a non-zero ω_ϕ and this shows the origin of rotation.

It is therefore interesting that in [36], the first order correction to the metric due to semi-classical corrections was found to generate a twist term in the metric. The g_{tr} term in the metric was exactly shown to have a form:

$$g_{tr} = \pm\frac{1}{1-\frac{r_g}{r}}\left(\frac{r_g}{r}\right)^{3/2}\tilde{t}\tilde{f} \ . \tag{3.86}$$

It is interesting that as $r \to r_g$ the g_{tr} as in (3.86) becomes finite, as the ratio $\frac{\tilde{t}}{(1-r_g/r)}$ is a ratio of two small numbers. However, the metric is singular at the horizon; therefore overall the correction is still a fluctuation at the horizon.

Thus we can sufficiently conclude that the first order fluctuations of the metric break the static nature of the Schwarzschild metric.

3.4.3 Non-spherical Space-time

The function $\tilde{f}$ in [36] was found to be

$$\tilde{f} = \frac{1}{P_e}\left(\frac{1}{P_e} - \coth(P_e)\right) \ , \tag{3.87}$$

where $P_e = \frac{r^2}{r_g^2}\sin\theta$ and thus a function of θ. The θ dependence in (3.86) thus breaks the spherical symmetry of the original metric. At this order of the semi-classical fluctuations no other twist is created [36]. However this single correction term spontaneously breaks the spherical symmetry and static nature of the metric.

3.4.4 The Strain

It is interesting that the above correction (3.86) can be interpreted as an effective quantum 'strain' on the metric. This is similar to the 'strain' caused when a gravity wave passes through a given background. The strain due to a 'fluctuation' is:

$$e_{ij} = \frac{1}{2}\left(g'_{ij} - g_{ij}\right) \ , \tag{3.88}$$

Therefore the 'fluctuation strain' is:

$$e_{tr} = \pm\frac{1}{2}g_{tr} \ . \tag{3.89}$$

If we are far away from the black hole, as would be on the Earth, we can compute the strain, as $\tilde{f}(P_e) \approx -\frac{1}{P_e} = -\frac{r_g^2}{r^2 \sin\theta}$. Using the specifications of the 'merged black hole' in LIGO [7]; $r = 1.3$ billion light years=1.23×10^{25}m, $r_g = 2GM = 1.57 \times 10^{22}$ m, this strain is computed to be,

$$e_{tr} = 7.67 \times 10^{-125}\text{cosec}\theta \ . \tag{3.90}$$

The order 10^{-125} suggests a relation to the cosmological constant [98], and it might be that the cosmological constant arises due to semi-classical fluctuations of the cosmological metric. This interesting aspect has to be investigated further.

This number is way smaller than the observed strain 10^{-21}, the amplitude of the gravity wave strain observed in LIGO. However, it has the same magnitude as observed in similar calculations of quantum corrections to gravity wave dispersion [99].

As we see that due to the nature of the correction, there is a cosecθ in the strain, which is rather strange. This term appears due to the $1/P_e$ form in the correction, which cannot be expanded in a spherical harmonic anymore. The g_{tr} strain has been obtained in a particular coordinate as expressed in equation (2.56). Therefore, the divergence of the $\csc\theta$ is a coordinate artefact. If we look at $g^{\phi\phi} = r^2 \csc^2\theta$, that also diverges at the poles. Exactly in

the same way, our strain seems to be divergent. If we smear the strain over a small surface, then we get a finite answer,

$$\int g_{tr} dS_r = \int g_{tr} \sin\theta d\theta d\phi \ . \tag{3.91}$$

From the above equation the strain would be finite as the $\csc\theta$ factor cancels.

3.5 Conclusion

In this section we briefly introduced the loop quantum gravity phase space from the canonical formulation of general relativity. The new result, we have found, is a semi-classical correction which is breaking the spherical symmetry of the Schwarzschild space-time. We have also computed a strain which is significantly smaller than our latest experimental ability. However, a small perturbation can generate a chaotic system in the unstable orbit of a black hole. A system of super-massive binary black holes might generate an observable strain effect. We have started our work by studying the effect in Schwarzschild black hole background as it is one of the simplest space-times. Starting in the next chapter, we will discuss the effect of this semi-classical correction in scalar, vector and tensor fields. As the correction is finite near the event horizon, it might generate a non-trivial effect around $r \to r_g$. Hence we will be studying the fields in near-horizon limit.

Chapter 4

Effect on The Scalar Field

The greatest enemy of knowledge is not ignorance,

it is the illusion of knowledge

– S. Hawking

Observing a quantum gravity effect in the real universe, is one of the most challenging tasks in modern experimental physics. With the discovery of the detectable quantum gravity effect, one can verify the quantization of gravity. Length scale of quantum gravity effects are around Planck length, very small to detect directly even with the latest model of accelerators. However, there are some recent searches for evidences of quantum gravity in observable astrophysical phenomena such as gamma ray bursts [100]. A particular astrophysical scenario where the loop quantum gravity fluctuation around the unstable orbits of the Schwarzschild black hole may give rise to a detectable effect [36] was discussed previously.

In this specific chapter, we will numerically analyse scalar field propagation with the same quantum gravity correction in the Schwarzschild black hole background predicted in the last chapter. The correction term will break the spherical symmetry of the classical Schwarzschild space-time. Even though the corrections are infinitesimal, it may produce an observable effect because of the non-linearity of the Einstein's evolution equations. The scalar field evolution in the black hole background generates different mode of thermal radiation called Hawking radiation [63]. Observational evidence of Hawking radiation has been claimed

by some researchers [38]. However the claim is still unverified. The semi-classical correction in the Schwarzschild black hole should affect the scalar field, and hence should affect the Hawking radiation as well. This result can be verified by a confirmed detection of the Hawking radiation. This entire chapter will follow the work given in the references [93] and [36].

We will start with the Klein-Gordon equation that describes a scalar field in quantum field theory [29]. The correction in background space-time will contribute an extra term in the classical Klein-Gordon equation. We will consider a toy model in order to solve the Klein-Gordon equation and numerically solve the toy model equation using the programming language RNPL [101, 102]. The output of the numerical analysis has been be plotted using XVS visualizing software [101, 102] and mathematica. We will compare the plots with and without the corrections, and will discuss the outcomes.

4.1 Corrected Scalar Field Evolution

The loop quantum gravity correction in the Schwarzschild metric affects the scalar field propagation in the black hole background. The effect can be studied by analysing the Klein-Gordon equation in the corrected Schwarzschild space-time. For the massless scalar field φ the equation can be written as,

$$\frac{1}{\sqrt{-g}}\partial_\mu(\sqrt{-g}g^{\mu\nu}\partial_\nu\varphi) = 0\ . \tag{4.1}$$

Now in the determinant of the metric g, the correction can be neglected as it is $O(\tilde{f}^2)$. However, the equation (4.1) can be expanded and given by,

$$-\partial_t^2\varphi + 2g^{tr}\partial_t\partial_{r^*}\varphi + \frac{1}{r^2}\partial_{r^*}(g^{tr}r^2)\partial_t\varphi + \partial_{r^*}^2\varphi + \left(1-\frac{r_g}{r}\right)\nabla_{\theta\phi}\varphi = 0\ , \tag{4.2}$$

where r^* is defined in Eddington-Finkelstein coordinate as $\frac{dr^*}{dr} = \frac{1}{1-r_g/r}$, $\nabla_{\theta\phi}$ contains the angular derivative terms [103].

Now in the limit, $r \to r_g$, the last term in equation (4.2) drops out leaving the equation without any angular derivative. Thus with the near horizon limit of a Schwarzschild black hole, the scalar field acts like the scalar field in a flat space-time with a *shift* term. In equation (4.2), the shift term comes due to the nonzero value of g^{tr}. Therefore, it is reasonable to discuss the solution of the Klein-Gordon equation for the scalar field propagation with a shift. This is where we will introduce the numerical method to solve the equations.

Numerical analysis is an extremely effective method to solve non-trivial differential equations. Very few problems of physics are exactly solvable even with the symmetries. Numerical methods provide us solutions for the problems, which are not exactly solvable, with an acceptable scale of precision. In the classical theory of general relativity, scalar gravitational collapse has already been studied by people using numerical relativity techniques [104, 105]. It has also been found that for the scalar field time evolution, there is a characteristic parameter p which is associated with the initial data. For some critical value of the parameter p^*, the scalar field will escape to infinity if $p < p^*$, otherwise it will collapse to a black hole. This universal scaling characteristic is also assigned with the mass of the black hole such that $M_{BH} \sim |p - p^*|^\gamma$ with an universal constant $\gamma \approx 0.37$. This scaling feature was first observed numerically by Choptuik and known as Choptuik scaling [106]. Here we will briefly discuss the scalar field evolution equations that are used in the numerical calculation. Let us consider a general ADM metric [80],

$$ds^2 = (-\alpha^2 + a^2\beta^2)dt^2 + 2\alpha^2\beta dt dr + a^2 dr^2 + r^2 b^2 d\Omega^2 \ , \tag{4.3}$$

where $d\Omega^2 = d\theta^2 + \sin^2\theta d\phi^2$, a and b are functions of both r and t, and β is a function of the radial coordinate only. Comparing the above equation to the equation (3.80), it can be concluded that the shift term β in the above equation is representing the correction term of the Schwarzschild metric. In the near horizon limit, the equation of motion for the scalar

field given by equation (4.2) is modified to the the following equations:

$$\begin{aligned} \partial_t \Phi &= \partial_r \left(\beta \Phi + \frac{\alpha}{a} \Pi \right) \\ \partial_t \Pi &= \frac{1}{r^2} \partial_r \left(r^2 \left(\beta \Pi + \frac{\alpha}{a} \Phi \right) \right) , \end{aligned} \tag{4.4}$$

where ,

$$\begin{aligned} \Phi(r,t) &= \partial_r \varphi \\ \Pi(r,t) &= \frac{a}{\alpha} (\partial_t \varphi - \beta \partial_r \varphi) . \end{aligned} \tag{4.5}$$

In Chapter 3, we have seen that for the canonical formalism of general relativity, the dynamics of the space-time are given by the Hamiltonian and momentum constraints. These constraints provide three independent time evolution equations for the variable a and the extrinsic curvatures of the space-time [101],

$$\begin{aligned} \dot{a} &= -\alpha a K_r^r + (a\beta)' \\ \dot{K_r^r} &= \beta K_r^{r'} - \frac{1}{a} \left(\frac{\alpha'}{a} \right)' + \alpha \left(\left(\frac{-2}{ra^2} \right)' + K K_r^r - 8\pi \frac{\Phi^2}{a^2} \right) \\ \dot{K_\theta^\theta} &= \beta K_\theta^{\theta'} + \frac{\alpha}{(rb)^2} - \frac{1}{a(rb)^2} \left(\frac{\alpha r}{a} \right)' + \alpha K K_\theta^\theta , \end{aligned} \tag{4.6}$$

where K_r^r and K_θ^θ are the components of extrinsic curvature and K is the trace of the extrinsic curvature. It is important to note that the shift term β in the metric (4.3) is a function of r only, where our correction term g^{tr} is a non-trivial function of both r and θ. Hence there will be an extra evolution equation for $K_{r\theta}$ as well. Numerically, coding all of these equations in three dimension is quite complicated. Hence we have decided to proceed step by step starting with one dimensional equation with a r dependent β. In the next section, we will study a toy model where we visualise the effect of the shift term in the one dimensional scalar wave equation.

4.2 Numerical Solution: New Result

This numerical calculation has been computed in the RNPL programming language, and visualized using XVS software [101, 102] and mathematica. The details of this programming method has been discussed in Appendix A. In any numerical theory, the most important job is to discretize the equations with proper boundary conditions. In this thesis, we will use *finite difference method* to discretize the time dependent partial differential equations and numerically solve it [107]. We will start with the one dimensional wave equation,

$$\partial_t^2 \varphi = \partial_x^2 \varphi \,. \tag{4.7}$$

This second order differential equation was simplified to two first order differential equations by redefining $\Phi = \partial_x \varphi$ and $\Pi = \partial_t \varphi$. Hence the equation (4.7) can be written as,

$$\begin{aligned} \partial_t \Pi &= \partial_x \Phi \\ \partial_x \Pi &= \partial_t \Phi \,. \end{aligned} \tag{4.8}$$

We have taken the boundary $[0,1]$ in the space dimension x and an arbitrary boundary $[0,T]$ in the time dimension t in order to achieve a finite result. These conditions provide the boundaries in equations (4.8):

$$\begin{aligned} \Pi(0,t) &= \Phi(0,t) \\ \Pi(1,t) &= -\Phi(1,t) \,. \end{aligned} \tag{4.9}$$

These boundary conditions ensure that no wave can enter from the left and right ends of the boundary in space. In order to discretize the continuous space-time, we will introduce

two indices n and j labelling the *time slice* and *space slice* respectively. Moreover, each unit time gap Δt is proportional to each unit space gap Δx and can be written as $\Delta t = \lambda \Delta x$, where λ is known as the *Courant number* [108]. Now using time step averaging operator $\mu_t = \frac{1}{2}(\phi_j^{n+1} + \phi_j^n)$ and the central derivative operator in space $D_x \Pi_j^n = \frac{1}{2\Delta x}(\Pi_{j+1}^n - \Pi_{j-1}^n)$ [109], one can rewrite the equations (4.8) as,

$$\begin{aligned} \frac{\Phi_j^{n+1} - \Phi_j^n}{\Delta t} &= \mu_t (D_x \Pi_j^n) \\ \frac{\Pi_j^{n+1} - \Pi_j^n}{\Delta t} &= \mu_t (D_x \Phi_j^n) \ . \end{aligned} \tag{4.10}$$

It is to be noted that in the LHS of the equation (4.10), we have taken forward time derivative, whereas the RHS contain central space derivative. The reason behind these different operations is that our aim is to get all the space informations about the future variables Φ_j^{n+1} and Π_j^{n+1}. Hence the forward derivatives provide us the future informations whereas the central derivatives provide us all of the space informations. However, the first spatial derivative should be taken as a forward derivative due to the lack of past information; also at the other boundary of x, a backward derivative should be taken to maintain the boundary condition. We have taken the initial form of the wave to be a *Gaussian wave* such as,

$$\varphi_j^0 = A \exp\left[-\frac{(x - x_c)^2}{(\Delta x)^2} \right] \ . \tag{4.11}$$

The Gaussian wave is chosen as it is a simple time-symmetric solution. However, other solutions can be chosen as well in order to study the behaviour of the correction in the space-time. Equation (4.10) has been coded numerically using RNPL with the boundary conditions (4.9) and initial conditions (4.11). The numerical solution was first plotted in XVS software which takes the output files of RNPL programme directly and shows the result as shown in the reference [93]. However, for a more compact understanding of the result, we have plotted the RNPL programming output in Mathematica. We have taken the

amplitude $A = 1$, position of the center of the peak $x_c = 0.5$, $\Delta x = 0.015$, and the Courant factor $\lambda = 0.8$. Also the iteration has been done for 128 number of time steps. As a result we got a Gaussian wave that eventually breaks into left and right moving wave with time iteration and exits at the x boundaries as shown in Figure 4.1. The rate of progress towards the boundary was same for both of the wave peaks. This outcome is expected as the solution of the wave equation (4.7) is a superposition of left and right moving waves [110].

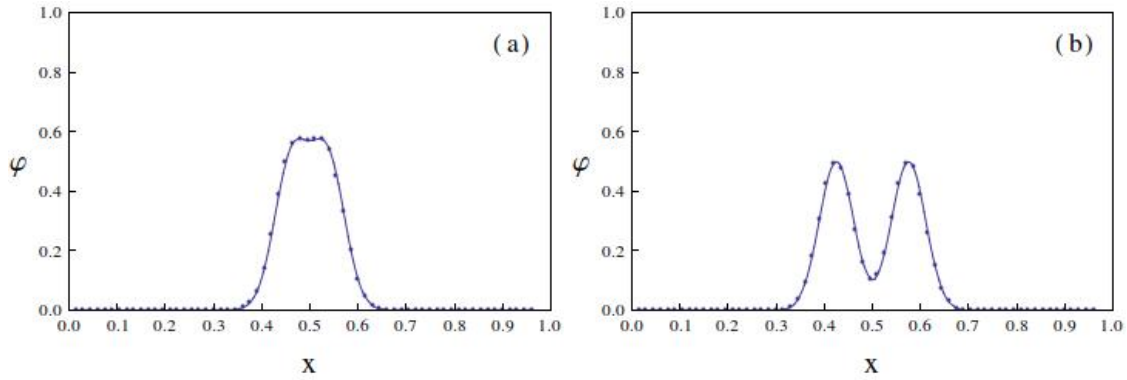

Figure 4.1: Plotting of the scalar field potential φ without correction as a function of the spatial variable x. (a) The Gaussian solution at time-slice t = 3; (b) The Gaussian solution at time-slice t = 6 [111].

However, this output shows a different feature when a twist field is added in the one-dimensional flat metric,

$$ds^2 \;=\; -dt^2 + dx^2 + \beta dt dx\,. \tag{4.12}$$

Equation of motion for the particle moving in this space-time metric is given by the following equation:

$$-\partial_t^2\varphi + \partial_x^2\varphi + \beta\partial_t\partial_x\varphi \;=\; 0\,. \tag{4.13}$$

Proceeding in a similar fashion to convert a second order differential equation into two first order dimensional equations , the above equation can be rewritten as:

$$\begin{aligned} \partial_t \Pi &= \partial_x \Phi \\ \partial_t \Phi &= \partial_x \Pi + (\partial_x \beta)\Phi + \beta \partial_x \Phi \,, \end{aligned} \tag{4.14}$$

with the redefinition :

$$\begin{aligned} \Pi &= \partial_t \varphi - \beta \partial_x \varphi \\ \Phi &= \partial_x \varphi \,. \end{aligned} \tag{4.15}$$

Discretizing the equations (4.14) with the help of the time average operator, the central spatial derivative operator and the forward time derivative operator, one can write:

$$\begin{aligned} \frac{\Phi_j^{n+1} - \Phi_j^n}{\Delta t} &= \mu_t(D_x \Pi_j^n) + \mu_t((D_x \beta_j^n)\Phi_j^n) + \mu_t(\beta_j^n (D_x \Phi_j^n)) \\ \frac{\Pi_j^{n+1} - \Pi_j^n}{\Delta t} &= \mu_t(D_x \Phi_j^n) \,. \end{aligned} \tag{4.16}$$

We have started with the form $\beta = x^2(x-1)^2$ with the boundary condition $\beta|_{x=0} = 0$ and $\beta|_{x=1} = 0$. As an output, we got two asymmetric wave peaks, split from the initial Gaussian function, moving away from each other towards the boundaries as shown in Figure 4.2. Again the rate of the progress remains the same for both of the peaks.

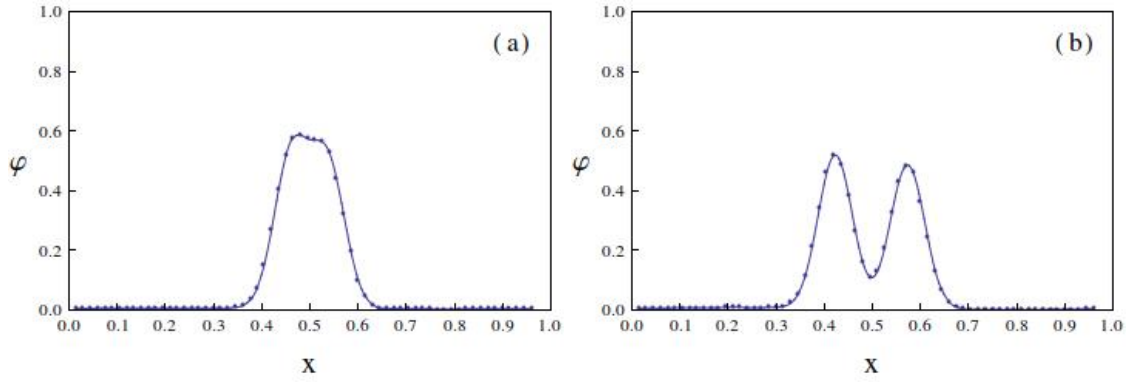

Figure 4.2: Plotting of the scalar field potential φ with twist term $\beta = x^2(x-1)^2$ as a function of the spatial variable x. (a) The Gaussian solution at time-slice t = 3; (b) The Gaussian solution at time-slice t = 6 [111].

Finally, we have taken $\beta = \sin^2(x^2(x-1)^2)$ with the same boundary conditions as the prior example. This time we have recorded an interesting behaviour of the wave function. The Gaussian wave generates two waves, one left and one right moving peak with larger asymmetry and the peaks approaching the boundaries with different progress rate. In Figure 4.3, it has been shown that at time slice $t = 40$, the left moving peak has disappeared from the frame while the right moving peak is still in the frame. This assymetric nature of the graphs can be shown for scalar field with the original quantum gravitational shift term as well. This is a work to appear.

This feature might have consequences for the Hawking radiation at the horizon as discussed in the reference [63]. The convergence of the output has been verified by taking different values of Δx. Starting with $\Delta x = 0.015$, we have taken $\Delta x/2$, $\Delta x/4$, $\Delta x/8$ and got the same image with different scales. Hence the result is converging. Therefore, these numerical results confirm that a correction in the metric will have an effect on the scalar field propagation.

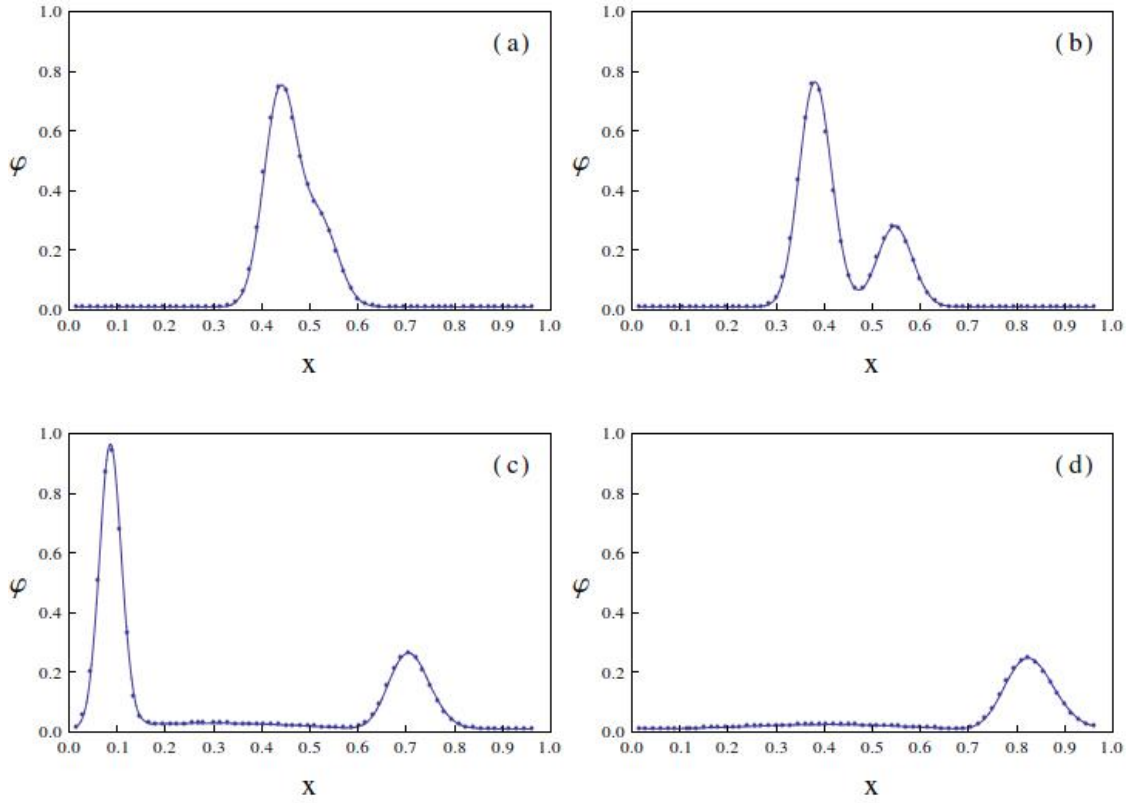

Figure 4.3: Plotting of scalar field potential φ with twist term $\beta = \sin^2(x^2(x-1)^2)$ as a function of the spatial variable x. (a) The Gaussian solution at time-slice t = 3; (b) The Gaussian solution at time-slice t = 6; (c) The Gaussian solution at time-slice t = 25; (d)The Gaussian solution at time-slice t = 40 [111].

4.3 Conclusion

In this chapter, we have seen the loop quantum gravity fluctuations generated in the coherent states give rise to a correction in the Schwarzschild metric and the correction induces the asymmetric behaviour of a scalar field in a near horizon limit. Though we have started our journey with the Schwarzschild space-time, our aim is to find the effect for the binary black hole system. The correction in the Schwarzschild black hole metric may not have a significant contribution to the one dimensional scalar field propagation though the asymmetry might influence processes like Hawking radiation. However, in the higher dimension, because of the non-linearity of the evolution equations, one can expect a non-trivial outcome. Also, it would be interesting to find out whether this correction imposes

any effect to other types of field propagations. In the next chapter, we will study this loop quantum gravity fluctuation effect on the vector field propagation in a Schwarzschild background.

Chapter 5

Effect on the Vector Field

Maxwell's Equations have had a
greater impact on human history
than any ten presidents.
– Carl Sagan

A vector is defined as a physical quantity that has a magnitude as well as direction. If a vector is defined at each point in a manifold, it is a vector field. In physics, the most common vector field is the *Electromagnetic field* which describes the propagation of the light wave. The electromagnetic field can be described by the Maxwell's equations which has been modified by Einstein. Maxwell's equations can be written in a covariant approach where the electromagnetic field is characterised by an antisymmetric tensor $F_{\mu\nu}$ as discussed in Chapter 2. Thus one can interpret the electromagnetic field propagation as a fluid flow [112]. In reference [64], the electromagnetic field propagation has been discussed for Reissner-Nordstrom and Schwarzschild black hole, and it has been shown that the black hole entropy is a consequence of vector field propagation in the black hole background. However, in this thesis, we will study the quantum gravity correction effect for the electromagnetic field propagation in the Schwarzschild black hole background.

We will start this chapter with the tensor description for the electromagnetic field. Then we will study the behaviour of the electromagnetic field propagation in the Schwarzschild black hole background. Next we will introduce the quantum corrected Schwarzschild met-

ric to review the vector field propagation. Our aim is to compare between classical and semi-classically corrected black hole scenario and look for a distinguishable feature in the electromagnetic field propagation.

5.1 Electromagnetic Field in Curved Space-Time

Maxwell's equations are given by the following equations, in natural units [113],

$$\begin{aligned} \nabla\cdot\mathbf{E} &= \frac{\rho}{\varepsilon_0}\,, \\ \nabla\times\mathbf{B} &= \frac{\partial\mathbf{E}}{\partial t}+\mu_0\mathbf{J}\,, \\ \nabla\cdot\mathbf{B} &= 0\,, \\ \nabla\times\mathbf{E} &= -\frac{\partial\mathbf{B}}{\partial t}\,, \end{aligned} \tag{5.1}$$

where $\mathbf{E}$ is the electric field, $\mathbf{B}$ is the magnetic field, ρ is the charge density, $\mathbf{J}$ is the current density, ε_0 is the permittivity of the free space and μ_0 is the permeability of the free space.

In the covariant description, the antisymmetric Faraday tensor $F_{\mu\nu}$ has been introduced such that for $\mathbf{E}=E_1\hat{i}+E_2\hat{j}+E_3\hat{k}$ and for $\mathbf{B}=B_1\hat{i}+B_2\hat{j}+B_3\hat{k}$, in natural unit with $c=1$ [47],

$$F_{\mu\nu}=\begin{pmatrix} 0 & -E_1 & -E_2 & -E_3 \\ E_1 & 0 & B_3 & -B_2 \\ E_2 & -B_3 & 0 & B_1 \\ E_3 & B_2 & -B_1 & 0 \end{pmatrix}. \tag{5.2}$$

The inner product of the Faraday tensor is invariant,

$$F^{\mu\nu}F_{\mu\nu}=2(B^2-E^2)\,. \tag{5.3}$$

Inhomogeneous Maxwell's equations can be written in covariant forms. From the equa-

tions (5.1), the first two equations can be expressed as,

$$\nabla_\mu F^{\mu\nu} = \mu_0 J^\nu \ , \tag{5.4}$$

and the last two equations can be written as,

$$\nabla_\tau F_{\mu\nu} + \nabla_\mu F_{\nu\tau} + \nabla_\nu F_{\tau\mu} = 0 \ . \tag{5.5}$$

The above equation is known as *Bianchi Identity* [113].

The antisymmetric property of the Faraday tensor together with equation (5.4) imply the conservation of charge,

$$\nabla_\mu J^\mu = 0 \ . \tag{5.6}$$

On the other hand, equation (5.5) allows us to write the Faraday tensor in terms of a *four-vector potential* A^μ [47],

$$F_{\mu\nu} = \partial_\mu A_\nu - \partial_\nu A_\mu \ . \tag{5.7}$$

It is to be noted that in the above equation, we have used the partial derivatives instead of the covariant derivatives. Particular for this equation, one can replace the covariant derivatives with the partial derivatives as the extra terms containing the affine connections will be cancelled out. However, we still have an extra degree of the freedom left: with the replacement of $A_\mu \to A_\mu + \partial_\mu \varphi$ (where φ is an arbitrary scalar potential), there will be no effect on equation (5.7). Here we need a *gauge fixing* in order to remove the freedom. Thus, with an appropriate choice of Lorentz-Gauge condition $\partial_\mu A^\mu = 0$ [64], one can simplify the Maxwell equations as,

$$\Box A_\mu = -\mu_0 J_\mu \ , \tag{5.8}$$

where the operator "$\Box$" represents the four-dimensional d'Alembert operator $\partial_\nu \partial^\nu = -\partial_t^2 + \nabla^2$. Moreover, Faraday tensor determines the energy-momentum tensor in the electromag-

netic field [113],

$$T_{\mu\nu} = -\frac{1}{\mu_0}\left[F_{\mu\tau}F^{\tau}_{\nu} + \frac{1}{4}g_{\mu\nu}F_{\alpha\beta}F^{\alpha\beta}\right]. \tag{5.9}$$

Thus we have introduced the electromagnetic field equations in covariant form and now one can look for the solution of the equations (5.4) and (5.5) in a curved space-time. In the next section, we solve Maxwell's equations with the Schwarzschild metric components. In the Minkowski space-time, these calculations are trivial compared to the curved space-time. In the curved background, one has to consider the coupling between the electromagnetic field and the geometry of the space-time. Things get more complicated when the background metric is non-diagonal, i.e. when the metric has cross-components from the coordinates. One may need to use numerical methods in order to solve the non-trivial differential equations.

5.2 Electromagnetic Field Propagation in Schwarzschild Background

Following reference [64], in this section, we will study the electromagnetic field propagation in the Schwarzschild black hole background. Maxwell's equations will be solved with the background of Schwarzschild metric and with a semi-classical approximation.
We will start with a coordinate transformation of the spherical coordinates in Schwarzschild black hole, because a stereo-graphic coordinate is more relevant and easier to deal with for further calculation. Referring to the Schwarzschild metric in Chapter 2, we have already seen that, in natural unit with $G = 1$,

$$ds^2 = -\left(1 - \frac{2M}{r}\right)dt^2 + \left(1 - \frac{2M}{r}\right)^{-1}dr^2 + r^2 d\theta^2 + r^2\sin^2\theta d\phi^2 \,. \tag{5.10}$$

The angular part of the above equation can be redefined as,

$$d\theta^2 + \sin^2\theta d\phi^2 = \frac{4}{(1+z\bar{z})^2}dz d\bar{z} \,, \tag{5.11}$$

where $z = \frac{\sin\theta e^{i\phi}}{1-\cos\theta}$ and $\bar{z} = \frac{\sin\theta e^{-i\phi}}{1-\cos\theta}$. Hence the non-zero metric components are redefined as,

$$g_{00} = -\left(1 - \frac{2M}{r}\right), \qquad g_{11} = \left(\frac{1}{1-\frac{2M}{r}}\right),$$
$$g_{23} = \frac{2r^2}{(1+z\bar{z})^2}\ . \tag{5.12}$$

It is to be noted we have changed the coordinate just to make the equations easily solvable. This part can be skipped if one is comfortable enough to deal with regular Schwarzschild coordinate system. Equation (5.4) without any source is,

$$\nabla_\mu F^{\mu\nu} = 0\ . \tag{5.13}$$

Using the form of $F^{\mu\nu}$ in terms of vector potential, i.e, $F_{\mu\nu} = \nabla_\mu A_\nu - \nabla_\nu A_\mu$, one can obtain,

$$\Box A_\mu - \nabla_\nu \nabla_\mu A^\nu = 0\ , \tag{5.14}$$

where $\Box = \nabla_\mu \nabla^\mu$. It is to be noted that this equation is different from equation (5.8) as we have not fix our gauge condition yet. We will choose our gauge later in this calculation in order to make the equations easier to solve.

However, the above equation can be written in terms of affine connection and partial derivatives such that,

$$LA_\mu = A_\nu \partial_\mu \Gamma^\nu + 2g^{\alpha\beta}\Gamma^\nu_{\alpha\mu}\partial_\beta A_\nu + \partial_\mu \nabla_\nu A^\nu\ , \tag{5.15}$$

where $\Gamma^\nu = g^{\alpha\beta}\Gamma^\nu_{\alpha\beta}$, L is the d'Alembert operator acting on functions such that $L = \frac{1}{\sqrt{|g|}}\partial_\mu \sqrt{|g|} g^{\mu\nu}\partial_\nu$.

From equation (5.15), we will get four independent equations for different values of μ,

$$
\begin{aligned}
LA_0 &= -\frac{2M}{r^2}(\partial_0 A_1 - \partial_1 A_0) + \partial_0 \nabla_\nu A^\nu \,, && (5.16)\\
LA_1 &= -\frac{2M}{r^2}\left[\partial_1 A_1 - (g^{00})^2 \partial_0 A_0\right] + \frac{2}{r^2}\left(1 - \frac{2M}{r}\right) A_1 \\
&\quad + \frac{2g^{23}}{r}(\partial_2 A_3 - \partial_3 A_2) + \partial_1 \nabla_\nu A^\nu \,, && (5.17)\\
LA_2 &= -\frac{2\bar{z}(1+z\bar{z})}{r^2}\partial_3 A_2 + \frac{2g^{11}}{r}(\partial_1 A_2 - \partial_2 A_1) + \partial_2 \nabla_\nu A^\nu \,, && (5.18)\\
LA_3 &= -\frac{2z(1+z\bar{z})}{r^2}\partial_3 A_3 + \frac{2g^{11}}{r}(\partial_1 A_3 - \partial_3 A_1) + \partial_3 \nabla_\nu A^\nu \,. && (5.19)
\end{aligned}
$$

Now it is time to choose a suitable gauge condition and we fix the gauge as $A_0 = 0$. This choice leads us to write equation (5.16),

$$\nabla_\nu A^\nu - \frac{2M}{r^2} A_1 = 0 \,. \tag{5.20}$$

After substituting the values of $\nabla_\nu A^\nu$ in the equations (5.17), (5.18), (5.19) and doing a little bit of calculation, one can obtain,

$$
\begin{aligned}
LA_r &= -\tfrac{2}{r^2}\partial_r (r g^{rr} A_r) \,, && (5.21)\\
\left[L + \tfrac{2\bar{z}(1+z\bar{z})}{r^2}\partial_{\bar{z}}\right] A_z &= \tfrac{2g^{rr}}{r}\partial_r A_z - \tfrac{2}{r}\left(1 - \tfrac{3M}{r}\right)\partial_z A_r \,, && (5.22)\\
\left[L + \tfrac{2z(1+z\bar{z})}{r^2}\partial_z\right] A_{\bar{z}} &= \tfrac{2g^{rr}}{r}\partial_r A_{\bar{z}} - \tfrac{2}{r}\left(1 - \tfrac{3M}{r}\right)\partial_{\bar{z}} A_r \,. && (5.23)
\end{aligned}
$$

There will be two sets of possible solutions for the above equations.

$$
\begin{aligned}
A^{(1)} &\equiv \left(0,\, 0,\, \frac{1}{\sqrt{2l(l+1)\omega}}\partial_z \Phi,\, \frac{1}{\sqrt{2l(l+1)\omega}}\partial_{\bar{z}}\Phi\right) \,, && (5.24)\\
A^{(2)} &\equiv \left(0,\, \sqrt{\frac{l(l+1)}{2\omega^3}}\frac{\Phi}{r^2},\, \frac{g^{rr}}{\sqrt{2l(l+1)\omega^3}}\partial_z\partial_r\Phi,\, \frac{g^{rr}}{\sqrt{2l(l+1)\omega^3}}\partial_{\bar{z}}\partial_r\Phi\right) \,, && (5.25)
\end{aligned}
$$

where $\Phi(t,r,z,\bar{z}) = e^{-i\omega t} f(r) Y_m^l(z,\bar{z})$ with spherical harmonics [114],

$$Y_{lm} = (-1)^m \sqrt{\frac{2l+1}{4\pi}(l+m)!(l-m)!}\frac{l!}{(1+z\bar{z})^l}\sum_n \frac{(-1)^n\, z^{(l-n)}\, \bar{z}^{(l-m-n)}}{n!(l-m-n)!(l-n)!(m+n)!} \ . \quad (5.26)$$

It can be shown that Φ follows the relation [64],

$$\Box\Phi = \frac{2g^{rr}}{r}\partial_r\Phi \ . \quad (5.27)$$

So, we have two possible vector field forms in a Schwarzschild black hole background. In the next section we will deal with the vector field in the corrected black hole background.

Motivation:

The correction in the Schwarzschild black hole will perturb the vector field and these perturbations can be used to test for stability of the space-time. Given the EHT which will try to obtain the image of a black hole, we can try to find quantum gravity correction to the image [115], as that is formed by electromagnetic wave or light deflected off the black hole field. The corrections might also shed light on the nature of the one loop corrections to black hole entropy.

5.3 Electromagnetic Field Propagation in Corrected Schwarzschild Black Hole: New Result

The quantum gravity correction, we have computed in the last section, is,

$$g^{tr} = \pm 2\frac{1}{1-f^2}\left(\frac{r_g}{r}\right)^{3/2}\tilde{t}\tilde{f}\left(\frac{P_{e_r}}{S_{e_r}}\right) \ . \quad (5.28)$$

For our convenience, we would redefine the correction term as

$$F(r,\theta) = \frac{1}{2}g^{tr} = \pm\frac{1}{1-f^2}\left(\frac{r_g}{r}\right)^{3/2}\tilde{t}\tilde{f}\left(\frac{P_{e_r}}{S_{e_r}}\right) \ . \quad (5.29)$$

For this calculation, we would not redefine the angular part of the metric as we did in the last section. Except that part, the calculation for the corrected Schwarzschild metric is quite straight-forward and will follow the same manner as the last section. From equation (5.15) with the gauge $A_0 = 0$, we would get the following equations,

$$\partial_0 \left[\nabla_j A^j - \tfrac{2M}{r^2} A_r\right] = \tfrac{r-2M}{r^3} \tfrac{\partial F}{\partial \theta} (\partial_1 A_2 - \partial_2 A_1) \ , \tag{5.30}$$

$$\begin{aligned} &\partial_r (\nabla_j A^j) + (\partial_t A_r) \tfrac{MF(r,\theta)}{r(r-2M)} + A_r \tfrac{2(r-2M)}{r^3} \\ &+ \tfrac{2}{r^3} (\partial_\theta A_\theta) + (\partial_t A_\theta) \tfrac{\partial F}{\partial \theta} \tfrac{1}{r(r-2M)} + A_\theta \tfrac{2\cot\theta}{r^3} + \tfrac{2}{r^3 \sin^2\theta} (\partial_\phi A_\phi) = 0 \ , \end{aligned} \tag{5.31}$$

$$\begin{aligned} &\partial_\theta (\nabla_j A^j) - (\partial_t A_r) \tfrac{\partial F}{\partial \theta} + \tfrac{2F}{r} (\partial_t A_\theta) \\ &- \tfrac{2(r-2M)}{r^2} (\partial_\theta A_r - \partial_r A_\theta) + \tfrac{2\cot\theta}{r^2 \sin^2\theta} (\partial_\phi A_\phi) + \tfrac{\csc^2\theta}{r^2} A_\theta = 0 \ , \end{aligned} \tag{5.32}$$

$$\begin{aligned} &\partial_\phi (\nabla_j A^j) + \tfrac{2F}{r} (\partial_t A_\phi - \partial_\phi A_t) \\ &+ \tfrac{2(r-2M)}{r} \left[\cot\theta (\partial_r A_\phi) - \tfrac{1}{r} (\partial_\phi A_r)\right] + \tfrac{2\cot\theta}{r} \left[(\partial_\theta A_\phi) - \tfrac{1}{r} (\partial_\phi A_\theta)\right] = 0 \ . \end{aligned} \tag{5.33}$$

We have ignored higher order terms of $F(r,\theta)$ because of their negligible contributions to the correction. As we can see here, there are some extra terms presented in the above equations due to the non-zero value of $F(r,\theta)$. With the approximation $F(r,\theta) \to 0$ and with the redefined angular part of the metric, these equations will coincide with the equations (5.16), (5.17), (5.18) and (5.19). However, the solution of the above equations will be non-trivial, as expected. It might be numerically solvable.

We initially try to solve the equations near the horizon, that is set $r \approx 2m$ as the correction is important near the horizon. That solves equation (5.30) as

$$\nabla_j A^j - \frac{2m}{r^2} A_r = \frac{r-2m}{r^3} \frac{\partial F}{\partial \theta} \int (\partial_r A_\theta - \partial_\theta A_r) \ dt + f(r,\theta,\phi) = \Pi(r,t,\theta) \ , \tag{5.34}$$

where we can set $f(r,\theta,\phi)$ to zero. Using this we can substitute $\nabla_j A^j$ in other equations, and assuming that $A(r,\theta)$ is independent of ϕ as the metric is independent of ϕ. Equation

(5.31) gives,

$$\partial_r\left(\frac{2M}{r^2}A_r+\Pi\right)+\partial_t A_r\lambda g_1+\partial_\theta A_\theta\left(\frac{2}{r^3}\right)+\partial_t A_\theta\lambda g_2+2\frac{\cot\theta}{r^3}A_\theta=0\ . \tag{5.35}$$

Similarly, equation (5.32) is

$$\partial_\theta\left(\frac{2M}{r^2}A_r+\Pi\right)-\partial_t A_r\lambda g_3+\partial_t A_\theta\lambda g_4+\frac{\csc^2\theta}{r^2}A_\theta=0\ , \tag{5.36}$$

and equation (5.33) is

$$\lambda g_4(\partial_t A_\phi)+\frac{2\cot\theta}{r}\partial_\theta A_\phi=0\ . \tag{5.37}$$

In the above, λ has been identified as the semi-classical parameter $\tilde{t}$ and

$$g_1 = \frac{MF}{\lambda r(r-2M)}\ , \tag{5.38}$$

$$g_2 = \frac{\partial F}{\partial\theta}\frac{1}{\lambda r(r-2M)}\ , \tag{5.39}$$

$$g_3 = \frac{1}{\lambda}\frac{\partial F}{\partial\theta}\ , \tag{5.40}$$

$$g_4 = \frac{1}{\lambda}\frac{2F}{r}\ . \tag{5.41}$$

As equation (5.33) is decoupled from A_r, we use equations (5.31) and (5.32) to analyse the system. We introduce an ansatz for the solution that $A_r=A_r^0+\lambda\tilde{A}_r$ and $A_\theta=A_\theta^0+\lambda\tilde{A}_\theta$. Then the order λ terms from equations (5.31) and (5.32) can be easily isolated. Therefore, from equation (5.31), we get,

$$\lambda\left[\partial_r\left(\frac{2M}{r^2}\tilde{A}_r\right)+\partial_\theta\tilde{A}_\theta\frac{2}{r^3}+\frac{2\cot\theta}{r^3}\tilde{A}_\theta+p(t,r,\theta)\right]=0\ , \tag{5.42}$$

and from (5.32), we get,

$$\lambda\left[\frac{2M}{r^2}\partial_\theta\tilde{A}_r+\frac{\csc^2\theta}{r^2}\tilde{A}_\theta+h(t,r,\theta)\right]=0\ , \tag{5.43}$$

where again we have redefined,

$$p(t,r,\theta) = g_1\partial_t A_r^0 + g_2\partial_t A_\theta^0 + \partial_r\Pi \,, \tag{5.44}$$

$$h(t,r,\theta) = -g_3\partial_t A_r^0 + g_4\partial_t A_\theta^0 + \partial_\theta\Pi \,. \tag{5.45}$$

Values of A_r^0 and A_θ^0 can be taken from the equation (5.24) as non-perturbed solutions. Therefore we can solve for $\tilde{A}_\theta$ from equation (5.43) and insert it in equation (5.42) to solve for $\tilde{A}_r$. The equation is of the form,

$$\frac{r^3}{4m}\partial_r\left(\frac{2m}{r^2}\tilde{A}_r\right) - \partial_\theta\left(\sin^2\theta\partial_\theta\tilde{A}_r\right) - \cos\theta\sin\theta\partial_\theta\tilde{A}_r = \Lambda(t,r,\theta) \,, \tag{5.46}$$

where $\Lambda(r,t,\theta)$ is

$$\Lambda(r,t,\theta) = \frac{r^2}{r_g}\partial_\theta\left(\sin^2\theta\, h(r,t,\theta)\right) + \frac{r^2}{r_g}\cos\theta\sin\theta\, h(r,t,\theta) - p(r,t,\theta) \,. \tag{5.47}$$

Next from the RHS of the equation we formulate $\tilde{A}_r = A(r)\Theta(\theta)$, where $\Theta(\theta)$ is an eigenstate of the angular operator with eigenvalue $\tilde{\lambda}$. Note this is not the same as the Legendre polynomial, but can be solved in terms of them. The equation has the form,

$$\frac{r^3}{4m}\partial_r\left(\frac{2m}{r^2}A(r)\right) - \tilde{\lambda}A(r) = \frac{1}{\Theta(\theta)}\Lambda(t,r,\theta) \,. \tag{5.48}$$

Given the form of the solution in the zeroth order as by equation (5.24), we can put $A_r^0 = 0$. In addition, if we choose $\theta = \pi/2$ we get for the non-zero term in $\Lambda(r,t)$,

$$\begin{aligned}\Lambda(r,t) &= \frac{r^2}{r_g}\partial_\theta\ \left(g_4\partial_t A_\theta^0\right) + \frac{r^2}{r_g}\partial_\theta^2\,\Pi \\ &= \left[\frac{r^2}{r_g}g_4\partial_\theta\partial_t\, A_\theta^0 + \frac{r^2}{r_g}\partial_\theta^2\left(\frac{r-r_g}{r^3}\frac{\partial F}{\partial\theta}\int\partial_r A_\theta^0 dt\right)\right]_{\theta=\frac{\pi}{2}} \,.\end{aligned} \tag{5.49}$$

This can be solved for any value of θ. However, from the solution (5.24), the A_θ^0 is non-

zero near the horizon. If we take as the solution $A^0_\theta = e^{i\omega r^*}e^{i\omega t}\partial_z Y_{lm}(z,\bar{z})$ with $r^* = r + 2M\ln|\frac{r}{2M}-1|$, again for simplicity, then the above reduces to,

$$\Lambda(r,t) = \frac{r^2}{r_g}\frac{2F}{r}(i\omega)e^{i\omega t}e^{i\omega r^*}\partial_\theta\partial_z Y_{lm}(z,\bar{z}) + 2\frac{r-r_g}{rr_g}\partial^2_\theta F \int (i\omega)\frac{dr^*}{dr}e^{i\omega t}e^{i\omega r^*}\partial_\theta\partial_z Y_{lm}(z,\bar{z})\,dt\ . \tag{5.50}$$

We use those values of $l,\ m$ for which the above equation is non-zero at $\theta = \frac{\pi}{2}$. We also have an estimate for the Φ field in this limit. $\Phi \sim e^{-i\omega t}e^{\pm i\omega r^*}$. Using this we can estimate a solution at some constant $\theta = c$, and time $t = \tau_c$ as,

$$\frac{dA}{dr} - (1+\tilde{\lambda})\frac{2A}{r} = \frac{2}{r\Theta(c)}\Lambda(\tau_c, r, c). \tag{5.51}$$

This is a first order equation, which can be solved. The solution for $A(r)$ is obtained as,

$$A(r) = r^{2(1+\tilde{\lambda})}\int \frac{2}{r}r^{-2(1+\tilde{\lambda})}\frac{\Lambda}{\Theta}dr\ . \tag{5.52}$$

Using various values of $\tilde{\lambda}$ a plot of the above gives us a non-trivial $A(r)$, though this wave's magnitude is small, it can be large near the horizon. The integral is comprised of several terms which can be computed using Maple. We are showing one of the terms of $A(r)$ in the Figure 5.1 for $\tilde{\lambda} = 0$. From the Figure, it is obvious that the term $A(r)$ has a non-trivial contribution near the horizon. Even though the effect faded far from the horizon, it might not give the same result for other values of $\tilde{\lambda}$. It is to be noted that this graph is not multiplied by the semi-classical parameter. Therefore the effect would be infinitesimal over all. However, the presence of the other modes of perturbation might generate a chaotic behaviour of the vector field that can be observed using EHT.

We can also get a solution for the angular part Θ. The equation for Θ is can be obtained from equation (5.46)

$$\sin^2\theta\frac{d^2\Theta}{d\theta^2} + 3\sin\theta\cos\theta\frac{d\Theta}{d\theta} - \tilde{\lambda}\Theta = 0\ . \tag{5.53}$$

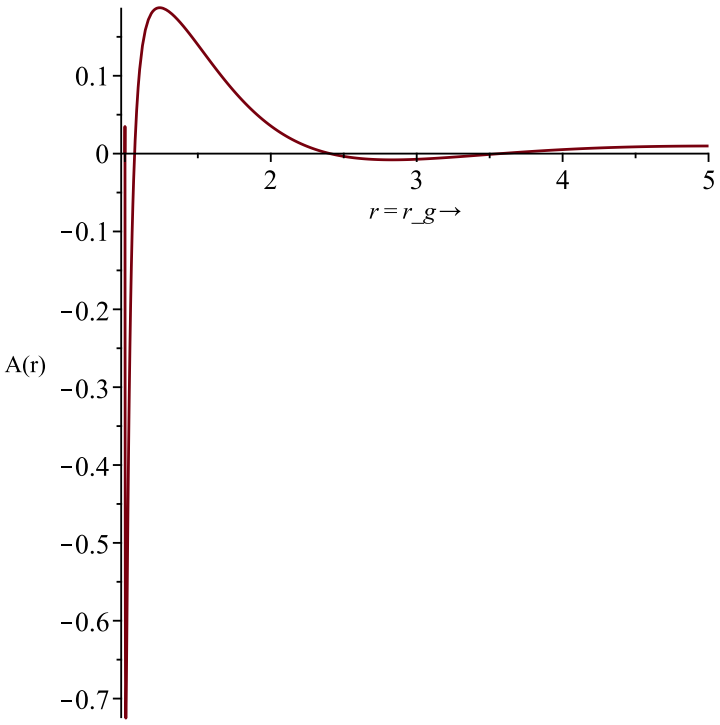

Figure 5.1: A(r) vs. r for $\tilde{\lambda} = 0$ [116]

If we redefine $\Theta = (\sin\theta)^{-1}\tilde{\Theta}$, then the equation for $\tilde{\Theta}$ is

$$\sin^2\theta\frac{d^2\tilde{\Theta}}{d\theta^2} + \sin\theta\cos\theta\frac{d\tilde{\Theta}}{d\theta} + (2\sin^2\theta - (1+\tilde{\lambda}))\Theta = 0\ . \tag{5.54}$$

This equation is in a form of Legendre differential equation [117], hence can be solved in terms of Legendre polynomial $p_l(\cos\theta)$ with,

$$l(l+1) = 2\ , \tag{5.55}$$

$$m^2 = 1+\tilde{\lambda}\ . \tag{5.56}$$

The above equation can be solved for different values of θ and $\tilde{\lambda}$. This work is still in progress. In experiment, we usually fix θ in order to observe the system in an equitorial plane. Therefore, with constant θ, the solution for Θ should modify the perturbation with a constant factor. However, it might be important to note the value of θ, for which the

perturbation is significant.

5.4 Conclusion

In this Chapter, we studied the behaviour of the electromagnetic field in the semi-classically corrected background. We find that the quantum fluctuations induce a non-zero A_r in the solution, and this can influence the computation of one loop corrections to the black hole entropy [64]. We have approximated our system for calculation convenience. However, without any approximation, the solution is quite complicated and the perturbation effect might generate an instability in the system. This effect can be tested by using numerical analysis. At this point, we can conclude that, even with the approximations, the quantum corrected Schwarzschild black hole is affecting the vector field; therefore, one can assure the quantum gravity correction effect with a suitable experimental design like EHT. Research on this topic is on progress. In the next chapter, we will discuss the correction effect in the tensor field propagation.

Chapter 6

Conclusion

The research on quantum gravity is significantly important, especially in this current era when LIGO has detected the strain produced by a gravity wave in the order of 10^{-21} [7]. The quality of the experimental set-up is improving fast with time. Therefore, we are looking forward to build an advanced technology that can detect even smaller changes in the system.

In this thesis, our aim was to get an observable quantum gravity effect that can verify the theory itself. We have studied the quantum gravity effect in the scalar, vector and tensor fields propagation in the semi-classically corrected black hole background. In the first three chapters, we have discussed the background theories that have been used in the calculations. After a brief introduction in Chapter 1, we started with the classical gravity theory in Chapter 2. The important outcome from this chapter was the Schwarzschild black hole solution. This solution is significant in this thesis, as we have taken our background space-time to be a Schwarzschild space-time in the later chapters. In Chapter 3, we have discussed basic canonical formulation of gravity and loop quantum gravity, which was our main framework to calculate the corrections in the classical Schwarzschild black hole.

The main work of this thesis begins with the quantum correction calculation in Chapter 3. In the classical Schwarzschild space-time, we got a correction generated from the coherent states of the loop quantum gravity variables. The effect of this correction has been studied for the scalar field propagation near the horizon of the black hole in Chapter 4. As a result, we found that the symmetry will be broken for a scalar ingoing and outgoing modes

at the horizon; not only that, the propagation velocity will be affected as well. This result implies that, the quantum gravity correction will have a significant effect on the scalar field. In the next chapter, we studied the correction effect on the vector field propagation with the corrected Schwarzschild background. Here, we ended up with an extra correction term in the form of a radial component of the vector potential which is zero for the classical Schwarzschild background.

6.1 Work in Progress: Effect on Gravitational Wave in Corrected Black Hole Background

Gravitational waves are vaccum solutions of the linearized Einstein equations with tansverse-traceless gauge as described in references [118, 119]. If we consider the weak gravitational field where our curved metric can be decomposed into the flat Minkowski metric such that $g_{\mu\nu} = \eta_{\mu\nu} + h_{\mu\nu} + O([h_{\mu\nu}]^2)$ with a small perturbation $|h_{\mu\nu}| << 1$, the perturbed Ricci tensor can be written as [119],

$$R_{\mu\nu} = \frac{1}{2}(h_{\mu}{}^{\alpha}{}_{,\nu\alpha} + h_{\nu}{}^{\alpha}{}_{,\mu\alpha} - h_{\mu\nu,}{}^{\alpha}{}_{\alpha} - h_{,\mu\nu}) + O([h_{\mu\nu}]^2) \ ,$$

where $h \equiv h^{\alpha}{}_{\alpha} = \eta^{\mu\alpha} h_{\mu\alpha}$ is the trace of the metric perturbations. With the transverse-traceless gauge [120], the linearized Einstein equation can be expressed as,

$$\Box h_{\mu\nu} = 0 \ . \tag{6.1}$$

It can shown that gravitational wave solutions of equation (6.1) are [119] ,

$$\overline{h}_{\mu\nu} = \Re\{A_{\mu\nu} \exp(i\kappa_{\alpha} x^{\alpha})\} \ , \tag{6.2}$$

with null four-vector κ^{α} and amplitude tensor

$$A_{\mu\nu} \equiv \begin{pmatrix} 0 & 0 & 0 & 0 \\ 0 & A_{xx} & A_{xy} & 0 \\ 0 & A_{xy} & -A_{xx} & 0 \\ 0 & 0 & 0 & 0 \end{pmatrix} . \tag{6.3}$$

In this thesis, our aim was to study the effect of quantum corrections on tensor fields, or gravity waves. For that purpose, we take the Schwarzschild metric, and study gravity waves in that. We then resolve the gravity wave propagation in the quantum corrected metric. Gravitational wave solutions with Schwarzschild black hole background can be expressed as odd parity perurbation solution under Regge-Wheeler gauge [121] and even parity perturbation solution under Zerilli gauge [122] as shown in reference [119]. These solutions are constrained by the Birkhoff's theorem [123, 124] where the solutions are spherically symmetric and asymptotically flat. However, if we consider the gravitational wave solutions with corrected Schwarzschild background, the solutions are not restricted by the Birkhoff's theorem. Therefore, we find difficulties in computing the modes of the gravitational wave. We found that the Einstein equation takes the form,

$$\delta R_{\mu\nu} = g^{\beta\alpha}\nabla_{\beta}\nabla_{\nu}h_{\mu\alpha} + g^{\beta\alpha}\nabla_{\beta}\nabla_{\mu}h_{\nu\alpha} - g^{\beta\alpha}\nabla_{\beta}\nabla_{\alpha}h_{\mu\nu} = 0 . \tag{6.4}$$

where $\delta R_{\mu\nu}$ is the difference between the Ricci tensor associated with corrected Schwarzschild metric and that of the original Schwarzschild metric. If we calculate equation (6.4) explicitly with Regge-Wheeler gauge, there will be no contribution from the components δR_{00}, δR_{01} and δR_{02}. However, there will be contributions from the components δR_{03} and δR_{ij}.

The general expressions for R_{0i} and R_{ij} are given by,

$$\begin{aligned}
\delta R_{0i} &= -g^{\alpha\beta}\nabla_\beta\nabla_i h_{0\alpha} + g^{\alpha\beta}\nabla_\beta\nabla_0 h_{\alpha i} - g^{\alpha\beta}\nabla_\alpha\nabla_\beta h_{0i} \\
&= g^{00}\nabla_0\nabla_i h_{00} + g^{01}\nabla_0\nabla_i h_{01} + g^{01}\nabla_0\nabla_0 h_{i1} - g^{01}\nabla_0\nabla_i h_{0i} \\
& \quad g^{10}\nabla_1\nabla_i h_{00} + g^{11}\nabla_1\nabla_i h_{01} + g^{11}\nabla_1\nabla_0 h_{i1} - g^{11}\nabla_1\nabla_1 h_{0i} \\
& \quad g^{22}\nabla_2\nabla_i h_{02} + g^{22}\nabla_2\nabla_0 h_{i2} - g^{22}\nabla_2\nabla_2 h_{0i} \\
& \quad g^{33}\nabla_3\nabla_i h_{30} + g^{33}\nabla_3\nabla_0 h_{i3} - g^{33}\nabla_3\nabla_3 h_{0i}
\end{aligned} \tag{6.5}$$

and,

$$\begin{aligned}
\delta R_{ij} &= -g^{\alpha\beta}\partial_\beta\partial_i h_{\alpha j} - g^{\alpha\beta}\partial_\beta\partial_j h_{\alpha i} + g^{\alpha\beta}\partial_\alpha\partial_\beta h_{ij} + g^{\alpha\beta}\Gamma^\tau_{i\beta}\partial_\tau h_{\alpha j} \\
&+ g^{\alpha\beta}\Gamma^\tau_{\beta j}\partial_\tau h_{\alpha i} + g^{\alpha\beta}\Gamma^\tau_{\alpha\beta}\partial_i h_{\tau j} + g^{\alpha\beta}\Gamma^\tau_{\alpha\beta}\partial_j h_{\tau i} \\
& \quad -g^{\alpha\beta}\Gamma^\lambda_{\alpha\beta}\partial_\lambda h_{ij} - g^{\alpha\beta}\Gamma^\lambda_{\alpha i}\partial_\beta h_{\lambda j} - g^{\alpha\beta}\Gamma^\lambda_{\alpha j}\partial_\beta h_{i\lambda} \\
& \quad +2g^{\alpha\beta}\partial_\beta(\Gamma^\lambda_{ij}h_{\alpha\lambda}) - g^{\alpha\beta}\Gamma^\tau_{\beta i}\Gamma^\lambda_{\tau j}h_{\alpha\lambda} \\
& \quad -g^{\alpha\beta}\Gamma^\tau_{\beta j}\Gamma^\lambda_{\tau i}h_{\alpha\lambda} - 2g^{\alpha\beta}\Gamma^\tau_{\alpha\beta}\Gamma^\lambda_{ij}h_{\tau\lambda} + g^{\alpha\beta}\Gamma^\lambda_{\alpha i}\Gamma^\tau_{\beta j}h_{\lambda\tau} \\
& \quad +g^{\alpha\beta}\Gamma^\lambda_{\alpha j}\Gamma^\tau_{\beta i}h_{\lambda\tau}\,.
\end{aligned} \tag{6.6}$$

Our calculations though are inconclusive at this stage, we will discuss the implications of the **new result** obtained. As we can see, the above equations (6.5) and (6.6) are quite complicated to solve explicitly. For the non-zero components of $\delta R_{\mu\nu}$, the solutions are expected to be non-trivial. The complete scenario with both of the odd-parity and even-parity perturbation may generate a complex situation. If we keep the odd parity waves, we find that δR_{11} and δR_{22} are zero, δR_{23} and δR_{13} are non-trivial and signify parity mixing. In the expression for δR_{13}, we have terms $-g^{01}\partial_1^2 h_{03}$ where g^{01} has a $\sin\theta$ that changes the parity of the expression. This will thus mix with δR_{13} from the even perturbations. This calculation is very cumbersome to follow. We hope to make progress using suitable computer software or coding which we are still developing. The use of Zerilli's equation, or Regge-

Wheeler's equation is restricted in this calculation. We find that we have to recalculate the system and obtain gauge invariant equations similar to the computations of Moncreif [125] for quantum fluctuations, which are not restricted to the spherical sector.

It is to be noted that we have computed the correction for the Schwarzschild black hole space-time, which is not a realistic version of actual black holes that exist in the universe. It would be more interesting to find a correction for Kerr black hole (black hole with rotation) and binary black hole system (two black holes revolving around each other). However, we have started the calculation with the simplest space-time and then we can proceed step by step to find a similar correction for a Kerr black hole followed by a binary black hole system.

There are different future research plans that can be carried on further. Few of the important plans are listed below.

- Implement the correction for the binary black hole collapse and study the effect.
- Calculation of the holonomy correction and corrections in all the corresponding momenta in spherical reduced phase space.
- Study the correction effect on gravitational wave emitted from different black holes and predict the nature of the black holes.
- The quantum gravity strain is of order (10^{-125}) which is very much similar to the order of the cosmological constant, research can be carried out to explore this coincidence.
- The event horizon telescope will be functional soon, and we can use the equations studied in this thesis to predict the behaviour of a 'image of the spherical black hole.'

Some of the above mentioned research projects are already in progress and hopefully the results will be presented in the very near future.

Bibliography

[1] J.B. Hartle. *Gravity: An Introduction to Einstein's General Relativity*. Addison-Wesley, 2003.

[2] Newtonian constant of gravitation, 2014. CODATA, http://physics.nist.gov/cgi-bin/cuu/Value?bg.

[3] Chris Pollock. Mercury's perihelion. http://www.math.toronto.edu/~colliand/426_03/Papers03/C_Pollock.pdf.

[4] Albert Einstein. Explanation of the Perihelion Motion of Mercury from the General Theory of Relativity. *Sitzungsber. Preuss. Akad. Wiss. Berlin (Math. Phys.)*, 1915:831–839, 1915.

[5] Avery E. Broderick, Ramesh Narayan, John Kormendy, Eric S. Perlman, Marcia J. Rieke, and Sheperd S. Doeleman. The Event Horizon of M87. *Astrophys. J.*, 805(2):179, 2015.

[6] Albert Einstein. Über Gravitationswellen. *Sitzungsber. Preuss. Akad. Wiss. Berlin (Math. Phys.)*, 1918:154–167, 1918.

[7] B. P. Abbott and et al. Gw151226: Observation of gravitational waves from a 22-solar-mass binary black hole coalescence. *Phys. Rev. Lett.*, 116:241103, Jun 2016.

[8] J. Surdej, C. Delacroix, P. Coleman, M. Dominik, S. Habraken, C. Hanot, H. Le Coroller, D. Mawet, H. Quintana, T. Sadibekova, and D. Sluse. The Optimal Gravitational Lens Telescope. *The Astronomical Journal*, 139:1935–1941, May 2010.

[9] Neil Ashby. Relativity in the Global Positioning System. *Living Rev. Rel.*, 6:1, 2003. [100 Years Of Relativity : space-time structure: Einstein and beyond, 257 (2005)].

[10] Joachim Wambsganss. Gravitational lensing in astronomy. *Living Rev. Rel.*, 1:12, 1998.

[11] Richard Massey, Thomas Kitching, and Johan Richard. The dark matter of gravitational lensing. *Rept. Prog. Phys.*, 73:086901, 2010.

[12] Steven Weinberg. *Cosmology*. Oxford, UK: Oxford Univ. Pr. (2008) 593 p, 2008.

[13] Kurt Godel. An Example of a new type of cosmological solutions of Einstein's field equations of graviation. *Rev. Mod. Phys.*, 21:447–450, 1949.

[14] M. S. Morris, K. S. Thorne, and U. Yurtsever. Wormholes, Time Machines, and the Weak Energy Condition. *Phys. Rev. Lett.*, 61:1446–1449, 1988.

[15] J. F. Hawley and K. A. Holcomb. *Foundations of modern cosmology*. New York: Oxford University Press, 1998.

[16] H. Kragh. *Quantum Generations; A History Of Physics In The Twentieth*. Orient Longman Limited, 2002.

[17] Max Planck and Max Planck. *Planck's Original papers in quantum physics / annotated by Hans Kangro ; translated by D. ter Haar and Stephen G. Brush*. Taylor and Francis London, german and english ed. edition, 1972.

[18] A. Einstein and J.J. Stachel. *Einstein's Miraculous Year: Five Papers that Changed the Face of Physics*. Princeton paperbacks. Princeton University Press, 2005.

[19] E. Schrödinger. An Undulatory Theory of the Mechanics of Atoms and Molecules. *Physical Review*, 28:1049–1070, December 1926.

[20] W. Heisenberg. Über den anschaulichen inhalt der quantentheoretischen kinematik und mechanik. *Zeitschrift für Physik*, 43(3):172–198, 1927.

[21] W. Heisenberg. The actual content of quantum theoretical kinematics and mechanics. *National Aeronautics and Space Administration (NASA)*, 1983.

[22] P. A. M. Dirac. The quantum theory of the emission and absorption of radiation. *Proceedings of the Royal Society of London A: Mathematical, Physical and Engineering Sciences*, 114(767):243–265, 1927.

[23] J. Huston. QCD: Experimental Review. In *Particles and fields. Proceedings, Meeting of the Division of the American Physical Society, DPF 2011, Providence, USA, August 9-13, 2011*, 2011.

[24] Ted Van Duzer and Charles W. Turner. *Principles of Superconductive Devices and Circuits, (Second Ed.)*. Prentice Hall PTR, Upper Saddle River, NJ, USA, 1999.

[25] Shun Lien Chuang. Physics of optoelectronic devices. *wiley New York*, 1995.

[26] Thaddeus D Ladd, Fedor Jelezko, Raymond Laflamme, Yasunobu Nakamura, Christopher Monroe, and Jeremy L O'Brien. Quantum computers. *Nature*, 464(7285):45–53, 2010.

[27] Alexandre Bresson, Yannick Bidel, Philippe Bouyer, Bruno Leone, Eamon Murphy, and P Silvestrin. Quantum mechanics for space applications. *Applied Physics B*, 84(4):545–550, 2006.

[28] P.C.W. Davies. Does quantum mechanics play a non-trivial role in life? *Biosystems*, 78(1–3):69 – 79, 2004.

[29] Michael E Peskin and Daniel V Schroeder. *An Introduction to Quantum Field Theory; 1995 ed.* Westview, Boulder, CO, 1995. Includes exercises.

[30] C. J. Isham. Canonical quantum gravity and the problem of time. In *19th International Colloquium on Group Theoretical Methods in Physics (GROUP 19) Salamanca, Spain, June 29-July 5, 1992*, pages 0157–288, 1992.

[31] L. Smolin. *Three Roads To Quantum Gravity*. Science masters series. Basic Books, 2002.

[32] Sabine Hossenfelder. Experimental Search for Quantum Gravity. In *Workshop on Experimental Search for Quantum Gravity NORDITA, Stockholm, Sweden, July 12-16, 2010*, 2010.

[33] Claus Kiefer. Quantum Gravity. In Abhay Ashtekar and Vesselin Petkov, editors, *Springer Handbook of Spacetime*, pages 709–722. 2014.

[34] Oliver Sim Brüning, Paul Collier, P Lebrun, Stephen Myers, Ranko Ostojic, John Poole, and Paul Proudlock. *LHC Design Report*. CERN, Geneva, 2004.

[35] R. L. Jaffe. The Casimir effect and the quantum vacuum. *Phys. Rev.*, D72:021301, 2005.

[36] Arundhati Dasgupta. Quantum Gravity Effects on Unstable Orbits in Schwarzschild Space-time. *JCAP*, 1005:011, 2010.

[37] S. W. Hawking. Particle creation by black holes. *Communications in Mathematical Physics*, 43(3):199–220, 1975.

[38] F. Belgiorno, S. L. Cacciatori, M. Clerici, V. Gorini, G. Ortenzi, L. Rizzi, E. Rubino, V. G. Sala, and D. Faccio. Hawking radiation from ultrashort laser pulse filaments. *Phys. Rev. Lett.*, 105:203901, 2010.

[39] S. Doeleman. Building an event horizon telescope: (sub)mm VLBI in the ALMA era. In *10th European VLBI Network Symposium and EVN Users Meeting: VLBI and the New Generation of Radio Arrays*, page 53, 2010.

[40] A. Einstein. Die grundlage der allgemeinen relativitätstheorie. *Annalen der Physik*, 354(7):769–822, 1916.

[41] Review b: Coordinate systems. `http://web.mit.edu/8.02t/www/materials/modules/ReviewB.pdf`.

[42] P. S. Wesson. The application of dimensional analysis to cosmology. *Space Science Reviews*, 27:109–153, oct 1980.

[43] C.W. Misner, K.S. Thorne, and J.A. Wheeler. *Gravitation*. Number pt. 3 in Gravitation. W. H. Freeman, 1973.

[44] Richard P. Feynman, Robert B. Leighton, and Matthew Sands. *The Feynman lectures on physics. Vol. 3: Quantum mechanics*. Addison-Wesley Publishing Co., Inc., Reading, Mass.-London, 1965.

[45] S. S. Shapiro and I. I. Shapiro. Gravitational deflection of light. *Einstein Online*, 04:1003, 2010.

[46] Albert Einstein. On the electrodynamics of moving bodies. *Annalen Phys.*, 17:891–921, 1905.

[47] D.J. Griffiths. *Introduction to Electrodynamics*. Prentice Hall, 1999.

[48] H. Minkowski and V. Petkov. *Space and Time: Minkowski's papers on relativity*. Minkowski Institute Press, 2013.

[49] Roger Penrose. *The road to reality : a complete guide to the laws of the universe*. Vintage, London, 2005.

[50] Susskind L. Lecture notes. `http://www.lecture-notes.co.uk/susskind/special-relativity/lecture-4/space-time-separation/`.

[51] Sergei A. Klioner. The problem of clock synchronization: A relativistic approach. *Celestial Mechanics and Dynamical Astronomy*, 53(1):81–109, 1992.

[52] Henry Poincaré. On the dynamics of the electron (english translation by Scott Walter). *Rendiconti del Circolo Matematico di Palermo*, 21:129–176, 1906.

[53] R. Katz. *An introduction to the special theory of relativity*. Van Nostrand momentum books. Published for the Commission on College Physics [by] D. Van Nostrand, 1964.

[54] Y. Zhang. *Special Relativity and Its Experimental Foundations*. Advanced Series on Artificial Intelligence. World Scientific, 1997.

[55] C. Christodoulides. *The Special Theory of Relativity: Foundations, Theory, Verification, Applications*. Undergraduate Lecture Notes in Physics. Springer International Publishing, 2016.

[56] Albert Einstein. On the influence of gravitation on the propagation of light. *Annalen Phys.*, 35:898–908, 1911. [Annalen Phys.14, 425 (2005)].

[57] Sean M. Carroll. Lecture notes on general relativity, 1997. `https://inspirehep.net/record/451850?ln=en`.

[58] C.J. Isham. *Modern Differential Geometry for Physicists*. World Scientific lecture notes in physics. World Scientific, 1999.

[59] B.F. Schutz. *A First Course in General Relativity*. Series in physics. Cambridge University Press, 1985.

[60] A. Dutta. Parallel transport of a vector on two sphere. *Figure is drawn in Xfig*, 2016.

[61] A. Dutta. Commutator of covariant derivatives. *Figure is drawn in Xfig*, 2016.

[62] Jeremy Bernstein. Spontaneous symmetry breaking, gauge theories, the Higgs mechanism and all that. *Rev. Mod. Phys.*, 46:7–48, Jan 1974.

[63] Daniel Harlow. Jerusalem Lectures on Black Holes and Quantum Information. *Rev. Mod. Phys.*, 88:15002, 2016.

[64] Guido Cognola and Paola Lecca. Electromagnetic fields in Schwarzschild and Reissner-Nordstrom geometry. Quantum corrections to the black hole entropy. *Phys. Rev.*, D57:1108–1111, 1998.

[65] Giovanni Modanese and Giorgio Fontana. Effect of the vacuum energy density on graviton propagation. *AIP Conf. Proc.*, 699:1198, 2004.

[66] Karl Schwarzschild. On the gravitational field of a mass point according to Einstein's theory. *Sitzungsber. Preuss. Akad. Wiss. Berlin (Math. Phys.)*, 1916:189–196, 1916.

[67] Oas. G. Full derivation of the Schwarzschild solution. `http://web.stanford.edu/~oas/SI/SRGR/notes/SchwarzschildSolution.pdf`.

[68] Roger Penrose. Gravitational collapse and space-time singularities. *Phys. Rev. Lett.*, 14:57–59, Jan 1965.

[69] Claes Uggla. Spacetime Singularities: Recent Developments. In *Proceedings, 13th Marcel Grossmann Meeting on Recent Developments in Theoretical and Experimental General Relativity, Astrophysics, and Relativistic Field Theories (MG13): Stockholm, Sweden, July 1-7, 2012*, pages 59–79, 2015.

[70] S. Chandrasekhar. On stars, their evolution and their stability. *Rev. Mod. Phys.*, 56:137–147, Apr 1984.

[71] G. 't Hooft. Perturbative quantum gravity. *Subnucl. Ser.*, 40:249–269, 2003.

[72] K. Becker, M. Becker, and J.H. Schwarz. *String Theory and M-Theory: A Modern Introduction*. Cambridge University Press, 2006.

[73] R. Gambini and J. Pullin. *A First Course in Loop Quantum Gravity*. OUP Oxford, 2011.

[74] Carlo Rovelli. Loop quantum gravity. *Phys. World*, 16N11:37–41, 2003.

[75] Bryce S. DeWitt. Quantum Theory of Gravity. 1. The Canonical Theory. *Phys. Rev.*, 160:1113–1148, 1967.

[76] Bryce S. DeWitt. Quantum Theory of Gravity. 2. The Manifestly Covariant Theory. *Phys. Rev.*, 162:1195–1239, 1967.

[77] Bryce S. DeWitt. Quantum Theory of Gravity. 3. Applications of the Covariant Theory. *Phys. Rev.*, 162:1239–1256, 1967.

[78] Carlo Rovelli and Lee Smolin. Knot theory and quantum gravity. *Phys. Rev. Lett.*, 61:1155–1158, Sep 1988.

[79] A. Ashtekar. New Variables for Classical and Quantum Gravity. *Phys. Rev. Lett.*, 57:2244–2247, 1986.

[80] R. Arnowitt, S. Deser, and C. W. Misner. Dynamical structure and definition of energy in general relativity. *Phys. Rev.*, 116:1322–1330, Dec 1959.

[81] R.M. Wald. *General Relativity*. University of Chicago Press, 1984.

[82] Thomas Thiemann. *Modern canonical quantum general relativity*. Cambridge University Press, 2008.

[83] R. K. P. Zia, E. F. Redish, and S. R. McKay. Making sense of the Legendre transform. *American Journal of Physics*, 77:614–622, July 2009.

[84] David L. Wiltshire. An Introduction to quantum cosmology. In *Cosmology: The Physics of the Universe. Proceedings, 8th Physics Summer School, Canberra, Australia, Jan 16-Feb 3, 1995*, pages 473–531, 1995.

[85] Edward Anderson. Problem of Time in Quantum Gravity. *Annalen Phys.*, 524:757–786, 2012.

[86] Soren Holst. Barbero's Hamiltonian derived from a generalized Hilbert-Palatini action. *Phys. Rev.*, D53:5966–5969, 1996.

[87] M. Ferraris, M. Francaviglia, and C. Reina. Variational formulation of general relativity from 1915 to 1925 "Palatini's method" discovered by Einstein in 1925. *General Relativity and Gravitation*, 14:243–254, March 1982.

[88] Giorgio Immirzi. Quantum gravity and Regge calculus. *Nucl. Phys. Proc. Suppl.*, 57:65–72, 1997.

[89] M. A. Clayton. Canonical general relativity: The Diffeomorphism constraints and spatial frame transformations. *J. Math. Phys.*, 39:3805–3816, 1998.

[90] B. Dittrich. Lecture Notes on Quantum Gravity. *Informal lectures given at University of New Brunswick*.

[91] A. Dutta and A. Dasgupta. Edge intersecting surface S. *Figure is drawn in Xfig*, 2016.

[92] Hermann Nicolai, Kasper Peeters, and Marija Zamaklar. Loop quantum gravity: An Outside view. *Class. Quant. Grav.*, 22:R193, 2005.

[93] A. Dutta and A. Dasgupta. Semi-Classicaly Corrected Gravity and Numerical Relativity. *Nova Science Publishers*, 2015.

[94] B Dittrich and T Thiemann. Testing the master constraint programme for loop quantum gravity: Iv. free field theories. *Classical and Quantum Gravity*, 23(4):1121, 2006.

[95] T. Thiemann and O. Winkler. Gauge field theory coherent states (GCS). 2. Peakedness properties. *Class. Quant. Grav.*, 18:2561–2636, 2001.

[96] Brian C Hall. The inverse segal–bargmann transform for compact lie groups. *Journal of Functional Analysis*, 143(1):98 – 116, 1997.

[97] G.A. Lemaitre and M.A.H. MacCallum. The Expanding Universe. *General Relativity and Gravitation*, 29:641–680, May 1997.

[98] John D. Barrow and Douglas J. Shaw. The Value of the Cosmological Constant. *Gen. Rel. Grav.*, 43:2555–2560, 2011. [Int. J. Mod. Phys.D20, 2875 (2011)].

[99] Martin Bojowald, Rituparno Goswami, Roy Maartens, and Parampreet Singh. A Black hole mass threshold from non-singular quantum gravitational collapse. *Phys. Rev. Lett.*, 95:091302, 2005.

[100] T. Piran. *Gamma-Ray Bursts as Probes for Quantum Gravity*, pages 351–362. Springer Berlin Heidelberg, Berlin, Heidelberg, 2005.

[101] The 3+1 formulation for general relativity. `http://laplace.physics.ubc.ca/2010-pi-nr/ref/387n-03-choptuik-3+1-formulation.pdf`.

[102] Examples of rnpl-based finite-difference calculations. `http://laplace.physics.ubc.ca/People/matt/Software/RNPL_main.html`.

[103] Dennis Philipp and Volker Perlick. Schwarzschild radial perturbations in Eddington–Finkelstein and Painlevé–Gullstrand coordinates. *Int. J. Mod. Phys.*, D24(09):1542006, 2015.

[104] Edward Seidel and Wai-Mo Suen. Towards a singularity-proof scheme in numerical relativity. *Phys. Rev. Lett.*, 69:1845–1848, Sep 1992.

[105] Frans Pretorius. Numerical relativity using a generalized harmonic decomposition. *Classical and Quantum Gravity*, 22(2):425, 2005.

[106] Matthew W. Choptuik. Universality and scaling in gravitational collapse of a massless scalar field. *Phys. Rev. Lett.*, 70:9–12, Jan 1993.

[107] K. W. Morton and D. F. Mayers. *Numerical Solution of Partial Differential Equations: An Introduction*. Cambridge University Press, New York, NY, USA, 2005.

[108] R. Courant, K. Friedrichs, and H. Lewy. On the Partial Difference Equations of Mathematical Physics. *IBM Journal of Research and Development*, 11:215–234, March 1967.

[109] Luis Lehner. Numerical relativity: A Review. *Class. Quant. Grav.*, 18:R25–R86, 2001.

[110] Julius O Smith. Physical audio signal processing. *Linear Predictive*, 2010.

[111] A. Dutta and A. Dasgupta. Plotting of scalar field potential with one spatial dimension. *Figure is drawn in Mathematica*, 2016.

[112] Christos G. Tsagas. Electromagnetic fields in curved spacetimes. *Class. Quant. Grav.*, 22:393–408, 2005.

[113] S. Weinberg. *Gravitation and cosmology: principles and applications of the general theory of relativity*. Wiley, 1972.

[114] R. Penrose and W. Rindler. *Spinors and Space-Time: Volume 1, Two-Spinor Calculus and Relativistic Fields*. Cambridge Monographs on Mathematical Physics. Cambridge University Press, 1987.

[115] J.-P. Luminet. Image of a spherical black hole with thin accretion disk. *Astronomy and Astrophysics*, 75:228–235, May 1979.

[116] A. Dutta and Arundhati Dasgupta. Plotting of A(r) vs. r. *Figure drawn in Maple*, 2016.

[117] D. Zwillinger. *Handbook of Differential Equations*. Number v. 1. Academic Press, 1998.

[118] Nigel T. Bishop and Luciano Rezzolla. Extraction of gravitational waves in numerical relativity. *Living Reviews in Relativity*, 19(1):2, 2016.

[119] Luciano Rezzolla. Gravitational waves from perturbed black holes and relativistic stars. In *Astroparticle physics and cosmology. Proceedings: Summer School, Trieste, Italy, Jun 17-Jul 5 2002*, pages 255–316, 2003.

[120] Richard H. Price and Yan Wang. The transverse traceless gauge and quadrupole sources. *American Journal of Physics*, 76(10):930–933, 2008.

[121] Tullio Regge and John A. Wheeler. Stability of a schwarzschild singularity. *Phys. Rev.*, 108:1063–1069, Nov 1957.

[122] Frank J. Zerilli. Effective potential for even parity Regge-Wheeler gravitational perturbation equations. *Phys. Rev. Lett.*, 24:737–738, 1970.

[123] R. D'Inverno. *Introducing Einstein's Relativity*. Clarendon Press, 1992.

[124] G.D. Birkhoff and R.E. Langer. *Relativity and Modern Physics*. Harvard University Press, 1923.

[125] V. Moncrief. Classical and quantum models of strong cosmic censorship. *General Relativity and Gravitation*, 15:309–314, April 1983.

Appendix A

RNPL Programming for Numerical Solution

RNPL program to solve the 1d wave equation with shift term $x^2(x-1)^2$

phi_tt = phi_xx

recast in first order form

pp_t = pi_x
pi_t = pp_x

where

pp := phi_x
pi := phi_t

The program uses Crank-Nicholson differencing with
(implicit) ingoing/outgoing radiation conditions, using
$O(h^2)$ forward and backwards differences, at the boundaries.

Initial data is a Gaussian for pp with pi = idsignum $*$ pp,
where

idsignum = -1, 0, 1 $\rightarrow$ ingoing, time-symmetric, outgoing
initial data, respectively

Definition of memory size (only needed for Fortran)

---

system parameter int memsiz := 1000000

Definition of parameters and associated default values.

Note that “xmin” and “xmax” are special in that they are
also implicitly declared to be parameters via the
definition of the coordinate system below.

```
parameter float xmin := 0.0
parameter float xmax := 1.0
```

The following four parameters are used in the
specification of the initial data.

```
parameter float amp := 1.0
parameter float xc := 0.5
parameter float xwid := 0.05
parameter float idsignum := 0.0
```

Definition of coordinate system, note that the first
coordinate is always assumed to be the time coordinate.

```
rect coordinates t, x
```

Definition of finite-difference grid: [1:Nx] specifies
the index range, {xmin:xmax} the coordinate range.

```
uniform rect grid g1 [1:Nx] {xmin:xmax}
```

Definition of grid functions: since a Crank-Nicholson
scheme is being used, the grid functions are defined at
“temporal offsets” 0 and 1, corresponding to “current” and
“advanced” time levels. The directive {out_gf = 1} enables
default output of the grid function (output can be disabled
via out_gf = 0, by omitting the directive completely, or
via modification of the file .rnpl.attributes prior to
program invocation).

```
float pp on g1 at 0,1 out_gf = 1
float pi on g1 at 0,1 out_gf = 1
```

FINITE DIFFERENCE OPERATOR DEFINITIONS

Crank Nicholson time derivative operator (first forward difference)

---

operator DCN(f,t) := $(<1>f[0]-<0>f[0])/dt$

Forward time averaging operator

---

operator MU(f,t) := $(<1>f[0]+<0>f[0])/2$

$O(h^2)$ centred spatial derivative operator

---

operator D0(f,x) := $(<0>f[1]-<0>f[-1])$ / $(2*dx)$

$O(h^2)$ backwards spatial derivative operator

---

operator DB(f,x) := $(3*<0>f[0]-4*<0>f[-1]+<0>f[-2])$ / $(2*dx)$

$O(h^2)$ forwards spatial derivative operator

---

operator DF(f,x) := $(-3*<0>f[0]+4*<0>f[1]-<0>f[2])$ / $(2*dx)$

DIFFERENCE EQUATION DEFINITIONS

---

evaluate residual pp
{
$[1:1]$:= DCN(pp,t) = MU(DF(pp,x),t) + MU(DF($(x*x)*((x-1)*(x-1)),x$)*pp,t) + MU($(x*x)*((x-1)*(x-1))$*DF(pp,x),t);
$[2:Nx-1]$:= DCN(pp,t) = MU(D0(pi,x),t) + MU(D0($(x*x)*((x-1)*(x-1)),x$)*pp,t) + MU($(x*x)*((x-1)*(x-1))$*D0(pp,x),t);
$[Nx:Nx]$:= DCN(pp,t) = MU(-DB(pp,x),t) + MU(DB($(x*x)*((x-1)*(x-1)),x$)*pp,t) + MU($(x*x)*((x-1)*(x-1))$*DB(pp,x),t);
}

evaluate residual pi
{
$[1:1]$:= DCN(pi,t) = MU(DF(pi,x),t);
$[2:Nx-1]$:= DCN(pi,t) = MU(D0(pp,x),t);
$[Nx:Nx]$:= DCN(pi,t) = MU(-DB(pi,x),t);

```
}

---------------------------------------------
INITIALIZATION STATEMENTS
---------------------------------------------

---------------------------------------------
Intialize to an ingoing,outgoing or time-symmetric
gaussian pulse (in the spatial derivative of the scalar
field), dependent on the value of idsignum.
---------------------------------------------
initialize pp
{
[1 : Nx] := amp * exp(-(x-xc)^2/xwid^2)
}
initialize pi
{
[1 : Nx] := idsignum * amp * exp(-(x-xc)^2/xwid^2)
}

auto initialize pp, pi

---------------------------------------------
Definition of type of time stepping algorithm. The use
of "iterative" here, combined with the "auto update ..."
statement below, results in a scheme whereby the
residuals defined above are iteratively relaxed using
a point-wise Newton-Gauss-Seidel technique, until the
residual norms are below a certain threshold.
---------------------------------------------
looper iterative

---------------------------------------------
The following statement directs RNPL to automatically
generate code to update the grid functions using the
residual definitions.
---------------------------------------------
auto update pp, pi
```